

DETrital ZIRCON GEOCHRONOLOGY OF THE SILURIAN–LOWER CRETACEOUS CONTINUOUS SUCCESSION OF THE SOUTH KITAKAMI BELT, NORTHEAST JAPAN

Hiroyuki OKAWA¹, Masanori SHIMOJO², Yuji ORIHASHI³, Koshi YAMAMOTO⁴,
Takafumi HIRATA⁵, Shin-ichi SANO⁶, Yasuo ISHIZAKI¹, Yoshikazu KOUCHI¹,
Shuichi YANAI⁷ and Shigeru OTOH¹

¹ Graduate School of Science and Engineering, University of Toyama, 3190 Gofuku, Toyama 930-8555, Japan

² Graduate School of Arts and Sciences, University of Tokyo, 3-8-1 Komaba, Meguro-ku, Tokyo 153-8902, Japan

³ Earthquake Research Institute, University of Tokyo, 1-1-1 Yayoi, Bunkyo-ku, Tokyo 113-0032, Japan

⁴ Graduate School of Environmental Studies, Nagoya University, Furo-cho, Chikusa-ku, Nagoya 464-8601, Japan

⁵ Graduate School of Science, Kyoto University, Kitashirakawaoiwa-cho, Sakyo-ku, Kyoto 606-8502, Japan

⁶ Fukui Prefectural Dinosaur Museum, 51-11 Terao, Muroko, Katsuyama, Fukui 911-8601, Japan

⁷ Japan Geocommunications Co., Ltd., 2-10 Yotsuya, Shinjuku-ku, Tokyo 160-0004, Japan

ABSTRACT

U-Pb analyses of more than 1,000 single detrital zircons from 16 formations of the Silurian–Lower Cretaceous continuous succession of the South Kitakami Belt (SKB), Northeast Japan, provide a detrital zircon reference for the complex continental-margin orogen of Japan. As a result, three tectonic phases were discriminated. Siluro–Devonian sandstone samples contain many syn-sedimentary zircons and 36.5–48.0% of Precambrian zircons scattering between 700 Ma and 3,000 Ma, suggesting that they were deposited along an active continental margin of East Gondwana. Permian–Early Jurassic sandstone samples contain virtually no Precambrian zircons, suggesting that they were deposited along the active margin of an oceanic island arc. Middle Jurassic–Early Cretaceous sandstone samples contain many 300–170 Ma zircons and up to 28% of Paleoproterozoic (around 1,850 Ma) zircons but no Neoproterozoic zircons. Moreover, the zircons during the magmatic hiatus in Korea (158–110 Ma) were detected only in one Lower Cretaceous sandstone sample. The age distribution suggests that the Paleoproterozoic zircons in the Middle Jurassic–Lower Cretaceous sandstone of the SKB were most likely supplied from a Paleoproterozoic orogen in the North China Block. Thus, the South Kitakami Paleoland, which accumulated the continuous succession of the SKB was born along a margin of Gondwana in the Silurian–Devonian, rifted from the continent and drifted in the Tethys ocean as an oceanic island arc in the Permian–Early Jurassic, and finally amalgamated along an active continental margin where detrital zircons of the North China Block were supplied in the Middle Jurassic.

Key words: U-Pb age, detrital zircon, LA-ICPMS, South Kitakami Belt, Northeast Japan, Gondwana

大川泰幸・下條将徳・折橋裕二・山本鋼志・平田岳史・佐野晋一・石崎泰男・高地吉一・柳井修一・大藤 茂 (2013) 東北日本, 南部北上帯のシルル～前期白亜紀連続層序における碎屑性ジルコン年代分布の推移. 福井県立恐竜博物館紀要 12: 35–78.

南部北上帯の浅海成シルル～下部白亜系連続層序から16層を選び、碎屑性ジルコンのウラン–鉛年代を測定した結果、日本列島の標準となる碎屑性ジルコン年代分布の推移が示された。①シルル～下部石炭系は1500–750 Maのジルコンを特徴的に含む多峰型年代分布をなし、新原生代ジルコンを産するゴンドワナ大陸北東縁からのジルコン供給を示唆する。②ペルム～下部ジュラ系は、いずれもほぼ堆積時ジルコンのみからなる単峰型年代分布をなす。③中部ジュラ～下部白亜系は、北中国地塊から供給されたと見られる古原生代(1850 Ma付近)ジルコンを含む二峰型年代分布をなす。以上より、本連続層序を堆積した南部北上古陸は、①シルル～前期石炭紀に位置したゴンドワナ大陸北東部の大陸縁から、②ペルム～前期ジュラ紀には分離してテチス海中の海洋性島弧として挙動し、③中期ジュラ紀には、北中国地塊からジルコンが供給される大陸縁に癒合したと見られる。

Received August 2, 2013. Accepted November 4, 2013.

Corresponding author—Shigeru OTOH

E-mail: shige@sci.u-toyama.ac.jp

INTRODUCTION

This paper aims (1) to introduce temporal transition of the detrital zircon age distributions recorded in the Silurian–Lower Cretaceous continuous succession of the South Kitakami Belt (SKB), Northeast Japan, and (2) to discuss the evolutionary history of the South Kitakami Paleoland, which accumulated the continuous succession of the SKB.

Recent progress in analytical technique has enabled rapid and exact U-Pb isotopic age determination of zircons using sensitive high-resolution ion-microprobe (SHRIMP) or inductively coupled plasma-mass spectrometry with laser ablation sampling (LA-ICPMS) (e.g., Compston, 1996; Kosler and Sylvester, 2003). Detrital zircon age distribution reflects the changes of provenance, paleogeography, and tectonic setting, and can be a powerful tool for inferring the plate tectonic evolution of a complex orogen like the Japanese Islands (e.g., Gehrels et al., 1995; Darby and Gehrels, 2006). To make such an inference, we have to know the temporal change of detrital zircon age distribution of each crustal block (or terrane) that makes up the orogen, and compare the data with the reference age distribution for the major crustal blocks in the world (e.g., Soreghan and Gehrels, 2000; Darby and Gehrels, 2006 and references therein). Such comparison enables us to know the origin and tectonic history of each crustal block in the orogen. The study of detrital zircon geochronology in Japan (Tsutsumi et al., 2000, 2003, 2006, 2009, 2011, 2012; Aoki et al., 2007, 2012; Otoh et al., 2010), however, is still local and is not comprehensive.

The SKB is the best target for a comprehensive study of detrital zircon geochronology in Japan, because it retains a 350-Myr continuous succession of shallow-marine to terrestrial beds formed during the Silurian to the Early Cretaceous (Kawamura et al., 1990; Mori et al., 1992; Ehiro and Kanisawa, 1999). The continuous succession of the SKB has already been studied as a standard succession of lithostratigraphy and paleobiogeography. It helps to estimate the transition of tectonic setting and affinities with the other crustal blocks or terranes of the Japanese Islands and East Asia (e.g., Kato, 1990; Nakamura and Tazawa, 1990; Otoh and Yanai, 1996; Ehiro and Kanisawa, 1999). The detrital zircon geochronological data of the SKB presented in this study will be another set of reference data. They can be much more useful than the paleobiogeographical data because even fossil-free sandstones of an accretionary prism or a metamorphic belt contain zircons, enabling to compare the SKB with any other belts but ultra-high-temperature metamorphic belts.

GEOLOGIC SETTING

The SKB consists mainly of basement rocks and overlying Ordovician to Early Cretaceous strata (Figs. 1 and 2). The outline of the basement rocks and the continuous succession we studied is described below.

Basement rocks

The basement rocks of the SKB are the Hayachine Complex (Ehiro et al., 1988) and its equivalents and the Hikami Granite (Murata et al., 1974).

The Hayachine Complex and its equivalents fringe northeastern to western boundary of the SKB (Fig. 1). They consist mainly of ultramafic to mafic rocks with small amounts of tonalite–trondhjemite–granodiorite (TTG). According to the petrological studies of Ozawa (1983, 1984) and Mori et al. (1992), they are fragments of volcanic-arc lithosphere. K-Ar hornblende ages of 421–484 Ma and a U-Pb zircon age of 462 Ma were reported from gabbro and tonalite, respectively (Ozawa et al., 1988; Shibata and Ozawa, 1992; Shimojo et al., 2010).

The Hikami Granite mainly exposes in the mid-eastern part of the SKB (Fig. 1). The Hikami Granite consists of massive to schistose granite, granodiorite, and tonalite, partly including blocks of gneissose metamorphic rocks (Tsubonusawa Metamorphic Rocks). Petrochemical studies suggested that the Hikami Granite is calc-alkaline, volcanic-arc granitoid (Kobayashi et al., 2000).

The Hikami Granite is unconformably overlain by the Silurian Kawauchi Formation (Murata et al., 1974, 1982), mentioned below, and has a SHRIMP U-Pb zircon age of 442 Ma (corresponding to the Late Ordovician; Watanabe et al., 1995). Shimojo et al. (2010), on the other hand, reported LA-ICPMS, U-Pb zircon ages of 416–403 Ma from four samples, suggesting that the granite at least partly forms Devonian intrusive bodies.

Silurian–Devonian strata

The Silurian to Devonian strata of the SKB crop out with the basement rocks (Fig. 1). They consist mainly of siliciclastic to volcaniclastic rocks with intercalations of felsic to mafic tuff and limestone, suggesting that they are deposits of a shallow-marine environment along an active continental margin.

In the northeastern part of the SKB, the Yakushigawa Formation overlies the Hayachine Complex and consists of interbedded basaltic volcaniclastic rocks, quartz-feldspathic sandstones, and felsic tuffs in the lower part, and of shales in the upper part. The shales of the Odagoe Formation, which yield a Silurian brachiopod *Trimerella* sp., overlie the Yakushigawa Formation (Ehiro et al., 1986). In the northern marginal part of the SKB to the south of Morioka (Fig. 1), the Hayachine Complex is associated with the Nameirizawa and Orikabetoge formations. The Nameirizawa Formation is lithologically correlated with the Yakushigawa Formation, whereas the Orikabetoge Formation consists of clastic rocks with orthoquartzite clasts (Okami et al., 1984) and yields Silurian fossils such as *Halysites kuraokaensis* and *Encrinurus* sp. (Kawamura et al., 1984; Yamazaki et al., 1984). In the Nagasaki area, western part of the SKB (Fig. 1), the Upper Devonian Tobigamori Formation overlies the Ohachimori Amphibolite, an equivalent of the Hayachine Complex, having K-Ar hornblende ages of 479–424 Ma (Kanisawa et al., 1992;

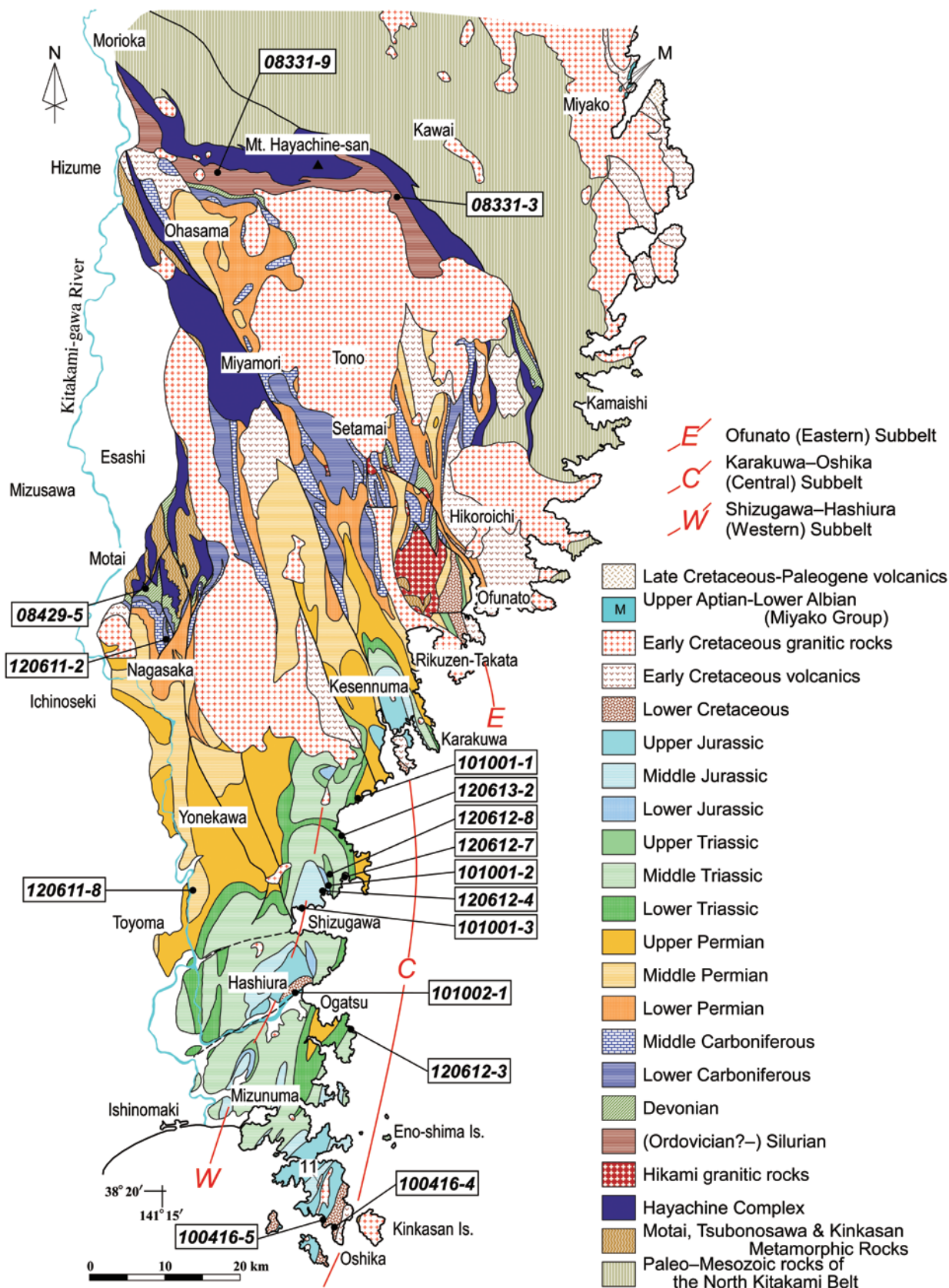


FIGURE 1. Geologic map of the South Kitakami Belt showing the sampling locations. Modified after Onuki (1981), Ehiro (1989), and Sasaki (2003). Abbreviations—Is.: Island, M: distribution of the Miyako Group.

Sasaki et al., 1997). The Tobigamori Formation consists of three members. The Lower Member consists of interbedded tuffaceous sandstone and shale yielding no fossils. The Middle Member consists of red conglomerate, sandstone, and shale, whereas the Upper Member consists mainly of sandy shale. The two members yield abundant brachiopod and plant fossils such as *Cyrtospirifer tobigamoriensis* and *Leptophloeum rhombicum*, and are correlated with the Famennian (Upper Devonian; Tachibana, 1950, 1952; Noda and Tachibana, 1959). Ehiro and Takaizumi (1992), on the other hand, found a Tournaisian ammonoid, *Protocanites* sp., from a float of the uppermost part of the Tobigamori Formation. In the Hikoroichi area, mid-eastern part of the SKB (Fig. 1), Siluro–Devonian Kawauchi, Ono, and Nakazato formations, in ascending order, lie on top of the Hikami Granite.

The Siluro–Devonian fauna and flora of the SKB have affinities with those of coeval northern East Gondwana: i.e., present-day Australia, South China, and the southern part of the Central Asian Orogenic Belt (CAOB). For example, tabulate corals from the Kawauchi Formation, such as *Schedohalysites* and *Falsicatenipora*, are abundant in the coeval strata of Australia and South China (e.g., Hamada, 1960; Kato, 1990), and the Eifelian brachiopod fauna from the Nakazato Formation has affinities with the coeval fauna from the CAOB in Inner Mongolia, China (Tazawa and Chen, 2001). Moreover, the Upper Devonian flora *Leptophloeum* of the Tobigamori Formation commonly occurs in the coeval strata of Australia, South China, CAOB, and the Imjingang Belt of North Korea (e.g., Kimura, 1987; Om et al., 1996; Tazawa et al., 2006).

Carboniferous strata

The distribution of the Carboniferous strata in the SKB is much wider than that of the Silurian to Devonian strata (Fig. 1). The Lower Carboniferous in the SKB is rich in felsic and mafic volcanic and pyroclastic rocks, whereas the Upper Carboniferous is rich in carbonate rocks (Kawamura and Kawamura, 1989a). Kawamura and Kawamura (1989b) and Kawamura et al. (1990) regarded that the Lower Carboniferous volcanic and pyroclastic rocks indicate the bimodal volcanism related to intra-arc rifting.

In the Nagasaki area, the Karaumestate Formation overlies the Tobigamori Formation, and is composed of interbedded sandstone and mudstone, felsic tuff, and calcareous sandstone (Kawamura and Kawamura, 1989a). The lower part of the Karaumestate Formation yields Tournaisian brachiopods, whereas the upper part yields Visean rugosa corals such as *Kueichouphyllum* sp. and *Dibunophyllum* sp., and brachiopods such as *Productus giganteus*. In the Hikoroichi area, the Lower Carboniferous Hikoroichi, Onimaru, and Lower to Upper Carboniferous Nagaiwa formations, in ascending order, overlies the Devonian Nakasato Formation. The Hikoroichi Formation, consisting mostly of felsic tuff and tuffaceous clastic rocks (Kawamura and Kawamura, 1989a), yields various rugosa corals such as *Amygdalophyllum etheridgei*, and brachiopods such as the *Rotaia-Marginatia-Syringothyris* assemblage and

Schizophoria resupinata, whereas the Onimaru Formation yields Late Visean rugosa corals such as *Kueichouphyllum glacie*, *Yuanophyllum kansuense*, and *Diphyphyllum hochangpingense*.

Two Carboniferous faunal provinces have been discriminated in the Eurasian realm: the northern province characterized by the rugosa coral *Gangamophyllum* and the southern province characterized by *Kueichouphyllum*. The northern province includes present-day northern Siberia, whereas the southern province includes present-day South China, Indochina, and northern Australia (Liao, 1990). Moreover, the mixed fauna of the northern and southern provinces has been recognized in the CAOB. Lower Carboniferous fauna of the SKB still has affinities with that of coeval northern East Gondwana. For example, the rugosa coral *Amygdalophyllum* from the Hikoroichi Formation is abundant in Australia (southern province). Occurrence of *Kueichouphyllum* and absence of *Gangamophyllum* in the Onimaru Formation also suggest an affinity with the southern province. The *Rotaia-Marginatia-Syringothyris* brachiopod assemblage, on the other hand, indicates an affinity with the CAOB (Tazawa, 1996). Late Carboniferous fauna from the SKB has various boreal elements (e.g., Kato, 1990), probably indicating the influence of global cooling at that time.

Permian to Middle Triassic strata

Permian strata

Permian strata in the SKB were subdivided, in ascending order, into the Sakamotozawan, Kanokuran, and Toyoman series (Minato et al., 1978), although we do not follow this local chronostratigraphic division and will call these “series” as “groups”. The Permian strata consist mostly of shallow marine epiclastic rocks and limestone, with small amounts of felsic to intermediate tuff in the Sakamotozawan Group.

The Sakamotozawan Group includes the Sakamotozawa Formation in the Hikoroichi–Setamai area, the Notsuchi Formation in the Nagasaki area, and the Nishikori Formation in the Toyoma area to the south of Nagasaki (Fig. 1). They consist mostly of sandstone, mudstone, and interbedded sandstone and mudstone, with some limestone beds particularly in the middle horizon (Kanmera and Mikami, 1965; Saito, 1966; Ehiro, 1989). The Sakamotozawan Group yields fusulinids such as *Zellia*, *Monodiexodina*, and *Pseudofusulina* (Kanmera and Mikami, 1965). Among them, genus *Monodiexodina* characterizes the *Monodiexodina* territory (Ishii et al., 1985), which includes the CAOB in Tarim, northeastern China, and Primorye in southeastern Russia (Ozawa, 1987). Moreover, the Nishikori (or Rodai) Formation yields the Maiya Flora consisting of *Gigantopteris*, *Taeniopteris*, and *Sphenophyllum*, common with the coeval strata in the Cathaysian Floristic Province in China and Korea (Asama, 1985).

The Kanokuran Group includes the Kanokura Formation in the Setamai area, the upper part of the Notsuchi Formation and the Usugino Conglomerates in the Nagasaki area, the Tenjinnoki Formation and the Yamazaki Conglomerates in the Toyoma area, and the Iwaizaki Limestones in the Motoyoshi

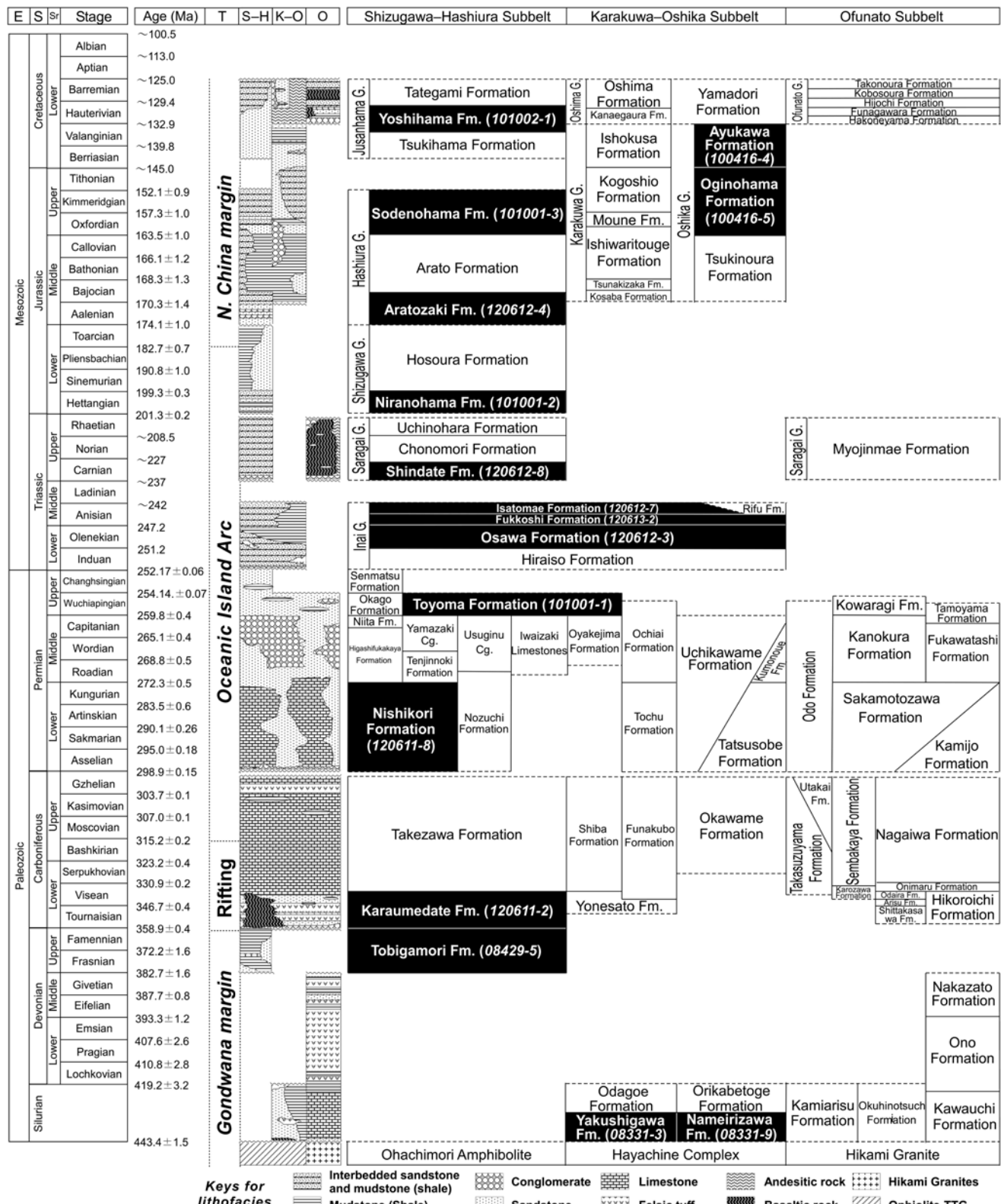


FIGURE 2. Stratigraphic division of the pre-Aptian sequences of the South Kitakami Belt showing the lithofacies and sampling horizons. Numerical ages for all systems are taken from International Commission on Stratigraphy (2013). Abbreviations—Cg.: Conglomerates, E: Erathem, Fm.: Formation, G: Group, K–O: Karakuwa–Oshika Subbelt, N: North China, O: Ofunato Subbelt, S: System, Sr: Series, S–H: Shizugawa–Hashiura Subbelt, T: Tectonic setting, TTG: Tonalite–trondhjemite–granodiorite.

area to the southeast of Nagasaka (Figs. 1 and 2). They consist generally of mudstone, sandstone, and conglomerate, with some interlayers of limestone. The conglomerate in the Kanokuran and overlying Toyoman groups is collectively called the Usuginutype Conglomerate with granitic clasts of 300–280 Ma (LA-ICPMS U-Pb ages; Okawa, unpublished data). The Usuginutype Conglomerate is particularly thick in the Kanokuran Group in the Nagasaka and Toyoma areas. The Kanokuran Group yields Roadian to Capitanian fusulinids of the *Monodexodina matsubaishi*, *Colania kotsuboensis*, and *Lepidolina multisepata* zones (Choi, 1973). The Kanokuran Group also yields such ammonoid genera as *Timorites*, *Paraceltites*, and *Cibolites*, and brachiopods such as *Leptodus nobilis* and *Spiriferellina cristata*. *Monodexodina matsubaishi* and *Spiriferellina cristata* indicates a faunal affinity with Mongolia and the southern margin of Siberia, whereas the ammonoids and *Leptodus nobilis* show the similarity with the Tethyan realm such as the South China Block (Ehiro, 1998; Tazawa, 1991, 2001).

The Toyoman Group includes the Kowaragi Formation in the Setamai–Karakuwa area and the Toyoma Formation in the Nagasaka, Toyoma, and Motoyoshi areas (Figs. 1 and 2). They consist mostly of black mudstone with some interlayers of sandstone, limestone, and conglomerate. The black mudstone bears strong slaty cleavage, particularly along the western limb of synclines (Sasaki, 2001, 2003), and partly contains carbonate and phosphate nodules (Kanisawa and Ehiro, 1986). The Toyoman Group yields Wuchiapingian to Changhsingian ammonoids such as *Araxoceras* sp. and *Paratirolites compressus* (Murata and Bando, 1975; Ehiro, 1996). Among them *Araxoceras* is a typical genus of the Tethys Ocean (Bando et al., 1987).

Lower to Middle Triassic strata

Lower to Middle Triassic strata of the SKB are collectively called the Inai Group (Fig. 2). The Inai Group is distributed in the southeastern part of the SKB and consists of two sedimentary cycles: the Hiraiso and Osawa formations constitute the first cycle, whereas the Fukkoshi and Isatomae formations constitute the second cycle (Onuki and Bando, 1959). The Hiraiso Formation consists of an upward fining sequence, beginning with basal conglomerate and coarse calcareous sandstone, overlain by interbedded sandstone and mudstone. Rare felsic tuff layers are intercalated in the lower part of the formation. The Hiraiso Formation yields *Pleuromeia* flora, which commonly occurs from the North China Block and the southern part of the CAOB (Kimura, 1987). The Hiraiso Formation also yields bivalves such as *Eumorphotis nipponicus* and “*Pecten*” aff. *ussuricus*. The Olenekian Osawa Formation consists mainly of calcareous mudstone, with some intercalations of sandstone and submarine sliding deposits (Kamada, 1983). The formation yields *Utatsusaurus hataii*, one of the earliest ichthyosaur fossils in the world. The Osawa Formation also yields abundant ammonoids of the *Columbites-Subcolumbites* fauna (Bando and Shimoyama, 1974), which is concentrated in the coeval strata in the Tethyan region (Bando et al., 1987). The Fukkoshi Formation consists mainly of bedded sandstone, with subordinate amount

of mudstone. The formation yields Anisian ammonoids such as *Bolatonites cf. kitakamicus*, *Hollandites* spp., and *Rikuzenites nobilis* (Shimizu, 1930; Yabe, 1949). The generic composition of the Anisian ammonoids from the SKB is the Pacific–Tethyan type (Ehiro, 1998) although they contain some common species with the coeval ammonoids from Primorye and Kolyma of eastern Russia (Nakazawa, 1991). The Fukkoshi Formation also yields brachiopods such as *Spiriferina* and *Terebratula* (Ichikawa, 1951). The Isatomae Formation consists of laminated muddy sandstone and mudstone, intercalated with some sandstone beds. The formation also yields Anisian Pacific–Tethyan ammonoids such as *Hollandites japonicus*, “*Danubites*” *naumanni*, and *Bolatonites kitakamicus* (Shimizu, 1930; Onuki and Bando, 1959; Bando, 1964; Ehiro, 1998).

Upper Triassic to Lower Cretaceous strata

Upper Triassic to Lower Cretaceous strata are distributed in the southeastern part of the SKB. They occur in three subbelts along the axes of three major synclines: the Shizugawa–Hashiura, Karakuwa–Oshika, and Ofunato subbelts from west to east (e.g., Yamashita, 1957; Takizawa, 1977, 1985; Fig. 1). The succession and thickness of the Mesozoic strata in the three subbelts substantially differ from each other. Sasaki (2003) reported that the regional strain is concentrated along the western limb of the major synclines and concluded that the major synclines are conical synclines with subvertical rotation axes and were formed through sinistral shearing along the high-strain zones (i.e., their western limbs at present).

Upper Triassic strata

Upper Triassic strata of the SKB are collectively called the Saragai Group (Fig. 2), which occurs in the Shizugawa–Hashiura and Ofunato subbelts but is absent in the Karakuwa–Oshika Subbelt (Fig. 1). The Saragai Group in the northern part of the Shizugawa–Hashiura Subbelt consists of the Shindate and Chonomori formations (Onuki and Bando, 1958), whereas the group in the Ofunato Subbelt is called the Myojinmae Formation (Kanagawa and Ando, 1983). The Shindate Formation consists mainly of massive feldspathic sandstone with subordinate amounts of mudstone, granule conglomerate, felsic tuff, and rare carbonaceous mudstone. The Carnian–Norian Chonomori Formation, overlying the Shindate Formation, consists of interbedded micaceous sandstone and mudstone. The Chonomori Formation is characterized by a rich *Monotis* fauna, which belongs to the Arcto-Pacific Realm (Kobayashi and Tamura, 1983; Tamura, 1987) and consists of *M. scutiformis*, *M. ochotica*, and *M. zabaikalica* (Nakazawa, 1964; Ando, 1987). The Myojinmae Formation in the Ofunato Subbelt consists mainly of tuff, with some andesite lava, tuffaceous sandstone, and volcanic conglomerate. A tuff clast in the conglomerate yields *Monotis ochotica* (Kanagawa and Ando, 1983).

Lower to lower Middle Jurassic strata

Lower to lower Middle Jurassic strata of the SKB is called the Shizugawa Group and occurs only in the Shizugawa–Hashiura Subbelt (Fig. 2). The Shizugawa Group in the type locality,

northern part of the Shizugawa–Hashiura Subbelt, consists of the Nirano-hama and Hosoura formations, in ascending order (Inai, 1939). The Nirano-hama Formation consists of brackish-water black mudstone and trigoniid-bearing coarse sandstone. The former yields paralic bivalves such as *Bakevella*, *Burmesia*, and *Geratrigonia*, whereas the latter is characterized by abundant occurrence of paralic bivalves (*Trigonia* and *Vaugonia*) and belemnites, together with middle to late Hettangian ammonoids such as *Alsatisites* (or *Yebisites*) *onoderai* (Matsumoto, 1956; Hayami, 1961; Sato and Westermann, 1991; Iba et al., 2012). The Hosoura Formation consists mostly of laminated sandy mudstone and yields Sinemurian to Aalenian ammonoids (Sato, 1957, 1962; Takahashi, 1969; Sato and Westermann, 1991). Many ammonoid and bivalve species from the Shizugawa Group are endemic and have not been found in other regions of East Asia (Hayami, 1990).

Middle Jurassic to Lower Cretaceous strata in the Shizugawa–Hashiura Subbelt

The Middle Jurassic to Lower Cretaceous strata in the Shizugawa–Hashiura Subbelt consists of the Hashiura and Jusanhamama groups, in ascending order (Fig. 2). The Hashiura Group in the northern part of the subbelt is subdivided into the Aratozaki, Arato, and Sodenohama formations (Mabuti, 1933; Matsumoto, 1953), whereas the strata correlative with the Aratozaki and Arato formations are called the Nakahara and Nagao formations, respectively, in the southern part of the subbelt (Mori, 1949; Kase, 1979). The Aratozaki Formation consists mainly of coarse quartz-feldspathic sandstone with some intercalations of conglomerate, and yields marine bivalves such as *Inoceramus morii* and *Vaugonia yokoyamai* (Hayami, 1961). The Arato Formation consists mainly of bedded black mudstone with interbedded mudstone and sandstone in its basal part. The Arato and Nagao formations yield abundant ammonoids such as Bajocian *Stephanoceras hashiuraense* and *Cadomites bandoi*, Callovian *Kepplerites mabutii*, and Oxfordian–Kimmeridgian *Kranaosphinctes cf. matsushima* and *Taramelliceras* sp. (Sato, 1962; Takahashi, 1969; Kase, 1979). Among these, *Kepplerites* is a typical boreal genus, whereas *Kranaosphinctes* is a Tethys–Pacific genus (Bando et al., 1987). Kase (1979) also reported from the uppermost part of the Nagao Formation a poorly-preserved ammonoid belonging to Olcostephanidae or Berriassellidae, and suggested that the horizon may be of Tithonian or younger age. The Sodenohama Formation consists of massive sandstone and interbedded sandstone and mudstone, and yields Kimmeridgian (Takahashi, 1969) or Tithonian ammonoids (Matsumoto, 1953). The Jusanhamama Group occurs only in the southern part of the subbelt and is subdivided into Yoshihama, Tategami, and Tsukihama formations, in ascending order (Mori, 1949; Kase, 1979). The Yoshihama and Tsukihama formations consist mostly of quartz-feldspathic sandstone, whereas the Tategami Formation consists of interbedded quartz-feldspathic sandstone and bituminous mudstone (Kase, 1979). Endemic species of such bivalve genus as *Filosina* and *Protocardia* occur in the Tategami Formation (Hayami, 1960), and Tashiro and Kozai (1989) pointed out that *Protocardia*

characterizes the Nankai Fauna, a southern Tethyan fauna occurring restrictively in the Kurosegawa and Southern Chichibu belts of the Outer Zone of Southwest Japan. Considering the age of the underlying Hashiura Group, the Jusanhamama Group is likely of Tithonian–Early Cretaceous age.

Middle Jurassic to Lower Cretaceous strata in the Karakuwa area, northern part of the Karakuwa–Oshika Subbelt

The Middle Jurassic to Lower Cretaceous strata in the Karakuwa area, northern part of the Karakuwa–Oshika Subbelt, are the Karakuwa and Oshima groups, in ascending order (Fig. 2). The Karakuwa Group is subdivided into the Kosaba, Tsunakizaka, Ishiwaritoge, Mone, Kogoshio, and Isokusa formations in ascending order (Shiida, 1940; Hayami, 1961), whereas the Oshima Group consists of the Kanaegaura and Yokonuma formations, in ascending order (Onuki, 1969).

Middle Jurassic to Lower Cretaceous strata in the Oshika area, southern part of the Karakuwa–Oshika Subbelt

The Middle Jurassic to Lower Cretaceous strata in the Oshika area, southern part of the Karakuwa–Oshika Subbelt, are the Oshika Group (Onuki, 1956) and Yamadori Formation (Inai and Takahashi, 1940), in ascending order (Fig. 2). The Oshika Group is subdivided into the Tsukinoura, Oginohama and Ayukawa formations, in ascending order (Takizawa et al., 1974; Takizawa, 1985). The Tsukinoura Formation consists of the lower sandstone and upper mudstone members. The upper part of the lower member yields ammonoids such as *Stephanoceras cf. plicatissimum* and *Normannites (Itinsaites)* sp. and is correlated with the *Otoites sauzei* and/or *Stephanoceras humphriesianum* zones of the European Middle Bajocian (Sato, 1972). The member also yields rich bivalves such as *Trigonia sumiyagura* and *Vaugonia kodaijimensis* (Hayami, 1961). The Oginohama Formation, consisting of sandstone and interbedded sandstone and mudstone with some layers of conglomerate, is subdivided into the Kitsunezaki Sandstone and Shale, Makinohama Sandstone, Kozumi Shale and Fukiura Shale and Sandstone members, in ascending order (Takizawa et al., 1974). The upper part of the Kozumi Shale Member yields late Oxfordian ammonoids such as *Perisphinctes (Perisphinctes) ozikaensis* and *Perisphinctes (Kranaosphinctes) cf. matsushima* and early Kimmeridgian ammonoids such as *Discosphinctes cf. kiritaniensis*, *Lithacoceras onukii*, and *Aulacostephanus (Pararasenia)* sp. (Fukada, 1950; Sato, 1962; Takahashi, 1969). The Fukiura Shale and Sandstone Member yields Tithonian ammonoids such as *Virgatosphinctes aff. communis* and *Aulacosphinctoides?* sp. (Takahashi, 1969; Takizawa et al., 1974). Further, abundant plant fossils belonging to the Ryoseki Flora occur from the upper part of each member (Kimura and Ohana, 1989). The Ayukawa Formation, consisting of quartz-feldspathic sandstone and mudstone, is subdivided into the Kiyosaki Sandstone, Kobitawatashi Sandstone and Shale, Futawatashi Shale, and Domeki Sandstone members, in ascending order (Takizawa et al., 1974). The lower part of the Kobitawatashi Sandstone Member yields Berriasian ammonoids such as *Berriasella* sp. (Takizawa, 1970), whereas the upper

part of the member and the upper part of the Futawatashi Shale Member yield Valanginian ammonoids such as *Thurmanniceras cf. isokusense*, *Kilianella* sp., and *Lyticoceras* sp. (Takizawa, 1970; Obata, 1988). The Yamadori Formation consists of andesitic to dacitic pyroclastic rocks and overlying basaltic lava and pyroclastic rocks (Takizawa et al., 1974).

Lower Cretaceous strata of the Ofunato Subbelt

The Ofunato Subbelt is mostly occupied by the Lower Cretaceous Ofunato Group, which is subdivided into the Hakoneyama, Funagawara, Hijochi, Kobosoura, and Takonoura formations, in ascending order (Onuki and Mori, 1961; Fig. 2). Among them, the Hakoneyama Formation, consisting mostly of volcanic conglomerate, has been interpreted to be a southern extension of the Upper Triassic Myojinmae Formation (Kanagawa and Ando, 1983).

SAMPLE DESCRIPTIONS

We studied the following 16 sandstone samples and examined their provenances from the age-distribution of detrital zircons. Here follow the descriptions of studied samples summarized in Fig. 3.

Silurian Nameirizawa Formation (Sample 08331-9; N39°32'55.8", E141°20'20.2")

Sample 08331-9 of the Silurian Nameirizawa Formation was collected from the middle part of the formation along the Nameirizawa River, Hanamaki City, Iwate Prefecture (Fig. 1). The sandstone sample was of medium to fine feldspathic wacke, with the matrix volume of a little more than 15%. The sandstone was angular and ill-sorted. The zircon grains were mostly abraded and anhedral, having columnar shapes with the longer dimension of 90–180 µm and the shorter dimension of 50–100 µm. Most of the zircons showed oscillatory zoning in cathodoluminescence (CL) images, a common feature of igneous zircons (Corfu et al., 2003), although few zircons were homogeneous or had metamorphic rim.

Silurian Yakushigawa Formation (Sample 08331-3; N39°32'06.8", E141°37'30.5")

Sample 08331-3 of the Silurian Yakushigawa Formation was collected from the lower part of the formation along the upper stream of the Yakushigawa River, Miyako City, Iwate Prefecture (Fig. 1). The sandstone sample was of angular and ill-sorted, fine feldspathic wacke. Although quartz veins with the width of 1 mm or less sparsely cut the sample, no zircons have been microscopically detected in it. More than half of the zircon grains we collected were abraded and the others were euhedral. The zircon grains generally had columnar shapes with the longer dimension of 50–200 µm and shorter dimension of 50–90 µm. Most of the zircons showed oscillatory zoning in CL images although few zircons were homogeneous or had a detritus core.

Devonian Tobigamori Formation (Sample 08429-5; N39°04'02.0", E141°14'37.0")

Sample 08429-5 of the Tobigamori Formation was collected from the Lower Member of the formation along the Natsuyama Logging Road, Ichinoseki City, Iwate Prefecture (Fig. 1). The sandstone sample was of very ill-sorted, angular, medium lithic wacke. Two thirds of the zircon grains we collected were euhedral and the others were abraded. Most of the zircon grains had columnar shape with the longer dimension of 70–220 µm and the shorter dimension of 50–100 µm. Most of the zircons showed oscillatory zoning in CL images although few zircons had metamorphic rim and few abraded zircons were homogeneous.

Lower Carboniferous Karaumestate Formation (Sample 120611-2; N39°0'25.10", E141°15'57.06")

Sample 120611-2 of the Lower Carboniferous Karaumestate Formation was collected approximately 50 m above the base of the formation, 1 km to the east of Mt. Karaumestateyama, Ichinoseki City, Iwate Prefecture (Fig. 1). The sandstone sample was of angular and ill-sorted, fine to medium lithic wacke. Nearly half of the zircon grains we collected were colorless and the others were brown. 80% of the zircon grains were euhedral and had columnar shapes with the longer dimension of 70–200 µm, the shorter dimension of 40–100 µm, and aspect ratio of 1.5–2.5. The other zircon grains, all brown colored, were abraded and had anhedral shapes. Larger zircon grains tended to have inclusions and microcracks. Most of the zircons showed oscillatory zoning in CL images.

Lower Permian Nishikori Formation (Sample 120611-8; N38°41'14.17", E141°17'24.39")

Sample 120611-8 of the Lower Permian Nishikori Formation was collected 20 m below the top of the formation along the lower stream of the Kitakamigawa River, Tome City, Miyagi Prefecture (Fig. 1). The sandstone sample was of ill-sorted, rounded to sub-rounded, medium- to coarse-grained lithic sandstone. The lithic fragments were mostly of volcanic rocks having plagioclase phenocrysts, with few polycrystalline quartz grains. Most of the zircon grains we collected were euhedral and colorless, having columnar shapes with the longer dimension of 70–400 µm, the shorter dimension of 40–200 µm, and the aspect ratio of 1.5–2. Most of them showed oscillatory zoning in CL images, and larger zircon grains tended to contain many inclusions.

Upper Permian Toyoma Formation (Sample 101001-1; N38°48'02.3", E141°33'04.0")

Sample 101001-1 of the Upper Permian Toyoma Formation was collected from the uppermost part of the formation along the Maehama Coast, Kesennuma City, Miyagi Prefecture (Fig. 1).

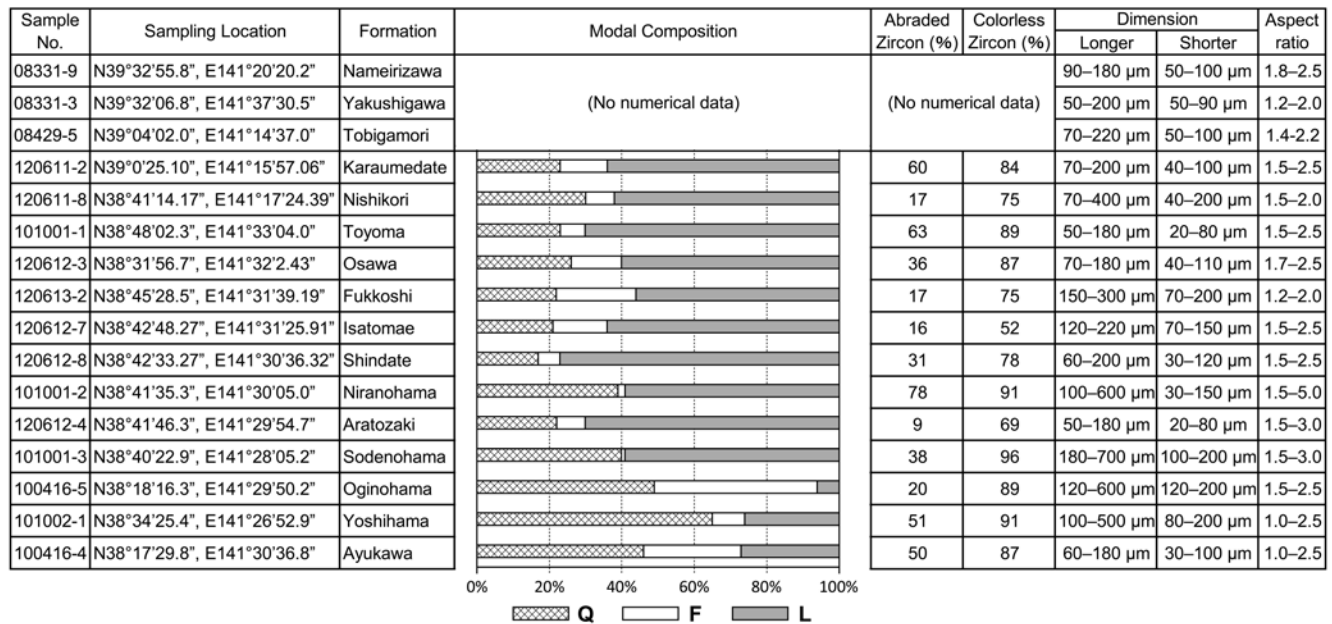


FIGURE 3. Diagram summarizing the sample description. Abbreviations—F: feldspars, L: lithic fragments, Q: single quartz.

The sandstone sample was of ill-sorted, sub-angular, and fine- to medium-grained lithic arenite. The zircon grains we collected were mostly euhedral and not abraded, among which 80% were colorless and the others were brown. The zircon grains had columnar shapes with the longer dimension of 50–180 µm, the shorter dimension of 20–80 µm, and the aspect ratio of 1.5–2.5. Most of them showed oscillatory zoning in CL images, and larger zircon grains tended to contain many inclusions and microcracks.

Lower Triassic Osawa Formation (Sample 120612-3; N38°31'56.7", E141°32'2.43")

Sample 120612-3 of the Lower Triassic Osawa Formation of the Inai Group was collected from the middle part of the formation on the east side of the Arahma Beach, Ishinomaki City, Miyagi Prefecture (Fig. 1). The sandstone sample was of well-sorted, sub-angular to sub-rounded, and fine- to medium-grained lithic arenite. The zircon grains we collected were mostly euhedral to subhedral and colorless, having columnar shapes with the longer dimension of 70–180 µm, the shorter dimension of 40–110 µm, and the aspect ratio of 1.7–2.5. All of them showed oscillatory zoning in CL images, and larger zircon grains tended to contain many inclusions and microcracks.

Middle Triassic Fukkoshi Formation (Sample 120613-2; N38°45'28.5", E141°31'39.19")

Sample 120613-2 of the Lower Triassic Fukkoshi Formation

was collected from the middle part of the formation along the Kesaiso Coast, Kesenuma City, Miyagi Prefecture (Fig. 1). The sampling horizon was 120 m below the top of the formation. The sandstone sample was of moderately-sorted, angular to sub-angular, and medium- to coarse-grained lithic arenite. The collected zircon grains were euhedral to subhedral and colorless, having columnar shapes with the longer dimension of 150–300 µm, the shorter dimension of 70–200 µm, and the aspect ratio of 1.2–2.0. Most of them showed oscillatory zoning in CL images, and few zircon grains contained inclusions and/or microcracks.

Middle Triassic Isatomae Formation (Sample 120612-7; N38°42'48.27", E141°31'25.91")

Sample 120612-7 of the Middle Triassic Isatomae Formation of the Inai Group was collected from the middle part of the formation along the coast on the northeast of Cape Bentenzaki, Minamisanriku Town, Miyagi Prefecture (Fig. 1). The sampling horizon was a little more than 500 m below the base of the Upper Triassic Saragai Group. The sandstone sample was of poorly- to moderately-sorted, angular to sub-angular, and medium-grained lithic arenite. The Isatomae sandstone is characterized by the lower content of volcanic-rock fragments and inclusion of K-feldspar grains. The zircon grains we collected were euhedral to subhedral and virtually not abraded, among which 70% were colorless and the others were brown. The zircon grains had columnar shapes with the longer dimension of 120–220 µm, the shorter dimension of 70–150 µm, and the aspect ratio of 1.5–2.5. Most of them showed oscillatory zoning in CL images,

and larger zircon grains tended to contain many inclusions and microcracks.

Upper Triassic Shindate Formation (Sample 120612-8; N38°42'33.27", E141°30'36.32")

Sample 120612-8 of the Upper Triassic Shindate Formation of the Saragai Group was collected from the horizon several meters below the top of the formation near the bottom of the Saragaizaka Slope, Minamisanriku Town, Miyagi Prefecture (Fig. 1). The Shindate Formation at this location, conformably lying beneath the Carnian–Norian Chonomori Formation, is probably of Carnian age. The sandstone sample was of moderately- to well-sorted, angular, and fine lithic arenite. The zircon grains we collected were mostly euhedral to subhedral and virtually not abraded, among which 90% were colorless and the others were brown. The zircon grains had columnar shapes with the longer dimension of 60–200 µm, the shorter dimension of 30–120 µm, and the aspect ratio of 1.5–2.5. Most of them showed oscillatory zoning in CL images, and larger zircon grains tended to contain many inclusions and microcracks.

Lower Jurassic Niranozama Formation (Sample 101001-2; N38°41'35.3", E141°30'05.0")

Sample 101001-2 of the Lower Jurassic Niranozama Formation of the Shizugawa Group was collected from the upper part of the formation (Fig. 1), the Niranozama or Hoinyashiki sandstone of Kobayashi and Mori (1955) and Takahashi (1969). The Niranozama Sandstone at this location is probably of Middle Hettangian age, because an ammonoid of this age, *Alsatis (Yebisites) onoderai*, was reported from the same sandstone close to this location (Matsumoto, 1956). The sandstone sample was of well-sorted, sub-angular, and very fine- to fine-grained feldspathic arenite. Most of the zircon grains we collected were euhedral and colorless, having columnar shapes with the longer dimension of 100–600 µm, the shorter dimension of 30–150 µm, and the aspect ratio of 1.5–5.0. Most of them showed oscillatory zoning in CL images, and larger zircon grains tended to contain many inclusions and microcracks.

Middle Jurassic Aratozaki Formation (Sample 120612-4; N38°41'46.3", E141°29'54.7")

Sample 120612-4 of the Middle Jurassic Aratozaki Formation of the Hashiura Group was collected from the horizon approximately 10 m above the base of the formation (Fig. 1) and is probably of Aalenian–Bajocian age. The sandstone sample was of ill-sorted, sub-angular, and fine- to medium-grained lithic arenite. The zircon grains we collected were mostly euhedral, among which 80% were colorless and the others were brown. The zircon grains had columnar shapes with the longer dimension of 50–180 µm, the shorter dimension of 20–80 µm, and the aspect ratio of 1.5–3.0. Most of them showed oscillatory zoning in CL images, and many zircon grains contained

inclusions and microcracks.

Upper Jurassic Sodenohama Formation (Sample 101001-3; N38°40'22.9", E141°28'05.2")

Sample 101001-3 of the Upper Jurassic Sodenohama Formation of the Hashiura Group was collected from the middle part of the formation on the coast near the Sodenohama Beach, 2 km to ESE from the center of the Minamisanriku Town, Miyagi Prefecture (Fig. 1). The Sodenohama Formation at this location is probably of Kimmeridgian age (Takahashi, 1969). The sandstone sample was of moderately-sorted, sub-angular to subrounded, and fine-grained lithic arenite. The zircon grains we collected were mostly euhedral to anhedral and colorless, having columnar shapes with the longer dimension of 180–700 µm, the shorter dimension of 100–200 µm, and the aspect ratio of 1.5–3.0. Most of them showed oscillatory zoning in CL images, and many zircon grains contained inclusions and microcracks.

Upper Jurassic Oginozama Formation (Sample 100416-5; N38°18'16.3", E141°29'50.2")

Sample 100416-5 of the Upper Jurassic Oginozama Formation of the Oshika Group was collected from the Fukiura Shale and Sandstone Member at the eastern end of the Kukunarihama Beach, Ishinomaki City, Miyagi Prefecture (Fig. 1), and is probably of Tithonian age. The sandstone sample was of ill-sorted, sub-angular, and fine- to medium-grained lithic arenite. The lithic fragments were mostly volcanic-rock fragments with minor polycrystalline quartz grains. The zircon grains we collected were euhedral or subhedral and virtually not abraded, among which 80% were colorless and the others were brown. The zircon grains had columnar shapes with the longer dimension of 120–600 µm, the shorter dimension of 120–200 µm, and the aspect ratio of 1.5–2.5. All of them showed oscillatory zoning in CL images and contained inclusions and microcracks.

Lower Cretaceous Yoshihama Formation (Sample 101002-1; N38°34'25.4", E141°26'52.9")

Sample 101002-1 of the Lower Cretaceous Yoshihama Formation of the Jusanhama Group was collected from the upper part of the formation at Jusanhama-Tsukihama, Ishinomaki City, Miyagi Prefecture (Fig. 1). The sandstone sample was of well-sorted, sub-angular, and fine-grained feldspathic arenite. The zircon grains we collected were mostly euhedral, among which 90% were colorless and the others were brown. The zircon grains had columnar shapes with the longer dimension of 100–500 µm, the shorter dimension of 80–200 µm, and the aspect ratio of 1.0–2.5. Most of them showed oscillatory zoning in CL images, and approximately 20% of these zircon grains, larger ones in particular, contained inclusions and microcracks.

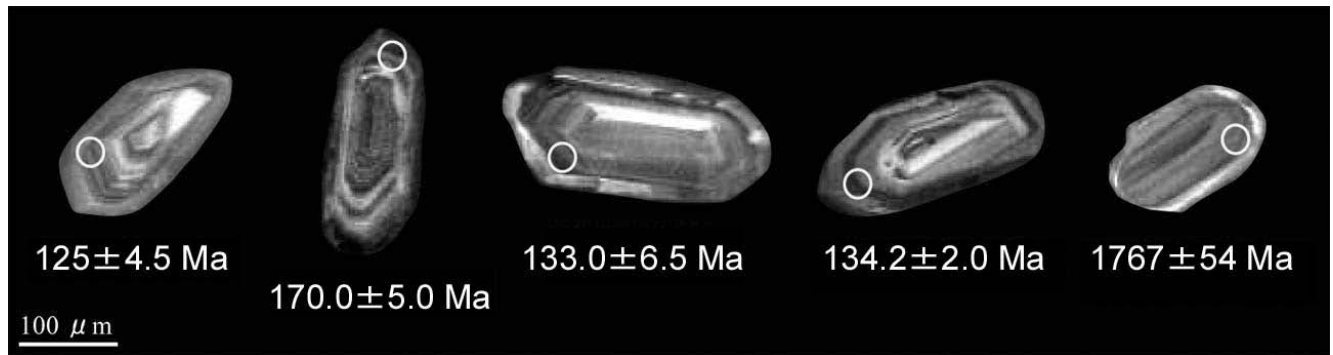


FIGURE 4. Cathodoluminescence images of some zircons from the Domeki Sandstone Member of the Ayukawa Formation, Oshika Group (sample 100416-4).

Lower Cretaceous Ayukawa Formation (Sample 100416-4; N38°17'29.8", E141°30'36.8")

Sample 100416-4 of the Lower Cretaceous Ayukawa Formation of the Oshika Group was collected from the Domeki Sandstone Member at the southeastern end of Ayukawa Port (Fig. 1), and must be of Valanginian or younger age. The sandstone sample was of ill-sorted, angular, and very coarse- to coarse-grained lithic wacke. The lithic fragments were mainly polycrystalline quartz grains with some volcanic-rock fragments. The zircon grains we collected were mostly euhedral, among which 90% were colorless and the others were brown. The zircon grains had columnar shapes with the longer dimension of 60–180 μm , the shorter dimension of 30–100 μm , and the aspect ratio of 1.0–2.5. Most of them showed oscillatory zoning in CL images (Fig. 3), and approximately 20% of these zircon grains, larger ones in particular, contained inclusions and microcracks.

ANALYTICAL METHOD

The zircon samples for analyses were prepared in accordance with the procedures described in Kawagoe et al. (2012). The measurement was carried out on laser ablation inductively coupled plasma mass spectrometers (LA-ICPMS) equipped in the (1) Department of Earth and Planetary Sciences, Graduate School of Science and Engineering, Tokyo Institute of Technology (TITech; former Hirata Laboratory), (2) Earthquake Research Institute of the University of Tokyo (ERI), and (3) Graduate School of Environmental Studies, Nagoya University (NU).

The ICPMS instrument equipped in TITech was a Thermo Electron VG Plasma Quad 2 quadropole-based ICPMS applied with a chicane-type ion lens system and connected with a MicroLas GeoLas 200CQ laser ablation system, which utilizes 193 nm wave-length ArF excimer laser (Iizuka and Hirata, 2004). The measurement conditions were as follows: the ablation pit size of 16–32 μm , energy density of 7–8 J/cm^2 , and

pulse repetition rate of 5–10 Hz. The analyses were carried out in a peak-jumping mode and the peaks of ^{202}Hg , ^{206}Pb , ^{207}Pb , ^{208}Pb , ^{232}Th , and ^{238}U were monitored. Data were acquired in sequences of 30 analyses, consisting of an analysis of gas blank, 4 NIST (National Institute of Standards and Technology, U.S.A.) SRM 610 glass standard, 4 standard zircon (91500 zircon with the $^{206}\text{Pb}/^{238}\text{U}$ age of 1062.4 ± 0.4 Ma; Wiedenbeck et al., 1995), 1 gas blank, 10 unknown, 4 SRM 610 standard, 4 91500 zircon, and 1 gas blank.

The ICPMS instrument equipped in ERI was a Thermo Elemental Plasma Quad 3 quadropole-based ICPMS connected with a New Wave UP-213 LA system, which used the frequency quintupled Nd-YAG 213-nm wavelength (Orihashi et al., 2008). The measurement conditions were as follows: the ablation pit size of 30 μm , energy density of 11–13 J/cm^2 , and pulse repetition rate of 10 Hz. The analyses were carried out in a peak-jumping mode and the peaks of ^{202}Hg , ^{206}Pb , ^{207}Pb , ^{208}Pb , ^{232}Th , and ^{238}U were monitored. Data were acquired in sequences of 28 analyses, consisting of 5 analyses of gas blank, 4 SRM 610 glass standard, 1 standard zircon (91500 zircon), 9 unknown, 4 SRM 610 standard, and 5 gas blank.

The ICPMS instrument equipped in NU was an Agilent 7700x quadropole-based ICPMS connected with a New Wave Research NWR-213-type LA system, which used the frequency quintupled Nd-YAG 213-nm wavelength. The measurement conditions, optimized to reduce matrix effects, were as follows: energy density of 11.7 J/cm^2 , pulse repetition rate of 10 Hz, pre-ablation time of 8 s, ablation time of 10 s, and the ablation pit size of 25 μm (Kouchi et al., 2012). The analyses were carried out in a peak-jumping mode and the peaks of ^{202}Hg , ^{206}Pb , ^{207}Pb , ^{208}Pb , ^{232}Th , and ^{238}U were monitored. Data were acquired in the same sequences with the ERI system.

Analytical bias among three laboratories was tested by using OD-3 zircon standard. The bias was within the range of their analytical errors (Iwano et al., 2013) and is neglected in the following discussion.

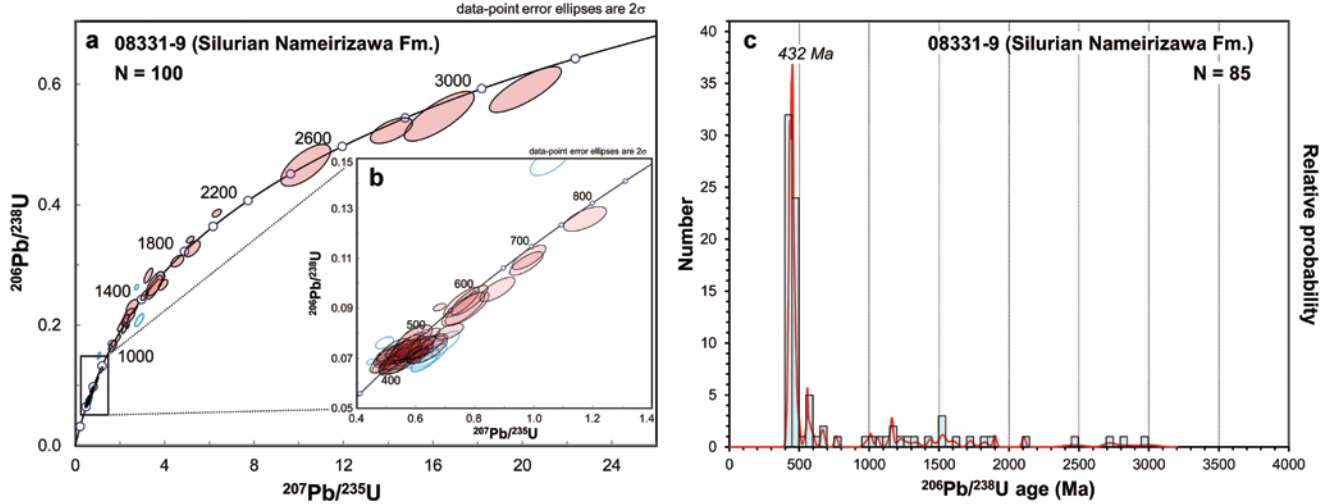


FIGURE 5. Analytical data of detrital zircons from sandstone of the Silurian Nameirizawa Formation (sample 08331-9). **a**, Concordia diagram for all data; **b**, Concordia diagram for 850–350 Ma data set; **c**, Probability density plot and histogram. Open (blue) circles in the concordia diagrams from Fig. 5 to Fig. 20 show the analytical data for discordant grains. Abbreviations(Figs. 5–20)—Fm.: Formation, N: total number of analyses.

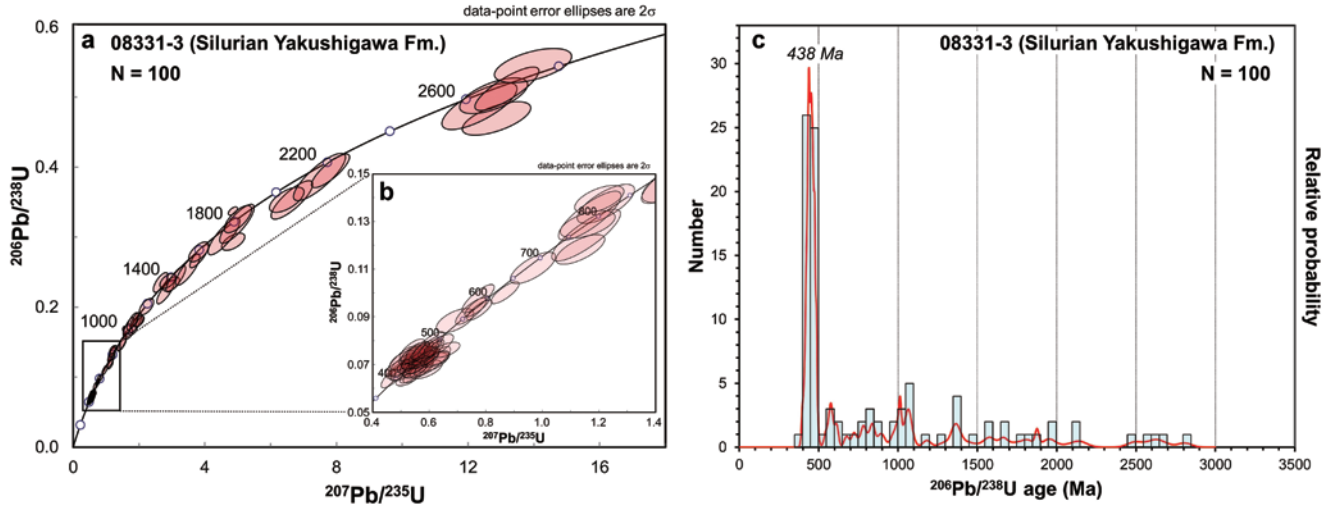


FIGURE 6. Analytical data of detrital zircons from sandstone of the Silurian Yakushigawa Formation (sample 08331-3). **a**, Concordia diagram for all data; **b**, Concordia diagram for 850–350 Ma data set; **c**, Probability density plot and histogram.

RESULTS

We sampled an outer part (rim or mantle) of collected zircon grains with the laser ablation technique, and analyzed with an ICPMS. After the analyses we first distinguished age clusters on a concordia diagram. Then we chose grains with the % conc value ($(100 \cdot ({}^{206}\text{Pb}/{}^{238}\text{U} \text{ age}) / ({}^{207}\text{Pb}/{}^{235}\text{U} \text{ age}))$) between 90 and 110 and drew a probability density plot and a histogram with the data interval of 50 Myr (${}^{206}\text{Pb}/{}^{238}\text{U}$ age). The data processing was

carried out using the Isoplot 3.70 software (Ludwig, 2008). Here follow the results of our analyses.

Silurian Nameirizawa Formation (Sample 08331-9)

We obtained 100 analyses from 97 zircon grains collected from sample 08331-9 of the Silurian Nameirizawa Formation in TITech; we sampled the outer and inner parts of 3 zircon grains. Detrital zircons were divided into 5 age groups on the concordia

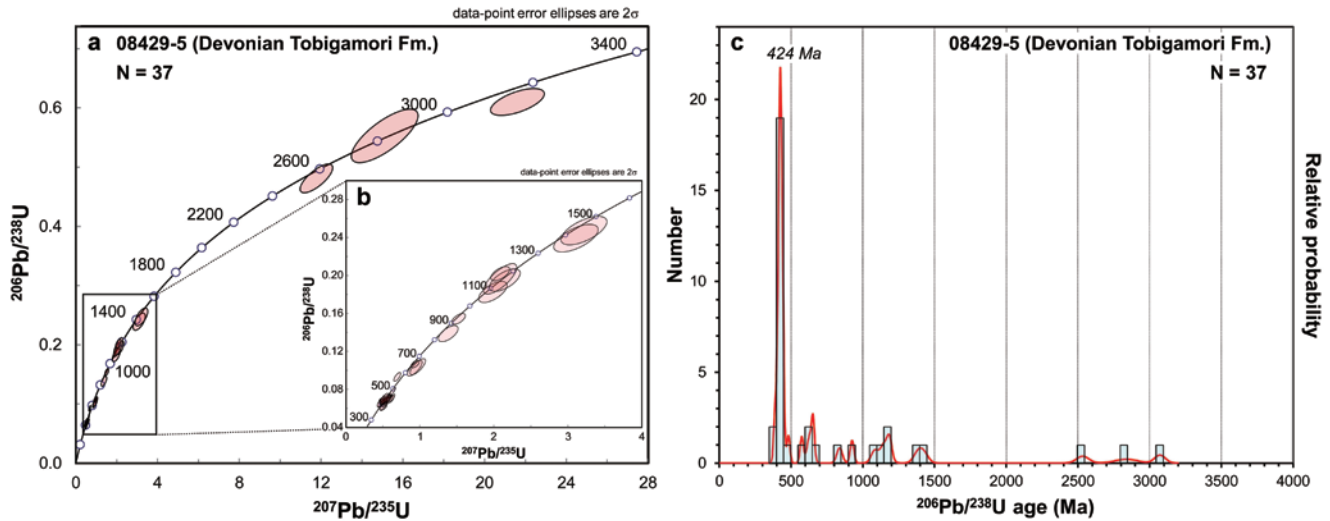


FIGURE 7. Analytical data of detrital zircons from sandstone of the Upper Devonian Tobigamori Formation (sample 08429-5). **a**, Concordia diagram for all data; **b**, Concordia diagram for 1600–300 Ma data set; **c**, Probability density plot and histogram.

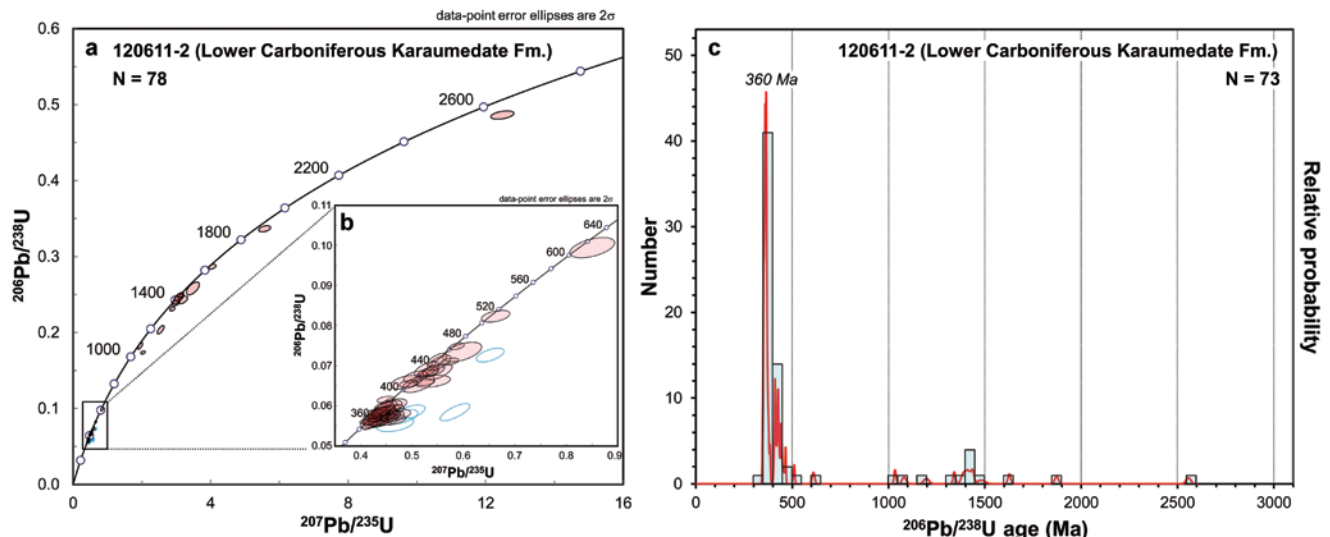


FIGURE 8. Analytical data of detrital zircons from sandstone of the Lower Carboniferous Karaumede Formation (sample 120611-2). **a**, Concordia diagram for all data; **b**, Concordia diagram for 640–320 Ma data set; **c**, Probability density plot and histogram.

diagram (Fig. 5a, b): 698–403 Ma (73%), 1087–945 Ma (4%), 1390–1111 Ma (7%), 1620–1402 Ma (5%), and 2955–2642 Ma (2%). We further chose 85 concordant grains with the % conc value between 90 and 110 and drew a probability density plot and a histogram with the data interval of 50 Myr ($^{206}\text{Pb}/^{238}\text{U}$ age; Fig. 5c). The histogram showed a multimodal pattern with the youngest concordant age of 416 ± 13 Ma (2σ) and %Pc of 36.5. The youngest peak on the probability density plot was 432 Ma. The Th/U ratio of each analysis was 0.22–2.22 and fell in

the range of igneous zircon, Th/U>0.1 (Rubatto and Hermann, 2003).

Silurian Yakushigawa Formation (Sample 08331-3)

We obtained 100 analyses from 100 zircon grains collected from sample 08331-3 of the Silurian Yakushigawa Formation in TITech. Detrital zircons were divided into 5 age groups on the concordia diagram (Fig. 6a, b): 868–385 Ma (65%), 1232–845

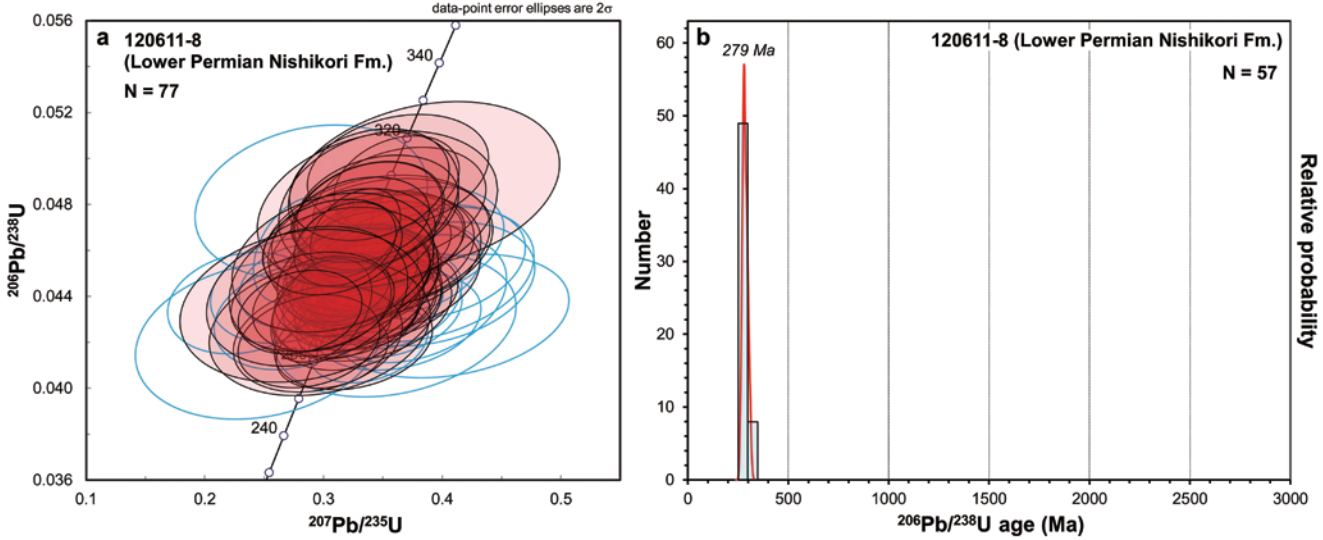


FIGURE 9. Analytical data of detrital zircons from sandstone of the Lower Permian Nishikori Formation (sample 120611-8). **a**, Concordia diagram for all data; **b**, Probability density plot and histogram.

Ma (13%), 1899–1220 Ma (13%), 2238–1845 Ma (4%), and 2891–2398 Ma (5%). All of the 100 grains had the % conc value between 90 and 110. The histogram of the $^{206}\text{Pb}/^{238}\text{U}$ ages of 100 concordant grains showed a multimodal pattern with the youngest concordant age of 398 ± 13 Ma and %Pc of 48.0. The youngest peak on the probability density plot was 438 Ma (Fig. 6c). The Th/U ratio of each analysis was 0.11–1.77 and fell in the range of igneous zircon.

Devonian Tobigamori Formation (Sample 08429-5)

We obtained 37 analyses from 37 zircon grains collected from sample 08429-5 of the Upper Devonian Tobigamori Formation in TITech. Detrital zircons were divided into 4 age groups on the concordia diagram (Fig. 7a, b): 503–367 Ma (59%), 673–589 Ma (8%), 1220–1033 Ma (11%), and 1449–1322 Ma (5%). The histogram of the $^{206}\text{Pb}/^{238}\text{U}$ ages of 37 concordant grains showed a multimodal pattern with the youngest concordant age of 386 ± 19 Ma and %Pc of 40.5. The youngest peak on the probability density plot was 424 Ma (Fig. 7c). The Th/U ratio of each analysis was 0.20–2.15 and fell in the range of igneous zircon.

Lower Carboniferous Karaumedeate Formation (Sample 120611-2)

We obtained, in ERI, 78 analyses from 78 zircon grains collected from sample 120611-2 of the Lower Carboniferous Karaumedeate Formation. Detrital zircons were divided into 3 age groups on the concordia diagram (Fig. 8a, b): 389–341 Ma (58%), 470–405 Ma (22%), and 1451–1365 Ma (7%). The histogram of the $^{206}\text{Pb}/^{238}\text{U}$ ages of 73 concordant grains showed

a multimodal pattern with the youngest concordant age of 348.9 ± 7.8 Ma and %Pc of 19.2. The youngest peak on the probability density plot was 360 Ma (Fig. 8c). The Th/U ratio of each analysis was 0.23–1.20 and fell in the range of igneous zircon.

Lower Permian Nishikori Formation (Sample 120611-8)

We obtained 77 analyses from 77 zircon grains collected from sample 120611-8 of the Lower Permian Nishikori Formation in NU. Detrital zircons formed a single cluster on the concordia diagram at 324–255 Ma (100%; Fig. 9a). The histogram of the $^{206}\text{Pb}/^{238}\text{U}$ ages of 57 concordant grains showed a unimodal pattern with the youngest concordant age of 263.0 ± 8.4 Ma and %Pc of 0. The peak on the probability density plot was 279 Ma (Fig. 9b). The Th/U ratio of each analysis was 0.31–1.16 and fell in the range of igneous zircon.

Upper Permian Toyoma Formation (Sample 101001-1)

We obtained 70 analyses from 70 zircon grains collected from sample 101001-1 of the Upper Permian Toyoma Formation in ERI (24 grains) and NU (46 grains). Detrital zircons are divided into 3 age groups on the concordia diagram (Fig. 10a, b): 374–224 Ma (78%), 468–445 Ma (3%), and 530–497 Ma (5%). The histogram of the $^{206}\text{Pb}/^{238}\text{U}$ ages of 59 concordant grains showed a quasi-unimodal pattern with the youngest concordant age of 227.8 ± 4.3 Ma and %Pc of 8.5. The youngest peak on the probability density plot was 249 Ma (Fig. 10c). The Th/U ratio of each analysis was 0.19–1.79 and fell in the range of igneous zircon.

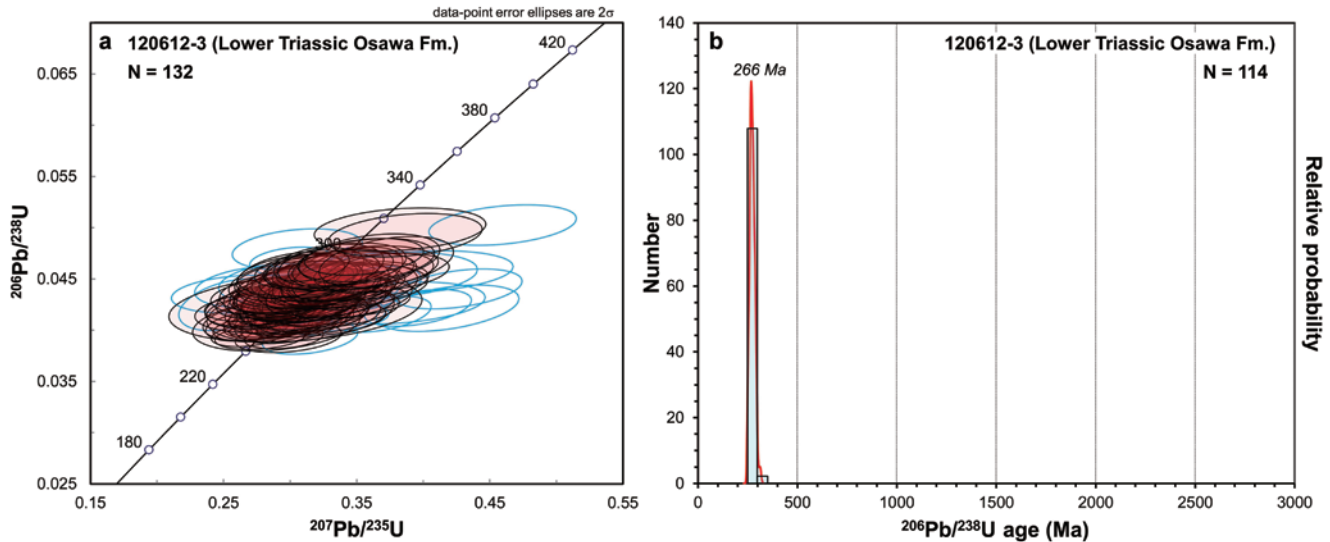


FIGURE 11. Analytical data of detrital zircons from sandstone of the Lower Triassic Osawa Formation of the Inai Group (sample 120612-3). **a**, Concordia diagram for all data; **b**, Probability density plot and histogram.

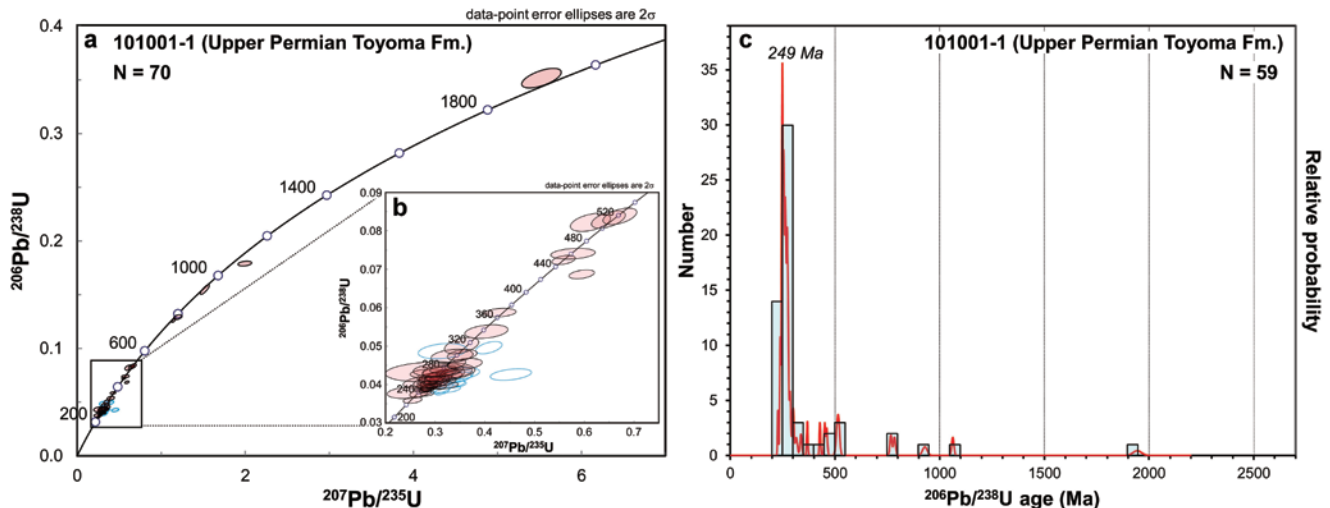


FIGURE 10. Analytical data of detrital zircons from sandstone of the Upper Permian Toyoma Formation (sample 101001-1). **a**, Concordia diagram for all data; **b**, Concordia diagram for 560–200 Ma data set; **c**, Probability density plot and histogram.

Lower Triassic Osawa Formation (Sample 120612-3)

We obtained 132 analyses from 132 zircon grains collected from sample 120612-3 of the Lower Triassic Osawa Formation of the Inai Group in NU. Detrital zircons formed a single cluster on the concordia diagram at 324–243 Ma (100%; Fig. 11a). The histogram of the $^{206}\text{Pb}/^{238}\text{U}$ ages of 114 concordant grains showed a unimodal pattern with the youngest concordant age of 248.6 ± 5.7 Ma and %Pc of 0. The youngest peak on the probability density plot was 266 Ma (Fig. 11b). The Th/U ratio of each

analysis was 0.42–1.09 and fell in the range of igneous zircon.

Middle Triassic Fukkoshi Formation (Sample 120613-2)

We obtained 107 analyses from 107 zircon grains collected from sample 120613-2 of the Middle Triassic Fukkoshi Formation of the Inai Group in NU. Detrital zircons formed a single cluster on the concordia diagram at 336–230 Ma (100%; Fig. 12a). The histogram of the $^{206}\text{Pb}/^{238}\text{U}$ ages of 90 concordant grains showed a unimodal pattern with the youngest concordant

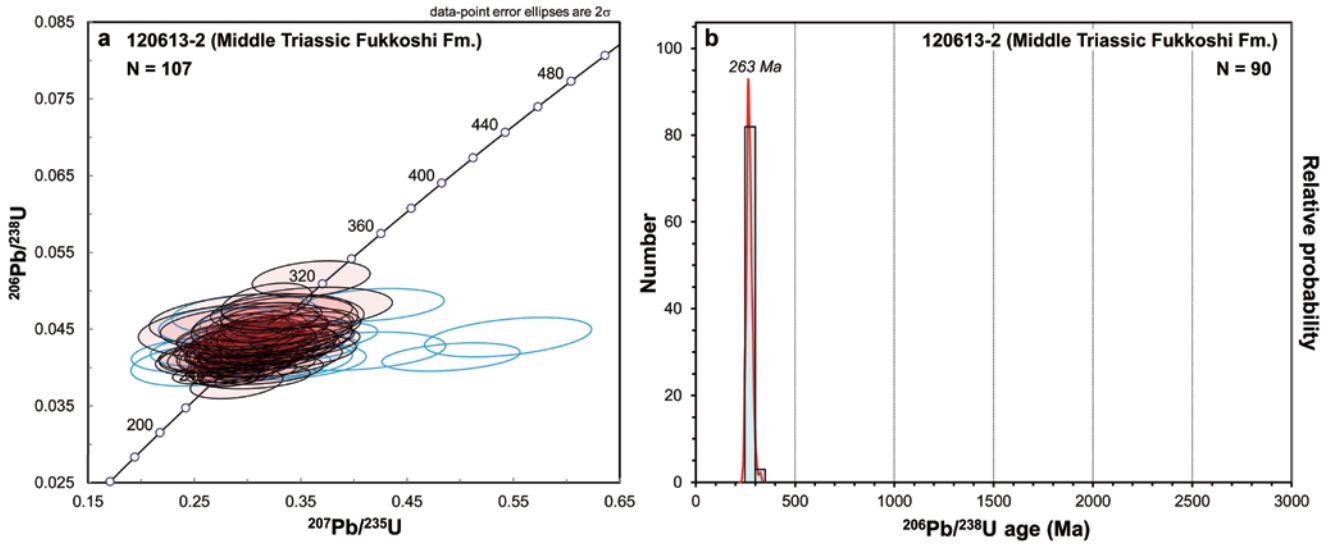


FIGURE 12. Analytical data of detrital zircons from sandstone of the Middle Triassic Fukkoshi Formation of the Inai Group (sample 120613-2). **a**, Concordia diagram for all data; **b**, Probability density plot and histogram.

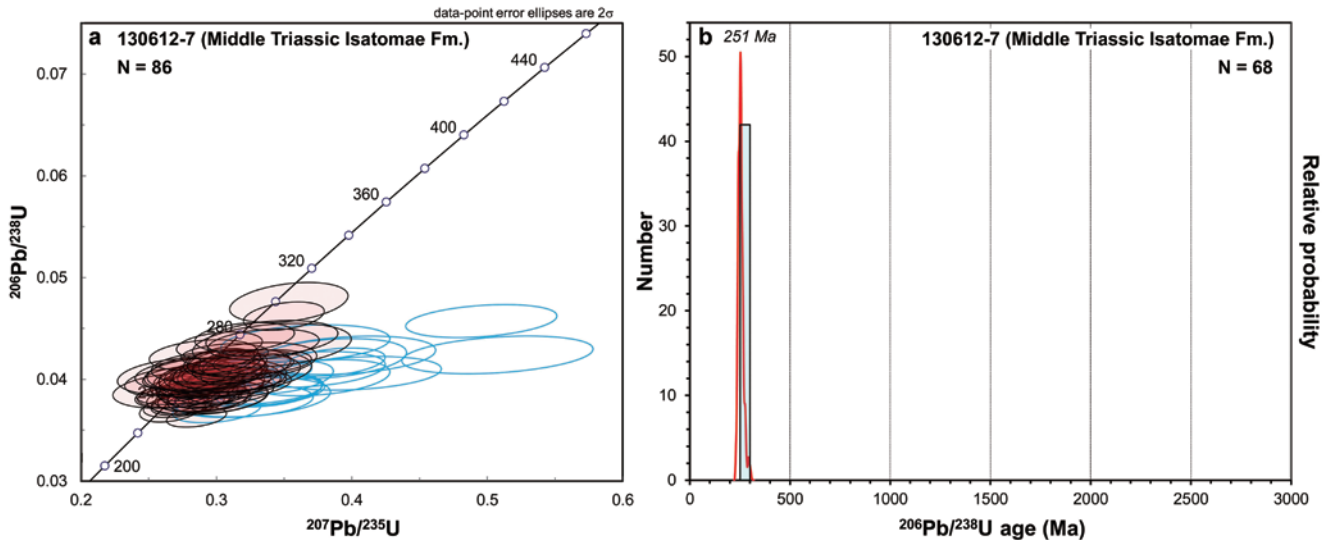


FIGURE 13. Analytical data of detrital zircons from sandstone of the Middle Triassic Isatomae Formation of the Inai Group (sample 130612-7). **a**, Concordia diagram for all data; **b**, Probability density plot and histogram.

age of 240 ± 10 Ma and %Pc of 0. The youngest peak on the probability density plot was 263 Ma (Fig. 12b). The Th/U ratio of each analysis was 0.3–0.9 and fell in the range of igneous zircon.

Middle Triassic Isatomae Formation (Sample 120612-7)

We obtained 86 analyses from 86 zircon grains collected from sample 120612-7 of the Middle Triassic Isatomae Formation

of the Inai Group in NU. Detrital zircons formed a single cluster on the concordia diagram at 310–223 Ma (100%; Fig. 13a). The histogram of the $^{206}\text{Pb}/^{238}\text{U}$ ages of 68 concordant grains showed a unimodal pattern with the youngest concordant age of 230.0 ± 5.1 Ma and %Pc of 0. The youngest peak on the probability density plot was 251 Ma (Fig. 13b). The Th/U ratio of each analysis was 0.37–1.16 and fell in the range of igneous zircon.

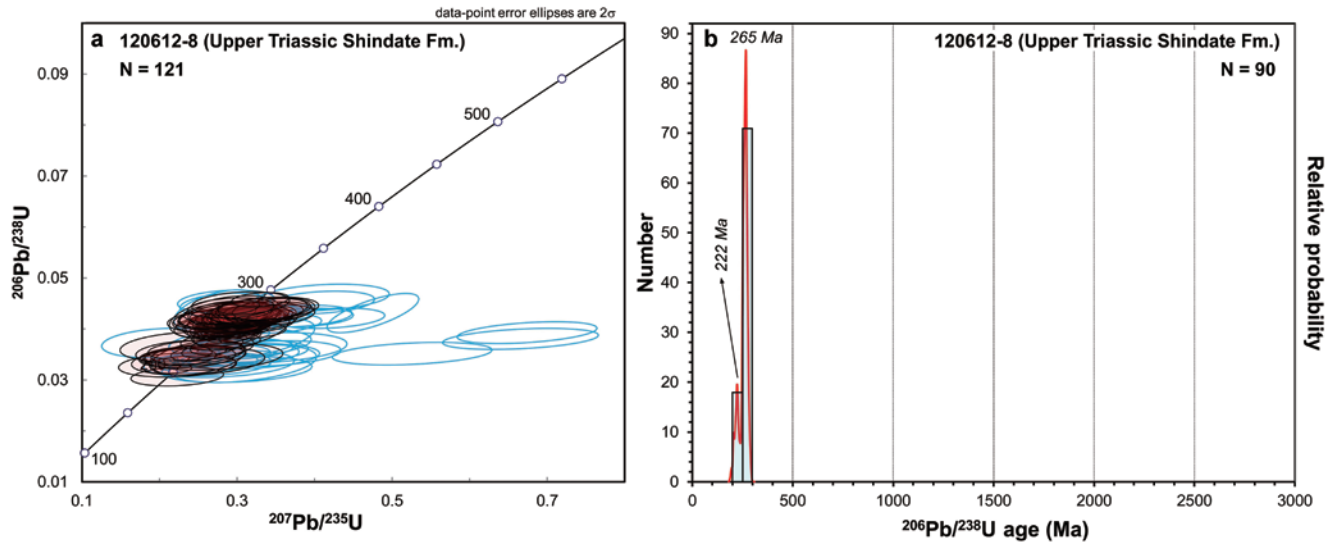


FIGURE 14. Analytical data of detrital zircons from sandstone of the Upper Triassic Shindate Formation of the Saragai Group (sample 120612-8). **a**, Concordia diagram for all data; **b**, Probability density plot and histogram.

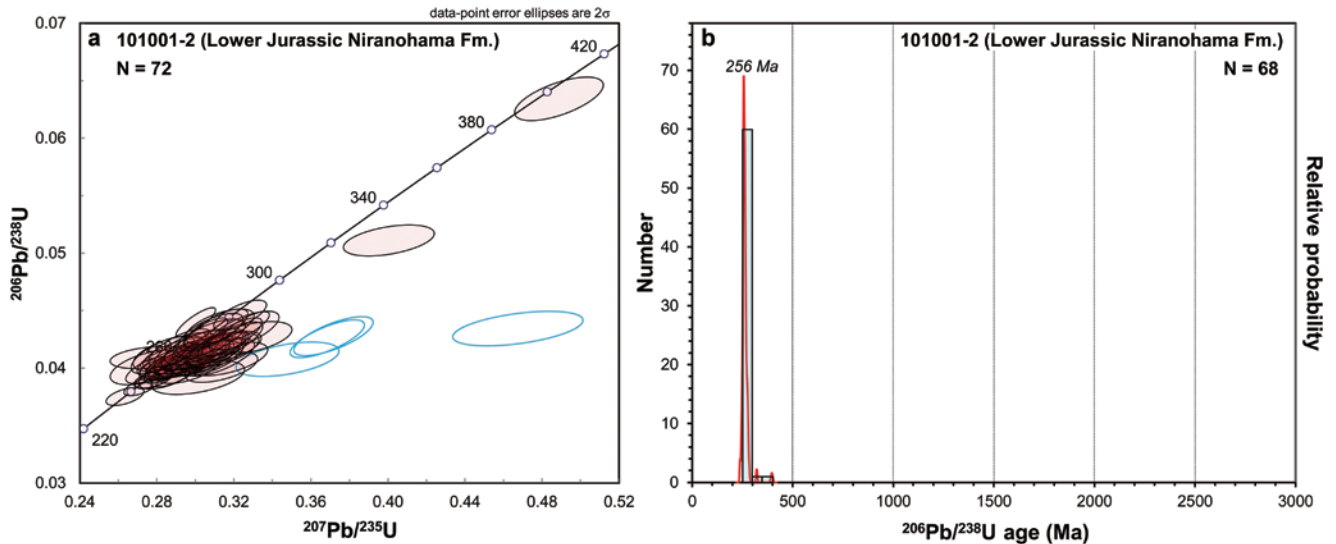


FIGURE 15. Analytical data of detrital zircons from sandstone of the Lower Jurassic Nirano-hama Formation of the Shizugawa Group (sample 101001-2). **a**, Concordia diagram for all data; **b**, Probability density plot and histogram.

Upper Triassic Shindate Formation (Sample 120612-8)

We obtained 121 analyses from 121 zircon grains collected from sample 120612-8 of the Upper Triassic Shindate Formation of the Saragai Group in NU. Detrital zircons formed a single cluster on the concordia diagram at 296–186 Ma (100%; Fig. 14a). The histogram of the $^{206}\text{Pb}/^{238}\text{U}$ ages of 90 concordant grains showed a unimodal pattern with the youngest concordant age of 195.1 ± 9.6 Ma and %Pc of 0. The youngest peak on the

probability density plot was 222 Ma (Fig. 14b). The Th/U ratio of each analysis was 0.39–1.33 and fell in the range of igneous zircon.

Lower–Middle Jurassic Nirano-hama Formation (Sample 101001-2)

We obtained 72 analyses from 72 zircon grains collected from sample 101001-2 of the Lower Jurassic Nirano-hama Formation

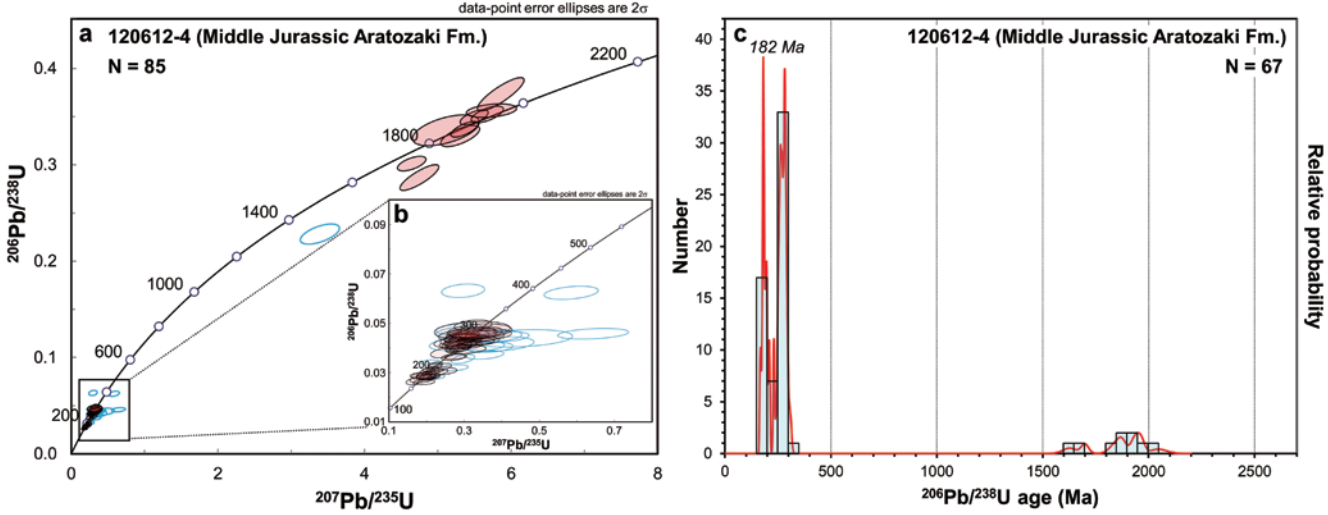


FIGURE 16. Analytical data of detrital zircons from sandstone of the Middle Jurassic Aratozaki Formation of the Hashiura Group (sample 120612-4). **a**, Concordia diagram for all data; **b**, Concordia diagram for 550–150 Ma data set; **c**, Probability density plot and histogram.

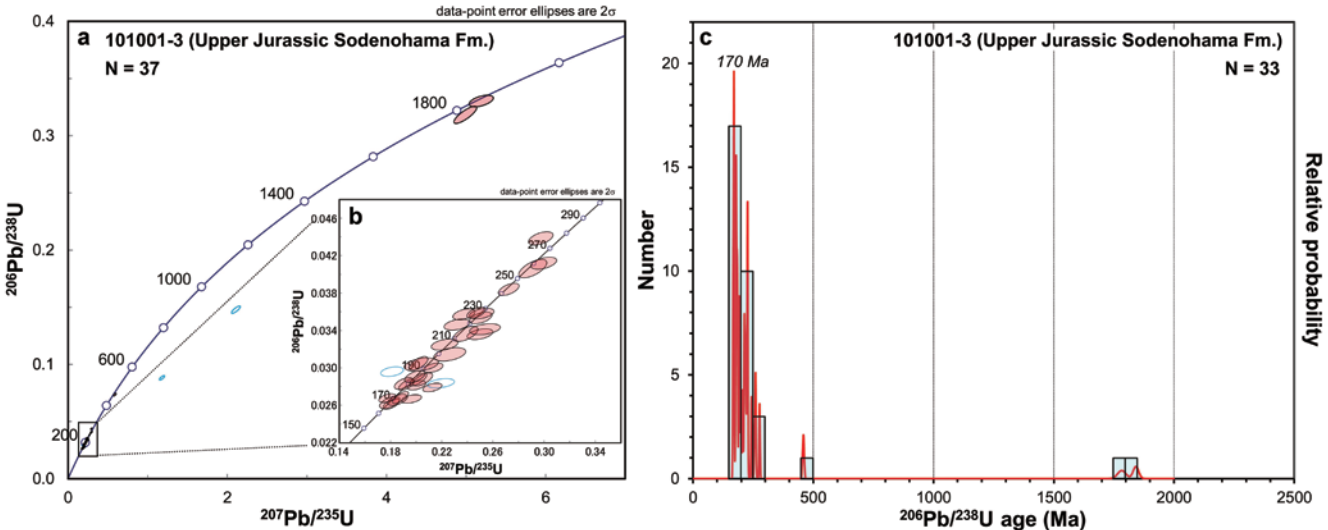


FIGURE 17. Analytical data of detrital zircons from sandstone of the Upper Jurassic Sodenohama Formation of the Hashiura Group (sample 101001-3). **a**, Concordia diagram for all data; **b**, Concordia diagram for 300–150 Ma data set; **c**, Probability density plot and histogram.

of the Shizugawa Group in ERI. Detrital zircons formed a single cluster on the concordia diagram at 288–234 Ma (100%; Fig. 15a). The histogram of the $^{206}\text{Pb}/^{238}\text{U}$ ages of 68 concordant grains showed a unimodal pattern with the youngest concordant age of 237.6 ± 4.0 Ma and %Pc of 0. The youngest peak on the probability density plot was 256 Ma (Fig. 15b). The Th/U ratio of each analysis was 0.26–1.28 and fell in the range of igneous zircon.

Middle Jurassic Aratozaki Formation (Sample 120612-4)

We obtained 85 analyses from 85 grains collected from sample 120612-4 of the lower Middle Jurassic Aratozaki Formation of the Hashiura Group in NU. Detrital zircons are divided into 3 age groups on the concordia diagram (Fig. 16a, b): 216–161 Ma (30%, 321–223 Ma (57%), and 2124–1789 Ma (10%). The histogram of the $^{206}\text{Pb}/^{238}\text{U}$ ages of 67 concordant grains showed a bimodal pattern with the youngest concordant age of $166.4 \pm$

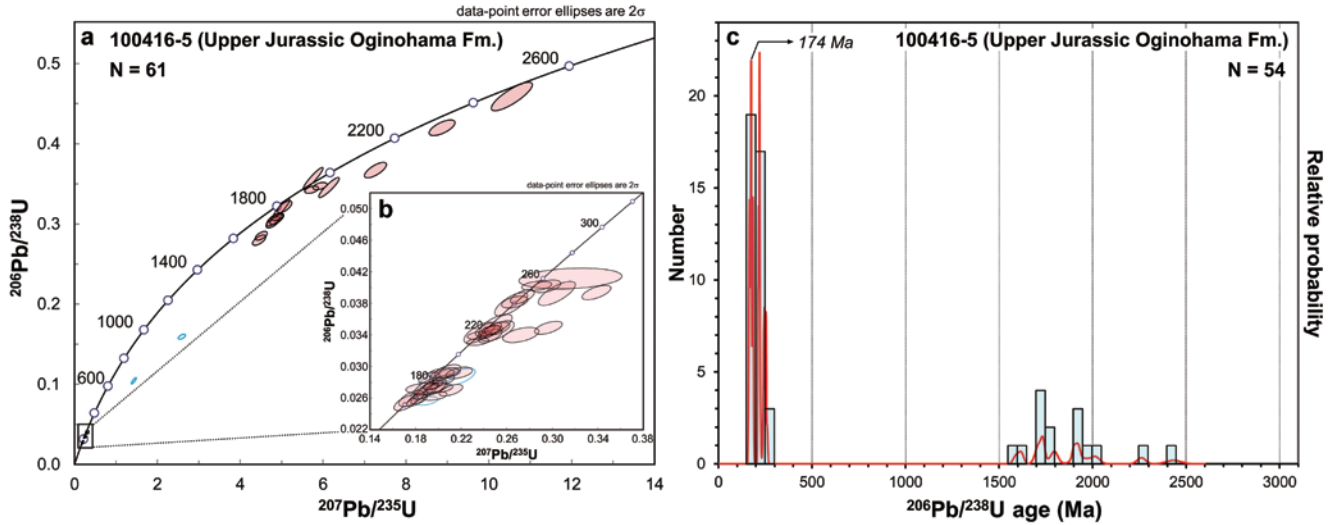


FIGURE 18. Analytical data of detrital zircons from sandstone of the Upper Jurassic Fukiura Shale and Sandstone Member of the Oginohama Formation, Oshika Group (sample 100416-5). **a**, Concordia diagram for all data; **b**, Concordia diagram for 340–150 Ma data set; **c**, Probability density plot and histogram.

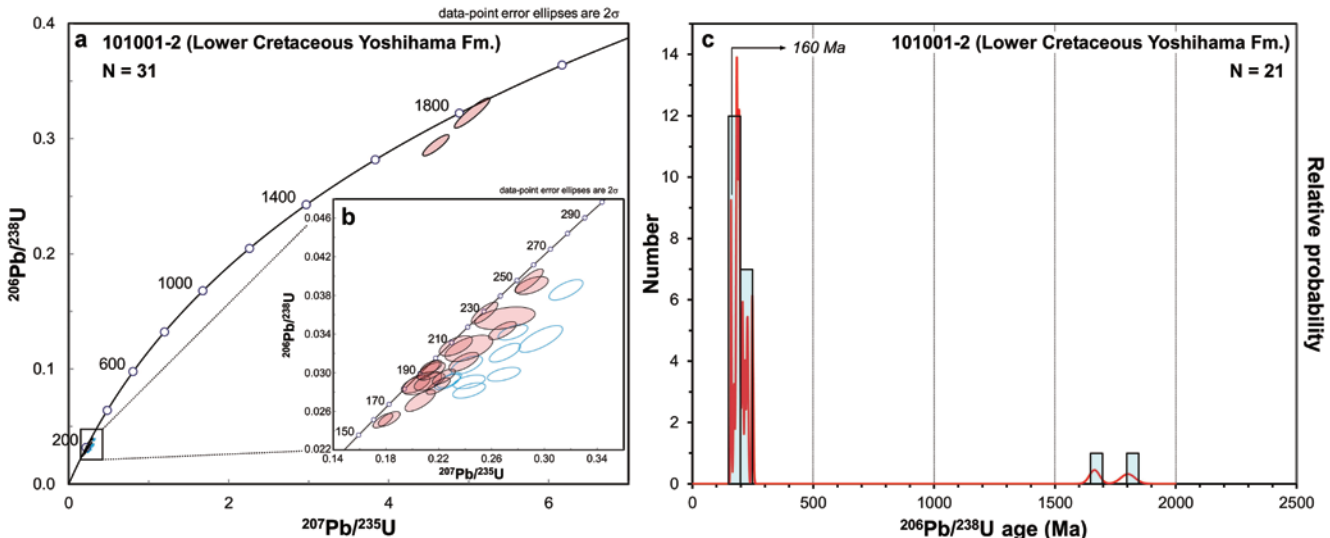


FIGURE 19. Analytical data of detrital zircons from sandstone of the Lower Cretaceous Yoshihama Formation of the Jusanhama Group (sample 101001-2). **a**, Concordia diagram for all data; **b**, Concordia diagram for 310–150 Ma data set; **c**, Probability density plot and histogram.

5.4 Ma and %Pc of 13.4. The youngest peak on the probability density plot was 182 Ma (Fig. 16c). The Th/U ratio of each analysis was 0.10–1.03 and fell in the range of igneous zircon.

Upper Jurassic Sodenohama Formation (Sample 101001-3)

We obtained 37 analyses from 37 zircon grains collected from sample 101001-3 of the Upper Jurassic (Kimmeridgian) Sodenohama Formation of the Hashiura Group in ERI. Detrital

zircons are divided into 3 age groups on the concordia diagram (Fig. 17a, b): 231–164 Ma (70%), 264–252 Ma (5%), and 1865–1749 Ma (5%). The histogram of the $^{206}\text{Pb}/^{238}\text{U}$ ages of 33 concordant grains showed a bimodal pattern with the youngest concordant age of 166.5 ± 3.0 Ma and %Pc of 7.7. The youngest peak on the probability density plot was 170 Ma (Fig. 17c). The Th/U ratio of each analysis was 0.18–1.49 and fell in the range of igneous zircon.

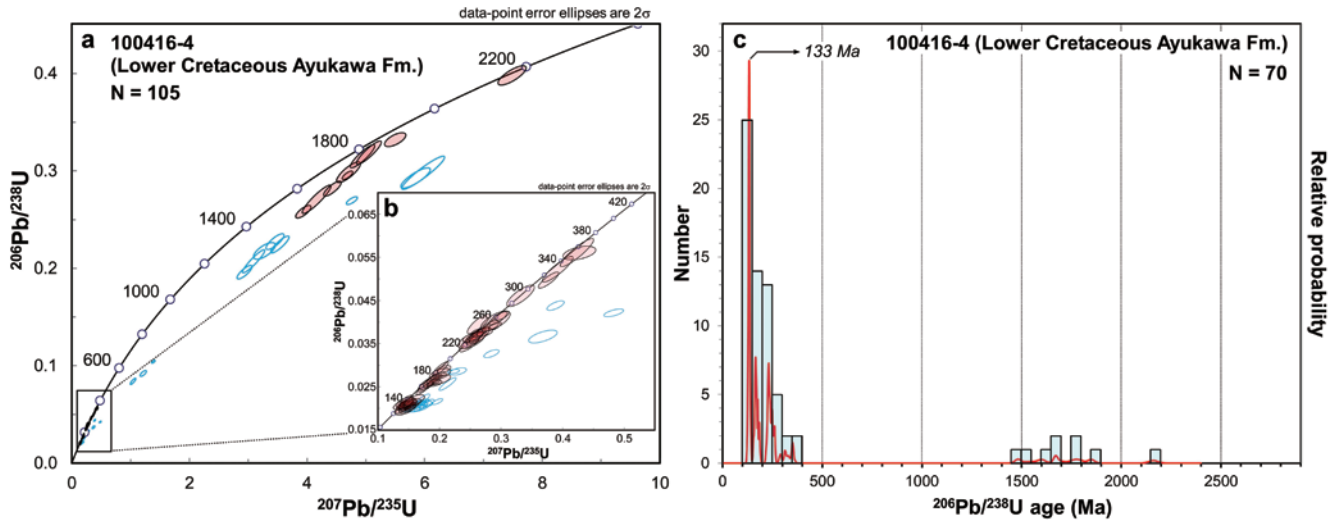


FIGURE 20. Analytical data of detrital zircons from sandstone of the Lower Cretaceous Domeki Sandstone Member of the Ayukawa Formation, Oshika Group (sample 100416-4). **a**, Concordia diagram for all data; **b**, Concordia diagram for 420–120 Ma data set; **c**, Probability density plot and histogram.

Upper Jurassic Oginohama Formation (Sample 100416-5)

We obtained, in ERI, 61 analyses from 61 zircon grains collected from sample 120416-5 of the Tithonian Fukiura Shale and Sandstone Member of the Oginohama Formation, Karakuwa Group. Detrital zircons are divided into 5 age groups on the concordia diagram (Fig. 18a, b): 191–157 Ma (35%), 267–208 Ma (37%), 1645–1562 Ma (4%), 1831–1671 Ma (11%), and 2030–1881 Ma (7%). The histogram of the $^{206}\text{Pb}/^{238}\text{U}$ ages of 54 concordant grains showed a bimodal pattern with the youngest concordant age of 161.7 ± 5.2 Ma and %Pc of 27.8. The youngest peak on the probability density plot was 174 Ma (Fig. 18c). The Th/U ratio of each analysis was 0.15–1.14 and fell in the range of igneous zircon.

Lower Cretaceous Yoshihama Formation (Sample 101002-1)

We obtained 31 analyses from 31 zircon grains collected from sample 101002-1 of the Lower Cretaceous Yoshihama Formation of the Jusanhamama Group in ERI. Detrital zircons are divided into 3 age groups on the concordia diagram (Fig. 19a, b): 165–156 Ma (10%), 235–167 Ma (74%), and 256–242 Ma (10%). The histogram of the $^{206}\text{Pb}/^{238}\text{U}$ ages of 21 concordant grains showed a bimodal pattern with the youngest concordant age of 159.6 ± 3.9 Ma and %Pc of 9.5. The youngest peak on the probability density plot was 160 Ma (Fig. 19c). The Th/U ratio of each analysis was 0.15–1.43 and fell in the range of igneous zircon.

Lower Cretaceous Ayukawa Formation (Sample 100416-4)

We obtained, in ERI, 105 analyses from 105 zircon grains collected from sample 100416-4 of the Valanginian or younger

Domeki Sandstone Member of the Ayukawa Formation, Oshika Group. Detrital zircons are divided into 4 age groups on the concordia diagram (Fig. 20a, b): 147–120 Ma (36%), 268–149 Ma (44%), 369–303 Ma (6%), and 1840–1451 Ma (10%). The histogram of the $^{206}\text{Pb}/^{238}\text{U}$ ages of 70 concordant grains showed a bimodal pattern with the youngest concordant age of 125.9 ± 6.3 Ma and %Pc of 15.3. The youngest peak on the probability density plot was 133 Ma. The Th/U ratio of each analysis was 0.12–1.99 and fell in the range of igneous zircon (Fig. 20c).

DISCUSSION

Comparison of the new U-Pb ages and the age of deposition of the studied samples

The accuracy of the U-Pb isotopic ratios obtained with the ICPMS instruments is guaranteed by comparing the weighted mean of several tens of measurements of a standard zircon and the published ID-TIMS (isotope dilution-thermal ionization mass spectrometry) or SHRIMP data for the same zircon. The weighted mean shows good agreement with the published isotopic ratio within $\pm 2\%$ (e.g., Orihashi et al., 2008). Hence the weighted mean of the youngest age cluster, which is usually close to the youngest peak age in the probability density plot, is a good measure of the depositional age, provided that syn-sedimentary volcanism in the hinterland supplied certain amount of igneous zircons to the measured sample. Figure 21 compares, for each sample, the youngest peak age in the probability density plot and the biostratigraphical age-range, i.e., the age-range previously inferred from stratigraphy and index fossils. For all samples except sample 101001-1 (Upper Permian Toyoma Formation), the youngest peak age falls in the biostratigraphical

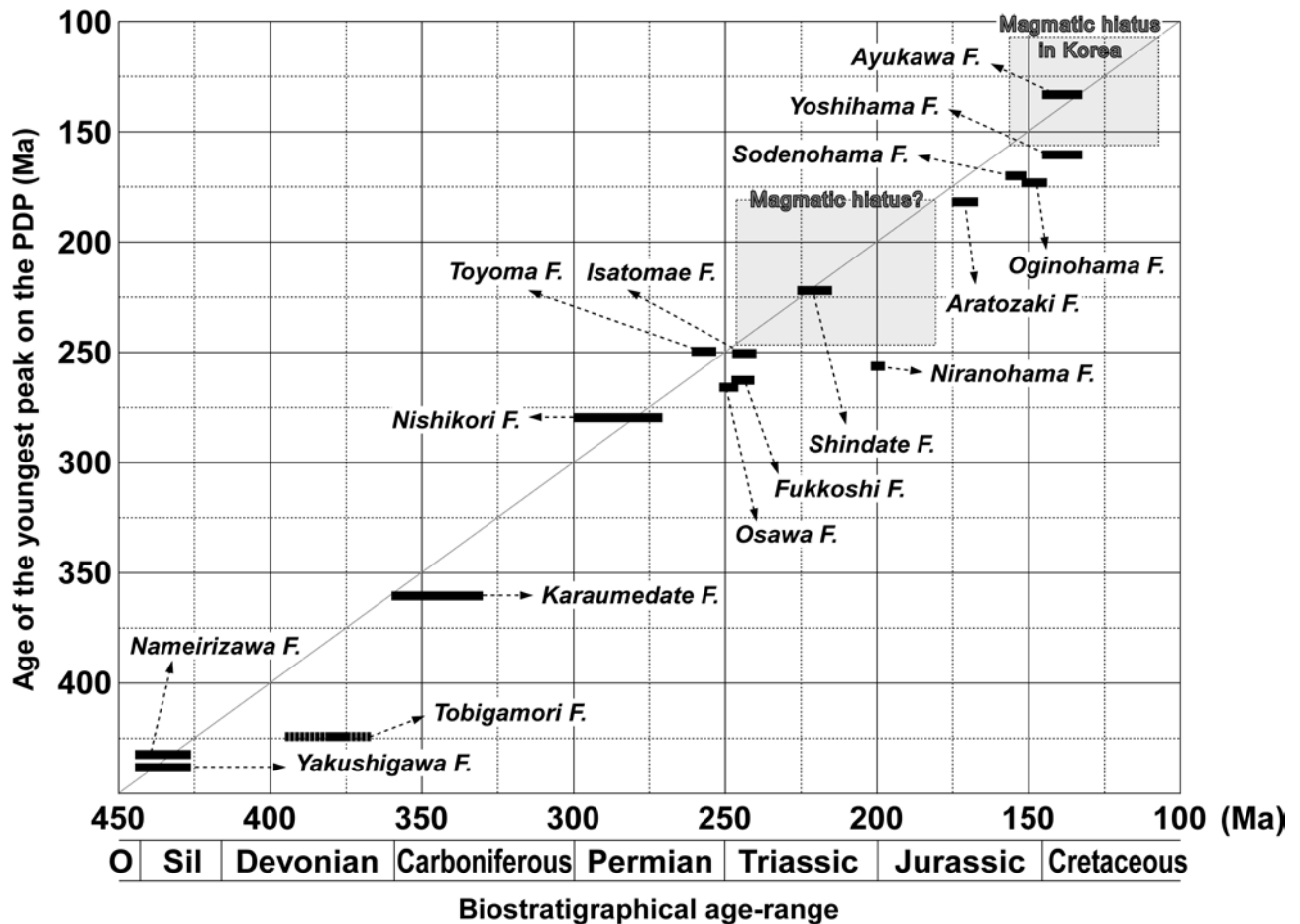


FIGURE 21. Diagram comparing the youngest peak age in the probability density plot (PDP; ordinate) and biostratigraphical age-range (abscissa). The age-range of the magmatic hiatus in Korea (158–110 Ma) and a possible magmatic hiatus during the Triassic and the Early Jurassic are also shown. Abbreviations—F.: Formation, O.: Ordovician, Sil: Silurian.

age-range or older than it. Thus we are convinced that the results of our measurement are mostly concordant with the litho- and biostratigraphy of the SKB.

The youngest peak ages of the following formations are significantly older than the biostratigraphical ages: Middle Triassic to Lower Jurassic formations (Osawa, Fukkoshi, and Nirano Fm.) and Middle Jurassic to Lower Cretaceous formations (Aratozaki, Sodenohama, Oginohama, and Yoshihama Fm.; Fig. 21). The fact suggests that there were no significant syn-sedimentary volcanism in Middle Triassic–Early Jurassic times and Middle Jurassic–Early Cretaceous times. The latter interval falls within the magmatic hiatus in Korea, 158–110 Ma (Sagong et al., 2005), and likely indicates its influence to the South Kitakami Paleoland.

Three tectonic stages of the South Kitakami Paleoland

Provenance analysis based on detrital zircon ages has been carried out in various parts of the world including eastern Asia

(e.g., Darby and Gehrels, 2006; Rojas-Agramonte et al., 2011; Yao et al., 2011, 2012; Diwu et al., 2012). According to these studies, the sand and sandstones of the North China Block are characterized by the abundance of 2.5 Ga and 1.85 Ga zircons and absence or very rare occurrence of Neoproterozoic zircons (Darby and Gehrels, 2006; Diwu et al., 2012; Choi et al., 2013). 2.5 Ga was the age of a major tectonothermal event associated with the crustal growth of the North China Block (Diwu et al., 2012). 1.85 Ga was the age of crustal assembly in the North China Block associated with the formation of the supercontinent Columbia (e.g., Rogers and Santosh, 2002; Zhao et al., 2004). Grenvillian tectonothermal event (1250–980 Ma) related to the formation of the supercontinent Rodinia was not recorded in the North China Block, which was isolated following the breakup of Rodinia (Yin and Nie, 1996). Zircons formed during the Grenvillian tectonothermal event are well preserved in the sand and sandstones of the South China Block (Yangtze and Cathaysia blocks), Australia, and some blocks in the CAOB including the Tarim Block (e.g., Rino et al., 2008; Iizuka et al.,

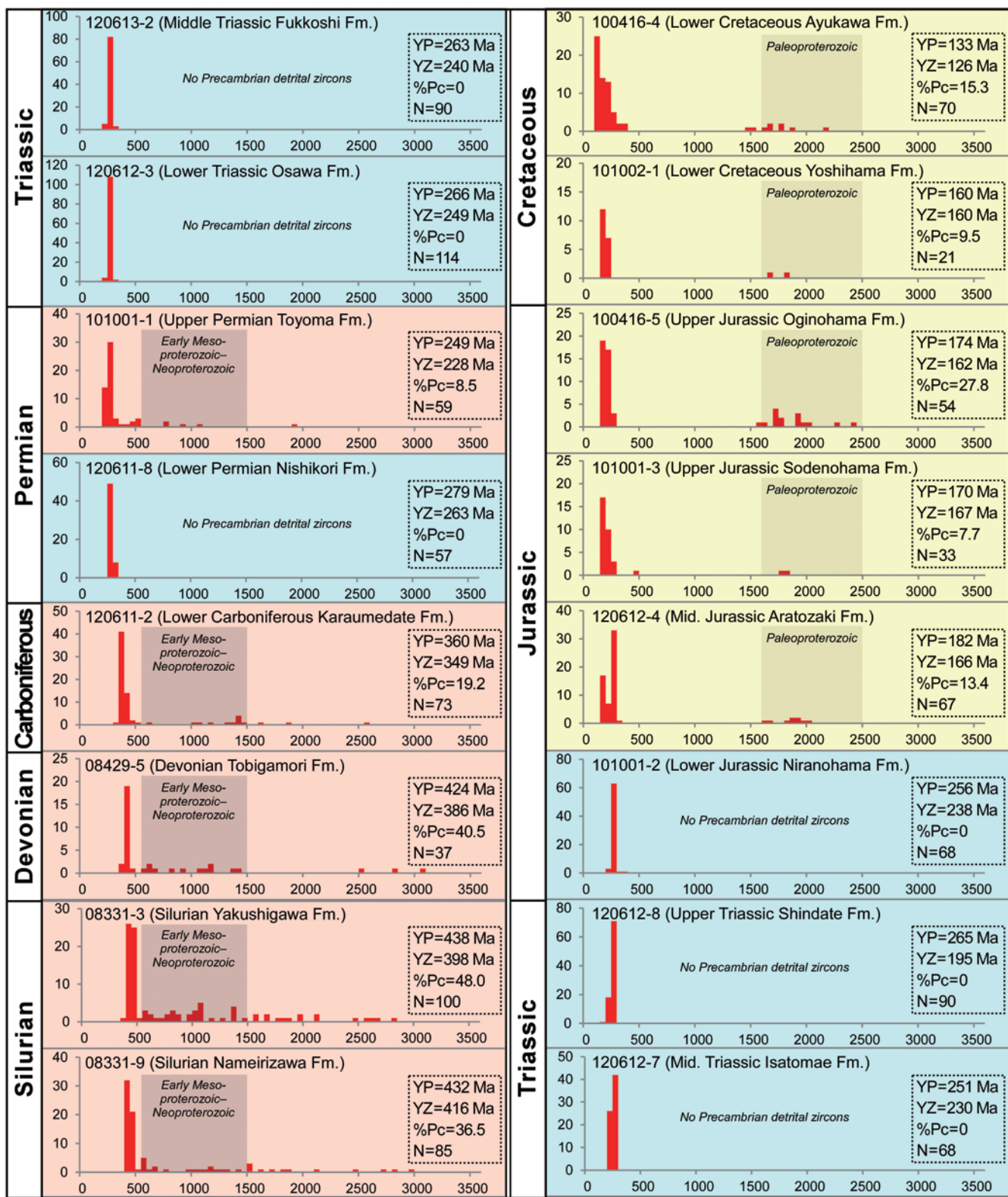


FIGURE 22. Histograms showing the age distributions of detrital zircon grains of all sandstone samples described in this study. The horizontal axes are for the age of zircon grains (best estimate in Ma) and the vertical axes are for the number of grains. Abbreviations—Fm.: Formation, N: total number of analyses, YP: age of the youngest peak in the probability density plot, YZ: age of the youngest zircon.

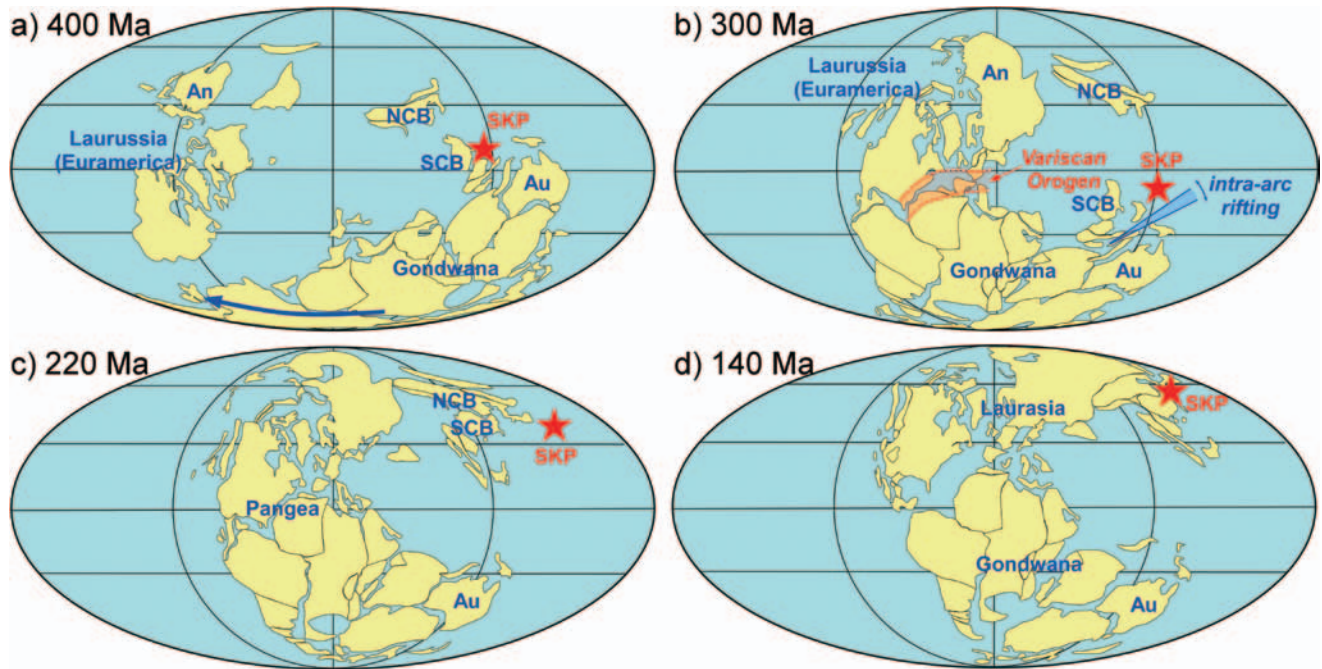


FIGURE 23 Plate reconstruction maps showing the position of the South Kitakami Paleoland at each period. The base reconstruction maps are taken from Lawver et al. (2009). **a**, 400 Ma (Early Devonian); **b**, 300 Ma (end Carboniferous); **c**, 220 Ma (Late Triassic); **d**, 140 Ma (end Jurassic). Abbreviations—An: Angara Craton, Au: Australia, NCB: North China Block, SCB: South China Block, SKP: South Kitakami Paleoland.

2010; Rojas-Agramonte et al., 2011; Yao et al., 2011, 2012; Diwu et al., 2012; Choi et al., 2013). All of these blocks were assembled in the northern part of East Gondwana during Early to Middle Paleozoic times (e.g., Scotese and McKerrow, 1990; Turner, 2010; Metcalfe, 2011).

By comparing the age distribution of detrital zircons of the SKB (Fig. 22) with that of Australia and continental blocks in eastern Asia, three stages of tectonic development have been discriminated of the SKB. From the following paragraph, we combine our new data with previous geological studies and present our model for the tectonic development.

Silurian–Early Carboniferous: Magmatic arc in the northern margin of East Gondwana

The age distribution of detrital zircons from the Siluro–Devonian sandstone of the SKB is characterized by more than 50% of syn-sedimentary zircons, i.e., zircons of ca. 500 Ma to the age of sedimentation, and relatively high proportion of Precambrian zircons (%Pc = 36.5–48.0). The abundance of syn-sedimentary detrital zircons, along with the abundant pyroclastic and volcaniclastic rocks in the Siluro–Devonian strata in the SKB, indicates an igneous activity in the provenance. Moreover the relatively high %Pc value suggests that the Siluro–Devonian sandstone was deposited in front of a continental magmatic arc with Precambrian basement rocks. The Precambrian detrital zircons on the concordia diagram shows several small clusters ranging in age from Neoarchean to Neoproterozoic. The presence of Neoarchean to Neoproterozoic zircons including

those of Grenvillian times excludes the North China Block from the candidates of the provenance. Considering the facts that the Siluro–Devonian corals, brachiopods, and plants of the SKB have affinities with those of Australia, South China, and the southern part of the CAOB (e.g., Hamada, 1960; Kato, 1990; Tazawa and Chen, 2001; Kimura, 1987; Tazawa et al., 2006), and that these blocks constituted northern East Gondwana in the Middle Paleozoic, the Siluro–Devonian sandstone must have been deposited along the northern margin of East Gondwana (Fig. 23a). Although Tazawa and Chen (2001) and Tazawa et al. (2006) demonstrated that the SKB was located in the eastern extension of the southern part of the CAOB (or the Tianshan–Xing'anling Belt) along the northern margin of the North China Block in the Devonian, the absence of 1.85 Ga zircons in the Devonian Tobigamori Formation denies their idea. Isozaki et al. (2010), on the other hand, stated that the Japanese Islands grew along the margin of an oceanic island arc originated from the ophiolite obduction within an oceanic plate (Paleo-Pacific plate). The Hayachine complex may have been a part of the obducted ophiolite that forms an oceanic island arc. However, the oceanic island arc, if existed, must have collided with the northern East Gondwana by the Silurian. The inclusion of some 40% of Precambrian zircons in the Siluro–Devonian sandstone of the SKB cannot be explained with the oceanic-island-arc setting, because Precambrian zircons are generally concentrated in the continental crust.

The Early Carboniferous sandstone of the Karaumede

Formation shows similar pattern of detrital zircon age distribution with the Siluro–Devonian sandstone although the %Pc value is significantly lower (19.2). The lower %Pc value likely indicate the commencement of the intra-arc rifting, mentioned in the next paragraph, and the decrease of the area of the hinterland with Precambrian rocks.

Permian–Early Jurassic: Oceanic island arc in the Tethys Ocean

Bimodal volcanic activity is recorded in the Lower Carboniferous sequence of the SKB and has been assumed to indicate intra-arc rifting (Kawamura et al., 1990). The Permian–Lower Jurassic sandstones that overlie the Carboniferous bimodal volcanic and pyroclastic rocks contain virtually no Precambrian zircons. The result is in contrast with the detrital zircon age distribution of coeval supracontinental strata of Korea (Pyeongan Supergroup on the Yeongnam Massif) that contain more than 80% of Paleoproterozoic zircons and show a strong affinity with the North China Block (Lee et al., 2012a). The absence of Precambrian zircons in the Permian–Lower Jurassic sandstones indicates that they were deposited along the margin of an oceanic island or microcontinent apart from a large continental block. The inclusion of syn-sedimentary igneous zircons in the Lower Permian Nishikori Formation (Fig. 21) suggests that the oceanic island or microcontinent had evolved to an active oceanic island arc by the Early Permian. Thus we interpret that the South Kitakami Paleoland was rifted from an active margin of East Gondwana in the Early Carboniferous and drifted as an oceanic island arc in the Tethys Ocean from the Early Permian (Fig. 23b). The unimodal age distribution of detrital zircons (centered at 280–250 Ma) in the Permian–Lower Jurassic sandstones indicates that the land surface of the oceanic island arc was mostly occupied by Permian igneous rocks. However, the detection of some Precambrian zircons from the Toyoma Formation (sample 101001-1; %Pc = 8.5) indicates that a certain amount of Precambrian basement rocks were exposed in the South Kitakami Paleoland.

The Siluro–Devonian faunal and floral affinity between the South Kitakami Paleoland and Australia disappeared in the Carboniferous; i.e., the South Kitakami Paleoland was in the tropical to subtropical Cathaysia floristic province, whereas Australia moved southward as a part of Gondwana to the Gondwana floristic province of the south polar region and partly covered with the continental ice sheet. The paleobiogeographical contrast between the SKB and Australia is concordant with the rifting model (Ehiro and Kanisawa, 1999). We suggest that the rifting was related to the clockwise rotation of Gondwana in Carboniferous–Permian times, which finally collided with the Laurussia or Euramerica continent to form a collision zone of the Variscan orogen in Europe, northwestern Africa, and eastern North America (Fig. 23b).

The South Kitakami Paleoland during the Carboniferous–Permian was paleobiogeographically allied to the South China or Indochina block (corals, fusulinids, and ammonoids; e.g., Minato and Kato, 1965; Nakazawa, 1991; Ozawa, 1987; Ehiro, 1998), the North China Block (plants; e.g., Asama, 1985), or

the CAOB along the northern and eastern margins of the North China Block at present (brachiopods; Tazawa, 1991, 2001). These studies indicated that the South Kitakami Paleoland was in the Tethyan realm (e.g., Ehiro, 1998), with some brachiopod genera indicating the mixture of boreal elements (e.g., Tazawa, 1991). Although we have a tentative idea that the South Kitakami Paleoland lay in the northern part of the Tethyan realm, between the continental blocks of CAOB and South China, and in the same climate zone with the North China Block, our detrital zircon data cannot indicate the exact position of the South Kitakami Paleoland in the Carboniferous–Permian. Our new data can only indicate that the South Kitakami Paleoland was not along the margin of a large continental block (Fig. 23c, d).

The boreal or arctic elements gradually increased in the Triassic strata. For example, the Anisian ammonoids contain some common species with the coeval ammonoids from Primorye and Kolyma (Nakazawa, 1991), and the Late Triassic *Monotis* fauna belongs to the Arcto-Pacific Realm (Kobayashi and Tamura, 1983; Tamura, 1987). Faunal connection between the SKB and the Angara Craton seems to have been strengthened through the Triassic. The Lower Jurassic Shizugawa Group is characterized by endemic species of ammonoids and bivalves (Hayami, 1990). The fact is concordant with our oceanic-island-arc model, but we have to evaluate the influence of mass extinction across the Triassic–Jurassic boundary.

Middle Jurassic–Early Cretaceous: Amalgamation with the North China Block

The age distribution of detrital zircons from the Middle Jurassic–Early Cretaceous sandstone of the SKB is characterized by more than 70% of syn-sedimentary zircons along with small amounts of Paleoproterozoic zircons (%Pc = 7.7–27.8), and absence of Neoproterozoic zircons. Although syn-sedimentary zircons are abundant, both the youngest zircon age and the youngest peak age in the probability density plot of the Upper Jurassic Sodenohama and Oginohama formations and of the Lower Cretaceous Yoshihama Formation are significantly younger than the age of sedimentation. Zircons younger than 160 Ma were not detected from the three formations. We interpret that the magmatic hiatus in South Korea (Sagong et al., 2005) gave an influence to the age composition of the detrital zircons in these formations. The absence of zircons younger than 160 Ma together with the absence of Neoproterozoic zircons strongly indicate that the South Kitakami Paleoland was along the margin of the North China Block during the sedimentation of the Aratozaki, Sodenohama, Oginohama, and Yoshihama formations (Fig. 23d). However the proportion of Paleoproterozoic zircons in these formations is significantly lower than that of the sandstone on the North China Block (e.g., the Jangsan Formation and Pyeongan Supergroup in South Korea; Lee et al., 2012a, b). Moreover the Ryoseki-type flora that flourished on South China, Indochina, and the Malay Peninsula in Late Jurassic to Early Cretaceous times occur from the Oginohama Formation. Hence we interpret that the South Kitakami Paleoland was a little far away from the Paleoproterozoic orogens in the North China

Block, e.g., the Jiao–Liao–Ji Belt in the eastern part of the North China Block (Zhao et al., 2005), in the Middle Jurassic–Early Cretaceous. The Lower Cretaceous Ayukawa Formation (sample 100416-4) contains many zircons in the period of the magmatic hiatus in South Korea, i.e., from 158 Ma to 110 Ma (Sagong et al., 2005). Considering the occurrence of the Ryoseki-type flora from the underlying Oginohama Formation (Kimura and Ohana, 1989), we interpret that the 150–130 Ma zircons in the Ayukawa sandstone came from the Jurassic–Cretaceous wide magmatic province in the Cathaysia Block (Li and Li, 2007), although their possible origin from the coeval metamorphic core complexes in the North China Block and CAOB (Davis et al., 1996, 2001; Wang et al., 2004) cannot be ruled out.

CONCLUSIONS

We carried out U–Pb analyses of more than 1,000 single detrital zircons from 16 formations of the Silurian–Early Cretaceous continuous succession of the South Kitakami Belt, Northeast Japan. The data set provides a detrital zircon reference for the complex continental-margin orogen of Japan for the first time. The results and interpretations can be summarized as follows.

1. Siluro–Devonian sandstone samples contain many syn-sedimentary zircons and 36.5–48.0% of Precambrian zircons, scattering in age between 700 Ma and 3000 Ma, suggesting that they were deposited along an active continental margin of northern East Gondwana.
2. Permian–Lower Jurassic sandstone samples contain virtually no Precambrian zircons, suggesting that they were deposited along the active margin of an oceanic island arc. From biostratigraphical evidence, the South Kitakami Paleoland seems to have drifted northward in the Tethyan realm between the continental blocks of CAOB (north) and South China (south) where boreal brachiopods and bivalves sometimes reached.
3. Middle Jurassic–Lower Cretaceous sandstone samples contain many 300–170 Ma zircons and up to 28% of Paleoproterozoic (around 1,850 Ma) zircons but no Neoproterozoic zircons. Moreover the zircons during the magmatic hiatus in Korea (158–110 Ma) were detected only in one Early Cretaceous sandstone sample. The age distribution suggests that the Paleoproterozoic zircons in the Middle Jurassic–Lower Cretaceous sandstone of the SKB were most likely supplied from a Paleoproterozoic orogen in the North China Block.
4. The South Kitakami Paleoland, which accumulated the continuous succession of the South Kitakami Belt, was thus born along a margin of Gondwana in the Silurian–Devonian, rifted from the continent and drifted in the Tethys ocean as an oceanic island arc in the Permian–Early Jurassic, and finally amalgamated along an active continental margin where detrital zircons of the North China Block were supplied in the Middle Jurassic.

ACKNOWLEDGMENTS

We would like to express our sincere gratitude to Emeritus Professor Kenji Konishi of Kanazawa University for his encouragement to submit our work to this issue; and to Professor Masaaki Shimizu and Associate Professor Kenji Kashiwagi of the University of Toyama for various discussions and instructions during the course of this study. Critical reviews of the submitted manuscript by Professor Yasufumi Iryu of Tohoku University, Professor Keitaro Kunugiza of the University of Toyama, Emeritus Professor Kenji Konishi, and Dr. Hiroto Ichishima of the Fukui Prefectural Dinosaur Museum are greatly appreciated. This study was supported by the Earthquake Research Institute (University of Tokyo) cooperative research program 2013-G-04, JSPS KAKENHI Grant Number 25400484, and the discretionary budget of the President of the University of Toyama.

REFERENCES

- Ando, H. 1987. Paleobiological study of the Late Triassic bivalve *Monotis* from Japan. The University Museum, the University of Tokyo Bulletin 30, Tokyo, 109 pp.
- Aoki, K., T. Iizuka, T. Hirata, S. Maruyama and M. Terabayashi. 2007. Tectonic boundary between the Sanbagawa belt and Shimanto belt in central Shikoku, Japan. Journal of the Geological Society of Japan 113: 171–183.
- Aoki, K., Y. Isozaki, S. Yamamoto, K. Maki, T. Yokoyama and T. Hirata. 2012. Tectonic erosion in a Pacific-type orogeny: Detrital zircon response to Cretaceous tectonics in Japan. Geology 40: 1087–1090.
- Asama, K. 1985. Permian to Triassic floral changes and some problems of the paleobiogeography, parallelism, mixed floras and origin of the angiosperms; pp. 199–218 in K. Nakazawa and J. M. Dickins (eds.), The Tethys. Tokai University Press, Tokyo.
- Bando, Y. 1964. The Triassic stratigraphy and ammonite fauna of Japan. Science Reports of the Tohoku University, Second Series, 36: 1–137.
- Bando, Y., T. Sato and T. Matsumoto. 1987. Chapter 3: Palaeobiogeography of the Mesozoic Ammonoidea, with special reference to Asia and the Pacific; pp. 65–95 in A. Taira and M. Tashiro (eds.), Historical Biogeography and Plate Tectonic Evolution of Japan and Eastern Asia. TERRAPUB, Tokyo.
- Bando, Y., and S. Shimoyama. 1974. Late Schythian ammonoids from the Kitakami Massif. Transactions and Proceedings of the Palaeontological Society of Japan, New Series, 94: 293–312.
- Choi, D. R. 1973. Permian fusulinids from the Setamai–Yahagi district, Southern Kitakami Mountains, N. E. Japan. Journal of the Faculty of Sciences, Hokkaido University, Series 4, 16: 1–132.
- Choi, T., Y. I. Lee, Y. Orihashi and H. I. Yi. 2013. The provenance of the southeastern Yellow Sea sediments constrained by detrital zircon U–Pb age. Marine Geology 337: 182–194.
- Compston, W. 1996. SHRIMP: Origins, impact and continuing

- evolution. *Journal of the Royal Society of Western Australia* 79: 109–117.
- Corfu, F., J. M. Hanchar, P. W. O. Hoskin and P. Kinny. 2003. Atlas of zircon textures; pp. 469–500 in J. M. Hanchar and P. W. O. Hoskin (eds.), *Zircon, Reviews in Mineralogy and Geochemistry* 53. Mineralogical Society of America, Washington, DC.
- Darby, B. J., and G. Gehrels. 2006. Detrital zircon reference for the North China block. *Journal of Asian Earth Sciences* 26: 637–648.
- Davis, G. A., X. Qian, Y. Zheng, H.-M. Tong, H. Yu, C. Wang, G. E. Gehrels, M. Shafiqullah and J. E. Fryxell. 1996. Mesozoic deformation and plutonism in the Yunmeng Shan: A metamorphic core complex north of Beijing, China; pp. 253–280 in A. Yin and T. M. Harrison (eds.), *The Tectonic Evolution of Asia*. Cambridge University Press, Cambridge.
- Davis, G. A., Y. Zheng, C. Wang, B. J. Darby, C. Zhang and G. E. Gehrels. 2001. Mesozoic tectonic evolution of the Yanshan fold and thrust belt, with emphasis on Hebei and Liaoning provinces, northern China; pp. 171–197 in M. S. Hendrix and G. A. Davis (eds.), *Paleozoic and Mesozoic Tectonic Evolution of Central Asia: From Continental Assembly to Intracontinental Deformation*, Geological Society of America Memoir 194. Geological Society of America, Boulder.
- Diwu, C. R., Y. Sun, H. Zhang, Q. Wang, A. Quo and L. Fan. 2012. Episodic tectonothermal events of the western North China Craton and North Qinling Orogenic Belt in central China: Constraints from detrital zircon U-Pb ages. *Journal of Asian Earth Sciences* 47: 107–122.
- Ehiro, M. 1989. Figure 2.1; p. 9 in Editorial Committee of “Geology of Japan 2 Tohoku District” (ed.), *Geology of Japan 2 Tohoku District*. Kyoritsu Shuppan, Tokyo.*
- Ehiro, M. 1996. Latest Permian ammonoid *Paratirorites* from the Ofunato district, Southern Kitakami Massif, Northeast Japan. *Transactions and Proceedings of the Palaeontological Society of Japan, New Series*, 184: 592–596.
- Ehiro, M. 1998. Permian ammonoid fauna of the Kitakami Massif, Northeast Japan—Biostratigraphy and paleobiogeography. *Palaeoworld* 9: 113–122.
- Ehiro, M., and S. Kanisawa. 1999. Origin and evolution of the South Kitakami Microcontinent during the Early Middle Palaeozoic; pp. 283–295 in I. Metcalfe (ed.), *Gondwana Dispersion and Asian Accretion: IGCP 321 Final Results Volume*. A.A. Balkema, Rotterdam.
- Ehiro, M., K. Okami and S. Kanisawa. 1988. Recent progress and further subject in studies on the “Hayachine Tectonic Belt” in the Kitakami Massif, Northeast Japan. *Earth Science (Chikyu Kagaku)* 42: 317–335.**
- Ehiro, M., and Y. Takaizumi. 1992. Late Devonian and Early Carboniferous ammonoids from the Tobigamori Formation in the Southern Kitakami Massif, Northeast Japan and their stratigraphic significance. *Journal of the Geological Society of Japan* 98: 197–204.
- Ehiro, M., J. Tazawa, M. Oishi and K. Okami. 1986. Discovery of *Trimerella* (Silurian Brachiopoda) from the Odagoe Formation, south of Mt. Hayachine in the Kitakami Massif, Northeast Japan and its significance. *Journal of the Geological Society of Japan* 92: 753–756.*
- Fukada, A. 1950. On the occurrence of *Perisphinctes* (s. s.) from the Ozika Peninsula in the southern Kitakami mountainland. *Journal of the Faculty of Science, Hokkaido University, Series 4*, 7: 211–216.
- Gehrels, G. E., W. R. Dickinson, G. M. Ross, J. H. Stewart and D. G. Howell. 1995. Detrital zircon reference for Cambrian to Triassic miogeoclinal strata of western North America. *Geology* 23: 831–834.
- Hamada, T. 1960. The Middle Palaeozoic formations in China and Korea, II. Northwest and South China. *Japanese Journal of Geology and Geography* 31: 219–239.
- Hayami, I. 1960. Pelecypods of the Jusanhama Group (Purbeckian or Wealden) in Hashiura area, northeast Japan. *Japanese Journal of Geology and Geography* 31: 13–21.
- Hayami, I. 1961. Successions of the Kitakami Jurassic. *Jurassic stratigraphy of South Kitakami, Japan*, I. *Japanese Journal of Geology and Geography* 32: 159–177.
- Hayami, I. 1990. Geographic distribution of Jurassic bivalve faunas in eastern Asia; pp. 361–369 in K. Ichikawa, S. Mizutani, I. Hara and A. Yao (eds.), *Pre-Cretaceous Terranes of Japan*. IGCP Project no. 224, Osaka.
- Iba, Y., S. Sano., J. Mutterlose. and Y. Kondo. 2012. Belemnites originated in the Triassic—A new look at an old group. *Geology* 40: 911–914.
- Ichikawa, K. 1951. Triassic formations in the southern part of the Kitakami Massif; pp. 7–26 in Geological Society of Japan (ed.), *The Triassic Stratigraphy of Japan*. Reports Special Number, Geological Survey of Japan.*
- Iizuka, T., and T. Hirata. 2004. Simultaneous determinations of U-Pb age and REE abundances for zircons using ArF excimer laser ablation-ICPMS. *Geochemical Journal* 38: 229–241.
- Iizuka, T., T. Komiya, S. Rino, S. Maruyama and T. Hirata. 2010. Detrital zircon evidence for Hf isotopic evolution of granitoid crust and continental growth. *Geochimica et Cosmochimica Acta* 74: 2450–2472.
- Inai, Y. 1939. Geology of the Environs of Sizugawa-mati, Miyagi Prefecture (preliminary report). *Journal of the Geological Society of Japan* 46: 231–242.*
- Inai, Y., and T. Takahashi. 1940. On the geology of the southernmost part of the Kitakami Massif. Contributions from the Institute of Geology and Paleontology, Tohoku University 34: 1–40.*
- International Commission on Stratigraphy. 2013. International chronostratigraphic chart, v2013/01. <http://www.stratigraphy.org/ICStrat/ChronostratChart2013-01.pdf>.
- Ishii, K., Y. Okimura and K. Ichikawa. 1985. Notes on Tethys biogeography with reference to Middle Permian fusulinaceans; pp. 131–155 in K. Nakazawa and J. M. Dickins (eds.), *The Tethys*. Tokai University Press, Tokyo.
- Isozaki, Y., K. Aoki, T. Nakama and S. Yanai. 2010. New insight into a subduction-related orogeny: A reappraisal of the geotectonic framework and evolution of the Japanese Islands.

- Gondwana Research 18: 82–105.
- Iwano, H., Y. Orihashi, T. Hirata, M. Ogasawara, T. Danbara, K. Horie, N. Hasebe, S. Sueoka, A. Tamura, Y. Hayasaka, A. Katsube, H. Ito, K. Tani, J. Kimura, Q. Chang, Y. Kouchi, Y. Haruta and K. Yamamoto. 2013. An inter-laboratory evaluation of OD-3 zircon for use as a secondary U-Pb dating standard. *Island Arc* 22: 382–394.
- Kamada, K. 1983. Triassic Inai Group in the Toyoma area in the southern Kitakami Mountains, Japan with special reference to the submarine sliding deosits in the Triassic Osawa Formation. *Earth Science (Chikyu Kagaku)* 37: 147–161.**
- Kanagawa, K., and H. Ando. 1983. Discovery of *Monotis* in the Ofunato area, southern Kitakami Mountains and its significance. *Journal of the Geological Society of Japan* 89: 187–190.*
- Kanisawa, S., and M. Ehiro. 1986. Occurrence and geochemical nature of phosphatic rocks and Mn-rich carbonate rocks in the Toyoman Series, Kitakami Mountains, Northeastern Japan. *Journal of the Japanese Association of Mineralogists, Petrologists and Economic Geologists* 81: 12–31.
- Kanisawa, S., M. Ehiro and K. Okami. 1992. K-Ar ages of amphibolites from the Matsugadaira–Motai Metamorphics and their significance. *Journal of Mineralogy, Petrology and Economic Geology* 87: 412–419.**
- Kammera, K., and T. Mikami. 1965. Succession and sedimentary features of the Lower Permian Sakamotozawa Formation. *Memoirs of the Faculty of Science, Kyushu University, Series D Geology*, 16: 265–274.
- Kase, T. 1979. Stratigraphy of the Mesozoic formations in the Hashiura area, Southern Kitakami Mountainland, northern Japan. *Journal of the Geological Society of Japan* 85: 111–122.**
- Kato, M. 1990. Paleozoic corals; pp. 307–312 in K. Ichikawa, S. Mizutani, I. Hara and A. Yao (eds.), Pre-Cretaceous Terranes of Japan. IGCP Project no. 224, Osaka.
- Kawagoe, Y., S. Sano, Y. Orihashi, H. Obara, Y. Kouchi and S. Otoh. 2012. New detrital zircon age data from the Totori Group in the Mana and Itoshiro areas of Fukui Prefecture, central Japan. *Memoir of the Fukui Prefectural Dinosaur Museum* 11: 1–18.
- Kawamura, M., M. Kato and Kitakami Paleozoic Research Group. 1990. Southern Kitakami Terrane; pp. 249–266 in K. Ichikawa, S. Mizutani, I. Hara and A. Yao (eds.), Pre-Cretaceous Terranes of Japan. IGCP Project no. 224, Osaka.
- Kawamura, T., and M. Kawamura. 1989a. The Carboniferous System of the South Kitakami Terrane, northeast Japan (Part 1)—Summary of the stratigraphy—. *Earth Science (Chikyu Kagaku)* 43: 84–97.**
- Kawamura, T., and M. Kawamura. 1989b. The Carboniferous System of the South Kitakami Terrane, northeast Japan (Part 2)—Sedimentary and tectonic environment—. *Earth Science (Chikyu Kagaku)* 43: 157–167.**
- Kawamura, T., H. Nakai and M. Kawamura. 1984. A new occurrence of Silurian fossils in the northern marginal part of the South Kitakami Belt. *Journal of the Geological Society of Japan* 90: 61–64.*
- Kimura, T. 1987. Chapter 6: Geographical distribution of Palaeozoic and Mesozoic plants in East and Southeast Asia; pp. 135–200 in A. Taira and M. Tashiro (eds.), Historical Biogeography and Plate Tectonic Evolution of Japan and Eastern Asia. TERRAPUB, Tokyo.
- Kimura, T., and T. Ohana. 1989. Late Jurassic plants from the Ogino-hama Formation, Oshika Group in the Outer Zone of Northeast Japan (I). *Bulletin of the National Science Museum, Series C Geology and Paleontology*, 15: 1–24.
- Kobayashi, T., and K. Mori. 1955. The Vaugoniinae from the Kitakami Mountains in north Japan. *Japanese Journal of Geology and Geography* 26: 73–88.
- Kobayashi, Y., H. Takagi, K. Kato, K. Sango and K. Shibata. 2000. Petrochemistry and correlation of Paleozoic granitic rocks in Japan. *Memoirs of the Geological Society of Japan* 56: 65–88.**
- Kobayashi, T., and M. Tamura. 1983. The Arcto-Pacific Realm and the Trigoniidae in the Triassic Period. *Proceedings of the Japan Academy, Series B*, 59: 207–210.
- Kosler, J., and P. J. Sylvester. 2003. Present trends and the future of zircon in geochronology: Laser ablation ICPMS; pp. 243–275 in J. M. Hanchar and P. W. O. Hoskin (eds.), Zircon, Reviews in Mineralogy and Geochemistry 53. Mineralogical Society of America, Washington, DC.
- Kouchi, Y., Y. Orihashi, H. Obara, T. Fujimoto, Y. Haruta, K. Tsukada and K. Yamamoto. 2012. U-Pb age dating for a zircon using 213 nm Nd-YAG laser ablation ICP mass spectrometry: An attempt on optimization of the analytical condition to reduce matrix effect. *Abstracts for the 59th annual meeting of the Geochemical Society of Japan*: 135.*
- Lawver, L.A., Dalziel, I.W.D., Norton, I.O., and Gahagan, L.M., The PLATES 2009 Atlas of Plate Reconstructions (750 Ma to Present Day), PLATES Progress Report 325-0509, 157 pp. <http://www.ig.utexas.edu/research/projects/plates/recons.htm>
- Lee, Y. I., T. Choi and Y. Orihashi. 2012a. Depositional ages of upper Pyeongan Supergroup strata in the Samcheok coalfield, eastern central Korea. *Journal of the Geological Society of Korea* 48: 93–99.***
- Lee, Y. I., T. Choi, H. S. Lim and Y. Orihashi. 2012b. Detrital zircon U-Pb ages of the Jangsan Formation in the northeastern Okcheon belt, Korea and its implications for material source, provenance, and tectonic setting. *Sedimentary Geology* 282: 256–267.
- Li, Z.-X., and X.-H. Li. 2007. Formation of the 1300-km-wide intracontinental orogeny and postorogenic magmatic province in Mesozoic South China: A flat-slab subduction model. *Geology* 35: 179–182.
- Liao, W. H. 1990. The biogeographic affinities of East Asian corals; pp. 175–179 in W. S. McKerrow and C. R. Scotese (eds.), Palaeozoic Palaeogeography and Biogeography, Geological Society Memoir 12. Geological Society, London.
- Ludwig, K. R. 2008. Isoplot 3.70: Geochronological Toolkit for Microsoft Excel. Berkeley Geochronology Center Special Publication 4, 77 p.

- Mabuti, S. 1933. Jurassic stratigraphy of the southern part of the Kitakami Mountainland, North-east Japan. Proceedings of the Imperial Academy of Japan 9: 313–316.
- Matsumoto, T. 1953. Chapter 17 Jurassic Period; pp. 325–377 in J. Makiyama (ed.), Historical Geology 2. Asakura Book Company, Tokyo.*
- Matsumoto, T. 1956. *Yebisites*, a new Lower Jurassic ammonite from Japan. Transactions and Proceedings of the Palaeontological Society of Japan, New Series, 23: 205–212.
- Metcalf, I. 2011. Palaeozoic–Mesozoic history of SE Asia; pp. 7–35 in R. Hall, M. A. Cottam and M. E. J. Wilson (eds.), The SE Asian gateway: History and tectonics of the Australia–Asia collision, Geological Society of London, Special Publications 355. Geological Society, London.
- Minato, M., and M. Kato. 1965. Waagenophyllidae. Journal of the Faculty of Science, Hokkaido University, Series 4, 12: 1–241.
- Minato, M., M. Kato, K. Nakamura, Y. Hasegawa, D. R. Choi and J. Tazawa. 1978. Biostratigraphy and correlation of the Permian of Japan. Journal of the Faculty of Science, Hokkaido University, Series 4, 18: 11–47.
- Mori, K. 1949. On the Jurassic formations in the Hashiura district, Province of Rikuzen. Japanese Journal of Geology and Geography 21: 315–322.
- Mori, K., K. Okami and M. Ehiro. 1992. Paleozoic and Mesozoic sequences in the Kitakami Mountains (29th IGC Field Trip A05); pp. 81–114 in M. Adachi and K. Suzuki (eds.), 29th IGC Field Trip Guide Book Vol. 1, Paleozoic and Mesozoic Terranes: Basement of the Japanese Islands Arcs. Nagoya University, Japan.
- Murata, M., and Y. Bando. 1975. Discovery of Late Permian *Araxoceras* from the Toyoma Formation in the Kitakami Massif, Northeast Japan. Transactions and Proceedings of the Palaeontological Society of Japan, New Series, 97: 22–31.
- Murata, M., S. Kanisawa, Y. Ueda and N. Takeda. 1974. Base of the Silurian system and the pre-Silurian granites in the Kitakami Massif, Northeast Japan. Journal of the Geological Society of Japan 80: 475–486.**
- Murata, M., K. Okami, S. Kanisawa and M. Ehiro. 1982. Additional evidence for the Pre-Silurian basement in the Kitakami massif, Northeast Honshu, Japan. Memoirs of the Geological Society of Japan 21: 245–259.
- Nakamura, K., and J. Tazawa. 1990. Faunal provinciality of the Permian brachiopods in Japan; pp. 313–320 in K. Ichikawa, S. Mizutani, I. Hara and A. Yao (eds.), Pre-Cretaceous Terranes of Japan. IGCP Project no. 224, Osaka.
- Nakazawa, K. 1964. On the Upper Triassic *Monotis* beds, especially, on the *Monotis typica* zone. Journal of the Geological Society of Japan 70: 523–535.**
- Nakazawa, K. 1991. The Permian and Triassic systems in the Tethys—their paleogeography; pp. 93–111 in K. Nakazawa and J. M. Dickins (eds.), The Tethys. Tokai University Press, Tokyo.
- Noda, M., and K. Tachibana. 1959. Some Upper Devonian cyrtospiriferids from the Nagasaki district, Kitakami Mountainland. Science Bulletin of the Faculty of Liberal Arts and Education, Nagasaki University 10: 15–21.
- Obata, I. 1988. Cretaceous formations in Northeast Japan. Earth Science (Chikyu Kagaku) 42: 385–395.*
- Okami, M., M. Ehiro, M. Yamazaki and M. Oishi. 1984. Orthoquartzite clasts from the Silurian Orikabetoge Formation, southern Kitakami Mountains, Northeast Japan. Journal of the Geological Society of Japan 90: 911–913.*
- Om, H. Y., C. C. Ryang, Y. H. Kim and D. S. Rim. 1996. Chapter 2 Section 4 Paleozoic Era; pp. 80–154 in Institute of Geology, State Academy of Sciences, DPR of Korea (ed.), Geology of Korea, Foreign Languages Books Publishing House, Pyongyang.
- Onuki, Y. 1956. Geology of the Kitakami Mountains. Explanatory text of the Geologic map of Iwate Prefecture (1:100,000) II. Iwate Prefecture, Morioka, 189 pp.
- Onuki, Y. 1969. Geology of the Kitakami Massif, Northeast Japan. Contributions from the Institute of Geology and Paleontology, Tohoku University 69: 1–239.**
- Onuki, Y. 1981. The Kitakami Massif; pp. 3–223 in Y. Onuki, N. Kitamura and H. Nakagawa (eds.), Explanatory text of the geological map around the Kitakami River in the scale 1:200,000. Hase Geological Survey Inc., Sendai.*
- Onuki, Y., and Y. Bando. 1958. On the Saragai Group of the Upper Triassic System. Journal of the Geological Society of Japan 64: 481–493.**
- Onuki, Y., and Y. Bando. 1959. On the Inai Group of the Lower and Middle Triassic System. Contributions from the Institute of Geology and Paleontology, Tohoku University 50: 1–69.**
- Onuki, Y., and K. Mori. 1961. Geology of the Ofunato district, Iwate Prefecture, southern part of the Kitakami Massif, Japan. Journal of the Geological Society of Japan 67: 641–654.**
- Orihashi, Y., S. Nakai and T. Hirata. 2008. U-Pb age determination for seven standard zircons using inductively coupled plasma-mass spectrometry coupled with frequency quintupled Nd-YAG ($\lambda = 213$ nm) laser ablation system: Comparison with LA-ICP-MS zircon analyses with a NIST glass reference material. Resource Geology 58: 101–123.
- Otoh, S., M. Shimojo, K. Aoki, T. Nakama, S. Maruyama and S. Yanai. 2010. Age distribution of detrital zircons in the psammitic schist of the Sanbagawa Belt, Southwest Japan. Journal of Geography 119: 333–346.**
- Otoh, S., and S. Yanai. 1996. Mesozoic inversive wrench tectonics in far east Asia: examples from Korea and Japan; pp. 401–419 in A. Yin and M. Harrison (eds.), The Tectonic Evolution of Asia. Cambridge University Press, Stanford.
- Ozawa, K. 1983. Relationships between tectonite and cumulate in ophiolites: The Miyamori ultramafic complex, Kitakami Mountains, northeast Japan. Lithos 16: 1–16.
- Ozawa, K. 1984. Geology of the Miyamori ultramafic complex in the Kitakami Mountains, northeast Japan. Journal of the Geological Society of Japan 90: 697–716.
- Ozawa, K., K. Shibata and S. Uchiumi. 1988. K-Ar ages of hornblende in gabbroic rocks from the Miyamori ultramafic complex of the Kitakami Mountains. Journal of Mineralogy,

- Petrology and Economic Geology 83: 150–159.**
- Ozawa, T. 1987. Chapter 2: Permian fusulinacean biogeographic provinces in Asia and their tectonic implications; pp. 45–63 in Taira, A. and M. Tashiro, (eds), Historical Biogeography and Plate Tectonic Evolution of Japan and Eastern Asia. TERRAPUB, Tokyo.
- Rino, S., Y. Kon, W. Sato, S. Maruyama, M. Santosh and D. Zhao. 2008. The Grenvillian and Pan-African orogens: World's largest orogenies through geologic time, and their implications on the origin of superplume. *Gondwana Research* 14: 51–72.
- Rogers, J. J. W., and M. Santosh. 2002. Configuration of Columbia, a Mesoproterozoic supercontinent. *Gondwana Research* 5: 5–22.
- Rojas-Agramonte, Y., A. Kröner, A. Demoux, X. Xia, W. Wang, T. Donskaya, D. Liu and M. Sun. 2011. Detrital and xenocrystic zircon ages from Neoproterozoic to Palaeozoic arc terranes of Mongolia: Significance for the origin of crustal fragments in the Central Asian Orogenic Belt. *Gondwana Research* 19: 751–763.
- Rubatto, D., and J. Hermann. 2003. Zircon formation during fluid circulation in eclogites (Monviso, Western Alps): Implications for Zr and Hf budget in subduction zones. *Geochimica et Cosmochimica Acta* 67: 2173–2187.
- Sagong, H., S. T. Kwon and J. H. Ree. 2005. Mesozoic episodic magmatism in South Korea and its tectonic implication. *Tectonics* 24: TC5002.
- Saito, Y. 1966. Geology of the Setamai district, Southern Kitakami Massif, Northeast Japan. Contributions from the Institute of Geology and Paleontology, Tohoku University 62: 56–67.**
- Sasaki, M. 2001. Restoration of Early Cretaceous sinistral displacement and deformation in the South Kitakami Belt, NE Japan: An example of the Motai–Nagasaki area. *Earth Science (Chikyu Kagaku)* 55: 83–101.
- Sasaki, M. 2003. Early Cretaceous sinistral shearing and associated folding in the South Kitakami Belt, northeast Japan. *Island Arc* 12: 92–109.
- Sasaki, M., K. Tsukada and S. Otoh. 1997. An outcrop of unconformity at the base of the Upper Devonian Tobigamori Formation, Southern Kitakami Mountains. *Journal of the Geological Society of Japan* 103: 647–655.**
- Sato, T. 1957. Biostratigraphie de la série de Shizukawa (Jurassique inférieur), au Japon septentrional. *Journal of the Faculty of Science of the University of Tokyo, Section 2*, 10: 313–350.
- Sato, T. 1962. Études Biostratigraphiques des ammonites du Jurassique du Japon. *Mémoires de la Société géologique de France, Nouvelle série*, 41: 1–122.
- Sato, T. 1972. Some Bajocian ammonites from Kitakami, Northeast Japan. *Transactions and Proceedings of the Palaeontological Society of Japan, New Series*, 85: 280–292.
- Sato, T., and G. E. G. Westermann. 1991. Japan and Southwest East Asia. pp. 81–108 in G. E. G. Westermann and A. C. Riccardi (eds.), *Jurassic Taxa Ranges and Correlation Charts for the Circum Pacific* 4, Newsletters on Stratigraphy 24. Schweizerbart Science Publishers, Stuttgart.
- Scotese, C., and W. McKerrow. 1990. Revised world maps and introduction; pp. 1–21 in W. S. McKerrow and C. R. Scotese (eds.), *Palaeozoic Palaeogeography and Biogeography*, Geological Society Memoir 12. Geological Society, London.
- Shibata, K., and K. Ozawa. 1992. Ordovician arc ophiolite, Hayachine and Miyamori complexes, Kitakami Mountains, Northeast Japan: Isotopic ages and geochemistry. *Geochemical Journal* 26: 85–97.
- Shiida, I. 1940. On the Geology in the environs of Kesennuma, Miyagi Prefecture. *Contributions from the Institute of Geology and Paleontology, Tohoku University* 33: 1–72.*
- Shimizu, S. 1930. On some Anisic ammonites from the *Hollandites* beds of the Kitakami Mountainland. *Science Report of the Tohoku Imperial University, Series 2*, 14: 63–74.
- Shimojo, M., S. Otoh, S. Yanai, T. Hirata, T. and S. Maruyama. 2010. LA-ICP-MS U-Pb age of some older rocks of the South Kitakami Belt, Northeast Japan. *Journal of Geography* 119: 257–269.**
- Soreghan, M. J., and G. E. Gehrels (eds.). 2000. *Paleozoic and Triassic Paleogeography and Tectonics of Western Nevada and Northern California*. Geological Society of America Special Paper 347. Geological Society of America, Boulder, 252 pp.
- Tachibana, K. 1950. Devonian plants first discovered in Japan. *Proceedings of the Japan Academy* 26: 54–60.
- Tachibana, K. 1952. On the Tobigamori Group of the Nagasaki district, Kitakami Mountainland. *Journal of the Geological Society of Japan* 58: 353–360.**
- Takahashi, H. 1969. Stratigraphy and ammonite fauna of the Jurassic System of the Southern Kitakami Massif, northeast Honshu, Japan. *Science Report of the Tohoku University, Series 2*, 41: 1–93.
- Takizawa, F. 1970. Ayukawa Formation of the Ojika Peninsula, Miyagi Prefecture, northeast Japan. *Bulletin of the Geological Survey of Japan* 21: 567–578.
- Takizawa, F. 1977. Some Aspects of the Mesozoic sedimentary basins in the South Kitakami Belt, Northeast Japan. *Monograph of the Association for the Geological Collaboration in Japan* 20: 61–73.**
- Takizawa, F. 1985. Jurassic sedimentation in the South Kitakami Belt, Northeast Japan. *Bulletin of the Geological Survey of Japan* 36: 203–320.
- Takizawa, F., N. Isshiki and M. Katada. 1974. Geology of the Kinkasan District, Quadrangle Series, Scale 1:50,000. *Geological Survey of Japan, Kawasaki*, 62 pp.**
- Tamura, M. 1987. Chapter 4: Distribution of Japanese Triassic bivalve faunas and sedimentary environment of megalodont limestone in Japan; pp. 97–110 in A. Taira and M. Tashiro (eds.), *Historical Biogeography and Plate Tectonic Evolution of Japan and Eastern Asia*. TERRAPUB, Tokyo.
- Tashiro, M., and T. Kozai. 1989. Bivalve faunal correlation of the Cretaceous System of Northeast Japan with that of Southwest Japan. *Earth Science (Chikyu Kagaku)* 43: 129–139.**

- Tazawa, J. 1991. Middle Permian brachiopod biogeography of Japan and adjacent regions in East Asia; pp. 213–230 in K. Ishii, X. Liu, K. Ichikawa and B. Huang (eds.), Pre-Jurassic Geology of Inner Mongolia, China: Report of China-Japan Cooperative Research Group, 1987–1989. Matsuya Insatsu, Osaka.
- Tazawa, J. 1996. *Rotaia* (Rhynchonellida, Brachiopoda) from the Lower Carboniferous of northeast Japan and its palaeobiogeographical significance. Scientific Papers of Niigata University, Series E (Geology), 11: 1–11.
- Tazawa, J. 2001. Middle Permian brachiopod faunas of Japan and South Primorye, Far East Russia: Their palaeobiogeographic and tectonic implications. Geosciences Journal 5: 19–26.
- Tazawa, J., and X. Chen. 2001. Middle Devonian brachiopods from the Nakazato Formation, South Kitakami Belt, northeast Japan and their palaeobiogeographical affinity with those of western Inner Mongolia. Journal of the Geological Society of Japan 107: 706–710.**
- Tazawa, J., K. Sasaki and A. Yokota. 2006. *Leptophloeum* from the Ainosawa Formation of the Soma area, Fukushima Prefecture, northeast Japan, and the tectono-sedimentary setting of the *Leptophloeum*-bearing Upper Devonian in Japan. Earth Science (Chikyu Kagaku) 60: 69–72.**
- Tsutsumi, Y., A. Miyashita, K. Horie and K. Shiraishi. 2012. Existence of multiple units with different accretionary and metamorphic ages in the Sanbagawa Belt, Sakuma–Tenryu area, central Japan. The Island Arc 21: 317–326.
- Tsutsumi, Y., A. Miyashita, K. Terada and H. Hidaka. 2009. SHRIMP U-Pb dating of detrital zircons from the Sanbagawa Belt, Kanto Mountains, Japan: Need to revise the framework of the belt. Journal of Mineralogical and Petrological Sciences 104: 12–24.
- Tsutsumi, Y., K. Yokoyama, K. Horie, K. Terada and H. Hidaka. 2006. SHRIMP U-Pb dating of detrital zircons in paragneiss from Oki-Dogo Island, western Japan. Journal of Mineralogical and Petrological Sciences 101: 289–298.
- Tsutsumi, Y., K. Yokoyama, K. Terada and H. Hidaka. 2011. SHRIMP Dating of detrital zircons from the Sangun-Renge Belt of Sangun Metamorphic Rocks, northern Kyushu, Southwest Japan. Bulletin of the National Museum of Nature and Science, Series C, 37: 5–16.
- Tsutsumi, Y., K. Yokoyama, K. Terada and Y. Sano. 2000. SHRIMP U-Pb dating of zircons in the sedimentary rocks from the Akiyoshi and Suo zones, Southwest Japan. Journal of Mineralogical and Petrological Sciences 95: 216–227.
- Tsutsumi, Y., K. Yokoyama, K. Terada and Y. Sano. 2003. SHRIMP U-Pb dating of detrital zircons in metamorphic rocks from northern Kyushu, western Japan. Journal of Mineralogical and Petrological Sciences 98: 181–193.
- Turner, S. A. 2010. Sedimentary record of late Neoproterozoic rifting in the NW Tarim Basin, China. Precambrian Research 181: 85–96.
- Wang, T., Y. Zheng, T. Li and Y. Gao. 2004. Mesozoic granitic magmatism in extensional tectonics near the Mongolian border in China and its implications for crustal growth. Journal of Asian Earth Sciences 23: 715–729.
- Watanabe, T., C. M. Fanning, K. Urano and H. Kano. 1995. Pre-Middle Silurian granitic magmatism and associated metamorphism in northern Japan: SHRIMP U-Pb zircon chronology. Geological Journal 30: 273–280.
- Wiedenbeck, M., P. Allé, F. Corfu, W. L. Griffin, M. Meier, F. Oberli, A. von Quadt, J. C. Roddick and W. Spiegel. 1995. Three natural zircon standards for U-Th-Pb, Lu-Hf, trace element and REE analyses. Geostandards Newsletter 19: 1–23.
- Yabe, H. 1949. A new Triassic ammonite from Yanaizu, north of Inai, near Isinomaki, Miyagi Prefecture. Proceedings of the Japan Academy 24: 168–174.
- Yamashita, N. 1957. The Mesozoic I. Geoscience Series 10, Association for Geological Collaboration of Japan, Tokyo, 94 pp.*
- Yamazaki, M., K. Okami, M. Ehiro and M. Oishi. 1984. The Silurian in the vicinity of Orikabe-Pass, northern marginal part of the Southern Kitakami Mountains. Earth Science (Chikyu Kagaku) 38: 268–272.*
- Yao, J., L. Shu and M. Santosh. 2011. Detrital zircon U-Pb geochronology, Hf-isotopes and geochemistry—New clues for the Precambrian crustal evolution of the Cathaysia Block, South China. Gondwana Research 20: 553–567.
- Yao, J., L. Shu, M. Santosh and J. Li. 2012. Precambrian crustal evolution of the South China Block and its relation to supercontinent history: Constraints from U-Pb ages, Lu-Hf isotopes and REE geochemistry of zircons from sandstones and granodiorite. Precambrian Research 208–211: 19–48.
- Yin, A., and S. Nie. 1996. A Phanerozoic palinspastic reconstruction of China and its neighboring region; pp. 442–485 in A. Yin and T. M. Harrison (eds.), The tectonic evolution of Asia. Cambridge University Press, Cambridge.
- Zhao, G., M. Sun, S. A. Wilde and S. Li. 2004. A Paleo–Meso–proterozoic supercontinent: Assembly, growth and breakup. Earth-Science Reviews 67: 91–123.
- Zhao, G., M. Sun, S. A. Wilde and S. Li. 2005. Late Archean to Paleoproterozoic evolution of the North China Craton: Key issues revisited. Precambrian Research 136: 177–202.

* : in Japanese

** : in Japanese with English abstract

*** : in Korean

< 地名・地層名 >

Arahama Beach	荒浜	Kitakamigawa River	北上川	Ofunato Group	大船渡層群
Arato Formation	荒砥層	Kitsunezaki Sandstone and Shale Member		Oginohama Formation	萩の浜層
Aratozaki Formation	荒砥崎層 狐崎砂岩頁岩部層		Ohachimori Amphibolite
Arisu Formation	有住層	Kiyosaki Sandstone Member	大鉢森角閃岩
Ayukawa Formation	鮎川層 清崎砂岩部層		Onimaru Formation	鬼丸層
Ayukawa Port	鮎川港	Kobitawatashi Sandstone and Shale Member	Ono Formation	大野層
Cape Bentenzaki	弁天崎 小長渡砂岩頁岩部層		Orikabetoge Formation	折壁峠層
Chonomori Formation	長の森層	Kobosoura Formation	小細浦層	Osawa Formation	大沢層
Domeki Sandstone Member	Kogoshio Formation	小々汐層	Oshika Group	牡鹿層群
..... ドウメキ砂岩部層		Kosaba Formation	小鯖層	Oshima Group	大島層群
Fukiura Shale and Sandstone Member	Kowaragi Formation	小原木層	Rodai Formation	樓台層
..... 福貴浦貢岩砂岩部層		Kozumi Shale Member	小積貢岩部層	Ryoseki	領石
Fukkoshi Formation	風越層	Kukunarihama Beach	十三成浜	Sakamotozawa Formation	坂本沢層
Funagawara Formation	船河原層	Kurosegawa	黒瀬川	Saragai Group	皿貝層群
Futawatashi Shale Member	Maehama Coast	前浜海岸	Saragaizaka Slope	皿貝坂
..... 長渡貢岩部層		Makinohama Sandstone Member	Sendai City	仙台市
Hakoneyama Formation	箱根山層 牧の浜砂岩部層		Setamai	世田米
Hanamaki City	花巻市	Minamisanriku Town	南三陸町	Shindate Formation	新館層
Hashiura	橋浦	Miyagi Prefecture	宮城県	Shittakasawa Formation	尻高沢層
Hayachine Complex	早池峰複合岩類	Miyako City	宮古市	Shizugawa	志津川
Hijochi Formation	飛定地層	Miyamori	宮守	Sodenohama Beach	袖の浜
Hikami Granite	水上花崗岩	Mone Formation	舞根層	South Kitakami Belt (SKB)
Hikoriochi	日頃市	Monobegawa Group	物部川層群 南部北上帶	
Hiraiso Formation	平磯層	Morioka City	盛岡市	Southern Chichibu Belt	南部秩父帶
Hoinskyiki	法印屋敷	Motoyoshi	本吉	Southwest Japan	西南日本
Hosoura Formation	細浦層	Mt. Hayachinesan	早池峰山	Takonoura Formation	蛸浦層群
Ichinoseki City	一関市	Mt. Hikamisan	水上山	Tategami Formation	立神層
Inai Group	稻井層群	Mt. Karaumedateyama	唐梅館山	Tenjinnoki Formation	天神ノ木層
Isatomae Formation	伊里前層	Myojinmae Formation	明神前層	Tobigamori Formation	鳶ヶ森層
Ishinomaki City	石巻市	Nagaiwa Formation	長岩層	Tome City	登米市
Ishigaritoge Formation	石割峠層	Nagao Formation	長尾層	Torinosu-type Limestone
Isokusa Formation	磯草層	Nagasaki	長坂 鳥巣式石灰岩	
Iwaizaki Limestones	岩井崎石灰岩層	Nakahara Formation	中原層	Toyoma Formation	登米層
Iwate Prefecture	岩手県	Nakazato Formation	中里層	Tsukihama Formation	月浜層
Jusanhama Group	十三浜層群	Nameirizawa Formation	名目入沢層	Tsunakizaka Formation	綱木坂層
Kamaishi City	釜石市	Nameirizawa River	名目入沢	Tsukinoura Formation	月の浦層
Kanaegaura Formation	鼎浦層	Natsuyama Logging Road	夏山林道	Usuginu-type Conglomerate
Kanokura Formation	叶倉層	Niranohama Formation	蘿の浜層 薄衣式礫岩	
Karakuwa	唐桑	Nishikori Formation	錦織層	Yakushigawa River	薬師川
Karaumedate Formation	唐梅館層	Northern Chichibu Belt	北部秩父帶	Yamadori Formation	山鳥層
Kawauchi Formation	川内層	Notsuchi Formation	野土層	Yamazaki Conglomerates	山崎礫岩層
Kesaiso Coast	今朝磯海岸	Odagoe Formation	小田越層	Yokonuma Formation	横沼層
Kesennuma City	気仙沼市	Odaira Formation	大平層	Yoshihama Formation	吉浜層

TABLE 1. U-Pb isotopic data for zircons from sandstone of the South Kitakami Belt. All errors are 2 σ . % conc = $100 \times \frac{^{206}\text{Pb}}{^{238}\text{U}}$ age)/($^{207}\text{Pb}/^{235}\text{U}$ age) is a measure of concordance between $^{206}\text{Pb}/^{238}\text{U}$ and $^{207}\text{Pb}/^{235}\text{U}$ ages. Analyses shown in italics are discordant and are not included in the probability density plot and histogram.

Grain	$^{206}\text{Pb}/^{238}\text{U}$	$^{207}\text{Pb}/^{235}\text{U}$	$^{207}\text{Pb}/^{238}\text{U}$	$^{207}\text{Pb}/^{235}\text{U}$	$^{207}\text{Pb}/^{238}\text{U}$	$^{207}\text{Pb}/^{235}\text{U}$	$^{207}\text{Pb}/^{238}\text{U}$	Grain	$^{206}\text{Pb}/^{238}\text{U}$	$^{207}\text{Pb}/^{235}\text{U}$	$^{207}\text{Pb}/^{238}\text{U}$	$^{207}\text{Pb}/^{235}\text{U}$	$^{207}\text{Pb}/^{238}\text{U}$	$^{207}\text{Pb}/^{235}\text{U}$	$^{207}\text{Pb}/^{238}\text{U}$	% conc Th/U
Silurian Nanemizawaya Formation (08331-9; N39°32'55.8"S, E141°20'20.2"E)																
NM-1	0.0767 ± 0.0025	0.6663 ± 0.036	4.77 ± 15	517 ± 22	92.3	0.50	NM-50	0.0745 ± 0.0020	0.6662 ± 0.029	4.63 ± 12	5.6 ± 18	89.8	0.41			
NM-2	0.0808 ± 0.0027	0.714 ± 0.039	501 ± 16	547 ± 23	91.5	0.46	NM-51	0.0729 ± 0.0020	0.559 ± 0.024	453 ± 12	451 ± 16	100.6	0.39			
NM-3	0.524 ± 0.017	14.15 ± 0.77	2715 ± 73	2760 ± 52	98.4	0.57	NM-52	0.0729 ± 0.0020	0.524 ± 0.023	453 ± 12	428 ± 15	106.0	0.54			
NM-4	0.0713 ± 0.0024	0.582 ± 0.032	444 ± 14	438 ± 10	95.3	0.81	NM-53	0.3068 ± 0.0079	4.57 ± 0.23	1725 ± 39	1745 ± 42	98.9	0.29			
NM-5	0.327 ± 0.011	5.24 ± 0.29	1825 ± 52	1860 ± 46	98.1	0.51	NM-54	0.0712 ± 0.0018	0.496 ± 0.025	443 ± 11	409 ± 17	108.4	0.47			
NM-6	0.2085 ± 0.0069	2.23 ± 0.12	1221 ± 37	1191 ± 38	102.5	0.63	NM-55	0.0721 ± 0.0018	0.587 ± 0.030	449 ± 11	469 ± 19	95.8	0.63			
NM-7	0.0717 ± 0.0024	0.556 ± 0.030	446 ± 14	449 ± 20	99.4	0.90	NM-56	0.1699 ± 0.0044	1.720 ± 0.087	1012 ± 24	1016 ± 32	99.6	0.71			
NM-8	0.0714 ± 0.0024	0.636 ± 0.035	445 ± 14	500 ± 21	88.9	0.45	NM-57	0.0751 ± 0.0019	0.575 ± 0.029	467 ± 12	461 ± 19	101.3	0.70			
NM-9	0.0704 ± 0.0023	0.540 ± 0.029	439 ± 14	438 ± 19	100.0	0.54	NM-58	0.0695 ± 0.0018	0.486 ± 0.025	433 ± 11	402 ± 17	107.6	0.62			
NM-10	0.0725 ± 0.0026	0.619 ± 0.030	451 ± 16	489 ± 19	92.2	0.50	NM-59	0.0762 ± 0.0020	0.495 ± 0.025	473 ± 12	408 ± 17	116.0	0.59			
NM-11	0.0717 ± 0.0026	0.609 ± 0.029	447 ± 15	483 ± 18	92.4	0.83	NM-60	0.0727 ± 0.0019	0.545 ± 0.028	453 ± 11	442 ± 18	102.5	0.74			
NM-12	0.0688 ± 0.0025	0.511 ± 0.024	429 ± 15	419 ± 16	102.3	0.61	NM-61	0.0686 ± 0.0018	0.490 ± 0.025	405 ± 17	405 ± 17	105.6	0.66			
NM-13	0.1951 ± 0.0070	2.23 ± 0.11	1149 ± 38	1189 ± 33	96.6	0.80	NM-62	0.0701 ± 0.0018	0.545 ± 0.028	437 ± 11	442 ± 18	98.9	0.60			
NM-14	0.1080 ± 0.0039	0.975 ± 0.047	661 ± 23	691 ± 24	95.7	0.40	NM-63	0.0667 ± 0.0021	0.482 ± 0.024	416 ± 13	399 ± 17	104.2	0.72			
NM-15	0.1105 ± 0.0040	0.984 ± 0.047	675 ± 23	695 ± 24	97.1	0.46	NM-64	0.0701 ± 0.0022	0.619 ± 0.031	437 ± 14	489 ± 20	89.2	0.88			
NM-16	0.283 ± 0.010	3.28 ± 0.16	1605 ± 51	1476 ± 37	108.7	0.66	NM-65	0.0761 ± 0.0024	0.627 ± 0.032	473 ± 15	494 ± 20	95.6	0.24			
NM-17	0.0730 ± 0.0026	0.578 ± 0.028	454 ± 16	463 ± 18	98.1	0.70	NM-66	0.0722 ± 0.0023	0.603 ± 0.031	450 ± 14	479 ± 19	93.8	0.61			
NM-17-2	0.0710 ± 0.0025	0.608 ± 0.029	442 ± 15	482 ± 18	91.7	0.65	NM-67	0.1975 ± 0.0063	2.04 ± 0.10	1162 ± 34	1128 ± 34	103.0	1.1			
NM-18	0.0676 ± 0.0030	0.529 ± 0.045	422 ± 18	431 ± 30	97.8	0.75	NM-68	0.1259 ± 0.0040	1.174 ± 0.059	764 ± 23	789 ± 28	96.9	0.51			
NM-19	0.230 ± 0.010	2.55 ± 0.22	1335 ± 54	1287 ± 63	103.8	0.59	NM-69	0.0722 ± 0.0023	0.598 ± 0.030	450 ± 14	476 ± 19	94.5	0.39			
NM-20	0.2163 ± 0.0097	2.42 ± 0.21	1263 ± 51	1249 ± 62	101.1	0.79	NM-70	0.1490 ± 0.0048	1.053 ± 0.053	896 ± 27	731 ± 26	122.6	0.32			
NM-21	0.0736 ± 0.0033	0.597 ± 0.051	458 ± 20	475 ± 33	96.2	0.52	NM-71	0.0744 ± 0.0024	0.554 ± 0.028	462 ± 14	448 ± 18	103.3	0.91			
NM-21-2	0.0732 ± 0.0033	0.560 ± 0.048	456 ± 20	452 ± 31	100.9	0.58	NM-72	0.0745 ± 0.0046	0.683 ± 0.054	467 ± 28	529 ± 32	88.4	0.55			
NM-22	0.0718 ± 0.0032	0.525 ± 0.045	447 ± 19	447 ± 30	104.3	0.50	NM-73	0.0704 ± 0.0043	0.644 ± 0.050	439 ± 26	505 ± 31	87.0	0.52			
NM-23	0.0699 ± 0.0031	0.616 ± 0.053	436 ± 19	488 ± 33	89.4	0.68	NM-74	0.0693 ± 0.0043	0.491 ± 0.038	432 ± 26	406 ± 26	106.4	0.65			
NM-24	0.0689 ± 0.0031	0.533 ± 0.046	429 ± 19	434 ± 30	99.0	1.0	NM-75	0.0739 ± 0.0045	0.563 ± 0.044	460 ± 27	454 ± 29	101.4	0.44			
NM-25	0.1654 ± 0.0074	1.68 ± 0.14	987 ± 49	971 ± 55	98.5	0.48	NM-76	0.0690 ± 0.0042	0.527 ± 0.041	430 ± 26	430 ± 27	100.1	0.33			
NM-26	0.0686 ± 0.0028	0.524 ± 0.048	456 ± 20	452 ± 31	100.9	0.58	NM-77	0.0744 ± 0.0043	0.676 ± 0.050	467 ± 28	529 ± 32	88.4	0.55			
NM-27	0.0705 ± 0.0029	0.570 ± 0.032	439 ± 17	458 ± 21	95.8	0.93	NM-78	0.0734 ± 0.0045	0.579 ± 0.045	457 ± 27	464 ± 29	98.4	0.63			
NM-28	0.0747 ± 0.0031	0.605 ± 0.034	464 ± 18	480 ± 21	96.6	0.48	NM-79	0.0900 ± 0.0055	0.774 ± 0.061	582 ± 35	582 ± 35	95.4	1.5			
NM-29	0.0976 ± 0.0040	0.877 ± 0.049	600 ± 23	639 ± 26	93.9	0.24	NM-80	0.263 ± 0.016	3.55 ± 0.28	1507 ± 83	1538 ± 62	98.0	0.42			
NM-30	0.0722 ± 0.0030	0.558 ± 0.031	450 ± 18	450 ± 20	99.9	0.45	NM-81	0.0933 ± 0.0049	0.782 ± 0.051	575 ± 34	593 ± 46	96.3	0.46			
NM-31	0.0679 ± 0.0028	0.626 ± 0.035	424 ± 17	428 ± 19	100.1	0.84	NM-82	0.592 ± 0.031	16.3 ± 1.3	2815 ± 140	2894 ± 75	97.3	0.49			
NM-32	0.2082 ± 0.0085	2.86 ± 0.16	1219 ± 45	1371 ± 42	88.9	0.66	NM-83	0.0755 ± 0.0040	0.580 ± 0.038	469 ± 24	465 ± 24	101.0	0.44			
NM-33	0.06864 ± 0.00092	0.448 ± 0.012	428.0 ± 5.5	375.9 ± 8.7	13.9	0.55	NM-84	0.0783 ± 0.0041	0.580 ± 0.038	486 ± 25	464 ± 24	104.7	0.46			
NM-34	0.06897 ± 0.00092	0.599 ± 0.015	429.9 ± 5.6	477 ± 10	90.2	0.56	NM-85	0.0701 ± 0.0037	0.536 ± 0.035	437 ± 22	436 ± 23	100.2	0.53			
NM-35	0.0712 ± 0.0010	0.606 ± 0.016	443.4 ± 5.7	481 ± 10	92.1	0.76	NM-86	0.0772 ± 0.0040	0.631 ± 0.041	480 ± 24	497 ± 26	96.5	0.68			
NM-36	0.1978 ± 0.0026	2.339 ± 0.060	1163 ± 14	1224 ± 18	95.0	2.2	NM-87	0.0744 ± 0.0039	0.617 ± 0.040	463 ± 23	488 ± 25	94.8	0.56			
NM-37	0.0726 ± 0.0010	0.637 ± 0.016	451.9 ± 5.8	500 ± 10	90.3	0.57	NM-88	0.0750 ± 0.0039	0.646 ± 0.042	466 ± 24	506 ± 26	92.0	0.64			
NM-38	0.3425 ± 0.0046	5.15 ± 0.13	1899 ± 22	1844 ± 22	103.0	1.6	NM-89	0.0925 ± 0.0048	0.755 ± 0.049	570 ± 29	571 ± 28	99.5	0.68			
NM-39	0.06941 ± 0.00093	0.563 ± 0.015	432.6 ± 5.6	453.7 ± 9.4	95.4	0.85	NM-90	0.0682 ± 0.0036	0.517 ± 0.034	425 ± 23	423 ± 23	100.5	0.53			
NM-40	0.0905 ± 0.0012	0.681 ± 0.018	558.6 ± 7.1	527 ± 11	106.0	0.82	NM-91	0.0689 ± 0.0042	0.550 ± 0.048	430 ± 25	445 ± 32	96.6	0.43			
NM-41	0.2632 ± 0.0035	2.739 ± 0.071	1506 ± 18	1339 ± 19	112.5	0.40	NM-92	0.0725 ± 0.0044	0.525 ± 0.046	451 ± 27	428 ± 31	105.4	0.81			
NM-42	0.3864 ± 0.0052	6.34 ± 0.16	2106 ± 24	204.1 ± 23	104.1	0.22	NM-93	1.537 ± 83	1.546 ± 70	506 ± 24	506 ± 26	99.4	0.75			
NM-43	0.2496 ± 0.0067	3.11 ± 0.13	1437 ± 35	1436 ± 33	100.1	0.50	NM-94	0.0684 ± 0.0042	0.534 ± 0.047	426 ± 25	434 ± 31	98.1	0.60			
NM-44	0.1788 ± 0.0048	1.921 ± 0.083	1061 ± 26	1089 ± 29	97.4	0.65	NM-95	0.0776 ± 0.0047	0.592 ± 0.052	482 ± 28	472 ± 33	102.0	0.50			
NM-45	0.0701 ± 0.0019	0.547 ± 0.024	437 ± 11	443 ± 16	98.5	0.54	NM-96	0.466 ± 0.028	10.31 ± 0.91	2466 ± 125	2463 ± 82	100.1	0.37			
NM-46	0.0679 ± 0.0018	0.560 ± 0.024	423 ± 11	452 ± 16	93.8	0.46	NM-97	0.0734 ± 0.0045	0.638 ± 0.056	457 ± 27	501 ± 35	91.1	0.83			
NM-47	0.2671 ± 0.0072	3.93 ± 0.17	1515 ± 37	1621 ± 35	94.2	0.37	NM-98	0.0701 ± 0.0020	0.523 ± 0.040	451 ± 27	451 ± 27	99.7	0.60			
NM-48	0.0701 ± 0.0019	0.553 ± 0.024	437 ± 11	447 ± 16	97.8	0.69	NM-99	0.0733 ± 0.0020	0.543 ± 0.044	457 ± 27	457 ± 27	99.1	0.83			

TABLE I. (Continued)

Grain	$^{206}\text{Pb}/^{238}\text{U}$	$^{207}\text{Pb}/^{235}\text{U}$	$^{208}\text{Pb}/^{238}\text{U}$	$^{207}\text{Pb}/^{235}\text{U}$ age (Ma)	$^{208}\text{Pb}/^{238}\text{U}$ age (Ma)	$^{207}\text{Pb}/^{235}\text{U}$ age (Ma)	$^{206}\text{Pb}/^{238}\text{U}$	Grain	$^{206}\text{Pb}/^{238}\text{U}$	$^{207}\text{Pb}/^{235}\text{U}$ age (Ma)	$^{208}\text{Pb}/^{238}\text{U}$ age (Ma)	% conc Th/U	
Slurian Yakushigawa Formation (08331-3; N39°32'06.8", E141°37'30.5")													
YKS-1	0.0637 ± 0.0022	0.519 ± 0.031	398 ± 13	425 ± 21	93.8	0.56	YKS-54	0.172 ± 0.011	1.69 ± 0.13	102.5 ± 60	100.3 ± 50	102.2 ± 0.50	
YKS-2	0.1691 ± 0.0058	1.643 ± 0.097	1007 ± 32	987 ± 37	102.1	0.55	YKS-54	0.354 ± 0.022	6.65 ± 0.52	195.2 ± 107	206.7 ± 69	94.5 ± 0.15	
YKS-3	0.1394 ± 0.0048	1.202 ± 0.071	841 ± 27	802 ± 33	105.0	0.33	YKS-55	0.222 ± 0.014	2.82 ± 0.22	129.4 ± 74	136.0 ± 58	95.2 ± 0.37	
YKS-4	0.0712 ± 0.0024	0.539 ± 0.032	443 ± 15	438 ± 21	101.2	0.74	YKS-56	0.177 ± 0.011	1.91 ± 0.15	105.2 ± 62	108.5 ± 52	96.9 ± 0.39	
YKS-5	0.0695 ± 0.0024	0.523 ± 0.031	433 ± 14	427 ± 21	101.3	0.38	YKS-57	0.1492 ± 0.0095	1.49 ± 0.12	89.6 ± 53	92.8 ± 47	96.6 ± 0.21	
YKS-6	0.1673 ± 0.0057	1.82 ± 0.11	997 ± 32	1052 ± 39	94.8	0.93	YKS-58	0.386 ± 0.028	7.49 ± 0.64	210.6 ± 128	217.2 ± 77	97.0 ± 0.56	
YKS-7	0.0727 ± 0.0025	0.627 ± 0.037	453 ± 15	494 ± 23	91.5	0.59	YKS-59	0.0715 ± 0.0051	0.500 ± 0.043	445 ± 31	412 ± 29	108.1 ± 0.58	
YKS-8	0.0762 ± 0.0026	0.661 ± 0.039	474 ± 16	515 ± 24	92.0	0.43	YKS-60	0.1243 ± 0.0089	1.55 ± 0.099	75.5 ± 51	78.0 ± 47	96.9 ± 0.19	
YKS-9	0.294 ± 0.010	4.87 ± 0.29	1661 ± 50	1797 ± 50	92.4	0.30	YKS-61	0.319 ± 0.023	4.98 ± 0.43	178.7 ± 111	181.6 ± 73	98.4 ± 0.30	
YKS-10	0.0689 ± 0.0025	0.540 ± 0.037	430 ± 15	438 ± 24	98.0	0.49	YKS-62	0.0713 ± 0.0051	0.611 ± 0.053	444 ± 31	484 ± 33	91.7 ± 0.51	
YKS-11	0.1802 ± 0.0066	2.00 ± 0.14	1068 ± 36	1114 ± 46	95.8	0.11	YKS-63	0.0660 ± 0.0047	0.480 ± 0.041	412 ± 29	398 ± 28	103.5 ± 0.48	
YKS-12	0.546 ± 0.020	13.98 ± 0.96	2807 ± 83	2748 ± 65	102.2	0.39	YKS-64	0.254 ± 0.018	3.49 ± 0.30	145.8 ± 93	152.4 ± 68	95.6 ± 1.4	
YKS-13	0.0732 ± 0.0027	0.569 ± 0.039	455 ± 16	458 ± 25	99.5	0.48	YKS-65	0.0682 ± 0.0049	0.555 ± 0.048	425 ± 29	448 ± 31	94.9 ± 0.72	
YKS-14	0.1289 ± 0.0047	1.161 ± 0.079	782 ± 27	782 ± 37	99.9	0.35	YKS-66	0.3022 ± 0.022	4.59 ± 0.39	169.9 ± 107	174.7 ± 72	97.2 ± 0.28	
YKS-15	0.2377 ± 0.0087	2.89 ± 0.20	1375 ± 45	1378 ± 52	99.7	0.36	YKS-67	0.0698 ± 0.0039	0.504 ± 0.038	435 ± 24	415 ± 26	105.0 ± 0.67	
YKS-16	0.0722 ± 0.0026	0.619 ± 0.042	449 ± 16	489 ± 27	91.8	0.69	YKS-68	0.488 ± 0.027	12.35 ± 0.93	256.1 ± 119	263.1 ± 71	97.3 ± 0.42	
YKS-17	0.2333 ± 0.0085	2.98 ± 0.20	1352 ± 45	1404 ± 52	96.3	0.48	YKS-69	0.180 ± 0.010	1.81 ± 0.14	106.7 ± 55	105.0 ± 49	101.6 ± 0.42	
YKS-18	0.1619 ± 0.0059	1.68 ± 0.12	967 ± 33	1002 ± 44	96.6	0.58	YKS-70	0.0728 ± 0.0041	0.554 ± 0.042	453 ± 25	448 ± 31	101.2 ± 0.71	
YKS-19	0.0884 ± 0.0041	0.691 ± 0.054	546 ± 25	534 ± 33	102.3	1.2	YKS-71	0.1483 ± 0.0083	1.49 ± 0.11	89.1 ± 47	92.7 ± 46	96.2 ± 0.35	
YKS-20	0.0680 ± 0.0032	0.589 ± 0.046	424 ± 19	470 ± 30	90.2	0.39	YKS-72	0.0711 ± 0.0040	0.568 ± 0.043	443 ± 24	457 ± 28	96.9 ± 0.70	
YKS-21	0.0718 ± 0.0034	0.509 ± 0.040	447 ± 20	418 ± 27	107.0	0.53	YKS-73	0.0681 ± 0.0038	0.511 ± 0.039	425 ± 23	419 ± 26	101.4 ± 0.45	
YKS-22	0.0682 ± 0.0032	0.560 ± 0.044	425 ± 19	451 ± 29	94.2	0.75	YKS-74	0.1106 ± 0.0038	0.633 ± 0.043	485 ± 23	498 ± 27	97.3 ± 0.71	
YKS-23	0.0681 ± 0.0032	0.490 ± 0.039	425 ± 19	405 ± 26	105.0	0.53	YKS-75	0.3226 ± 0.016	5.01 ± 0.34	182.0 ± 77	182.1 ± 57	99.9 ± 0.72	
YKS-24	0.0670 ± 0.0031	0.506 ± 0.040	418 ± 19	416 ± 27	100.6	0.52	YKS-76	0.0726 ± 0.0035	0.548 ± 0.037	452 ± 21	444 ± 24	101.8 ± 0.85	
YKS-25	0.2012 ± 0.0094	2.24 ± 0.18	1182 ± 51	1193 ± 55	99.1	0.99	YKS-77	0.0748 ± 0.0037	0.545 ± 0.037	465 ± 22	442 ± 24	105.2 ± 0.45	
YKS-26	0.0709 ± 0.0033	0.6077 ± 0.040	442 ± 20	482 ± 30	91.7	0.51	YKS-78	0.1106 ± 0.012	2.66 ± 0.18	136.4 ± 60	131.9 ± 50	103.4 ± 1.6	
YKS-27	0.0682 ± 0.0028	0.551 ± 0.036	425 ± 17	445 ± 24	95.5	0.69	YKS-79	0.1106 ± 0.0054	0.967 ± 0.066	676 ± 31	687 ± 34	98.4 ± 0.26	
YKS-28	0.2779 ± 0.012	3.83 ± 0.25	1588 ± 59	1598 ± 53	99.4	0.68	YKS-80	0.1375 ± 0.0067	1.225 ± 0.083	830 ± 38	812 ± 38	102.2 ± 0.29	
YKS-29	0.0730 ± 0.0030	0.587 ± 0.039	454 ± 18	469 ± 25	96.8	0.59	YKS-81	0.0762 ± 0.0037	0.540 ± 0.037	452 ± 22	438 ± 24	108.0 ± 0.99	
YKS-30	0.470 ± 0.020	12.87 ± 0.86	2670 ± 62	93.0	1.5	YKS-82	0.0748 ± 0.0037	13.18 ± 0.79	266.7 ± 108	269.3 ± 57	99.1 ± 0.87		
YKS-31	0.0720 ± 0.0030	0.574 ± 0.038	448 ± 18	461 ± 24	97.3	0.56	YKS-83	0.0704 ± 0.0035	0.571 ± 0.034	439 ± 21	459 ± 22	95.6 ± 1.6	
YKS-32	0.503 ± 0.021	12.78 ± 0.84	2625 ± 90	2664 ± 62	98.5	1.0	YKS-84	0.395 ± 0.020	7.83 ± 0.47	214.7 ± 71	221.1 ± 54	97.1 ± 0.65	
YKS-33	0.354 ± 0.015	6.50 ± 0.43	1953 ± 70	2045 ± 58	95.5	0.27	YKS-85	0.0977 ± 0.0048	0.773 ± 0.047	60.1 ± 28	58.1 ± 27	103.3 ± 0.32	
YKS-34	0.0706 ± 0.0010	0.541 ± 0.013	440.0 ± 6.0	439.4 ± 8.3	100.1	0.74	YKS-86	0.0925 ± 0.0046	0.748 ± 0.045	570 ± 27	567 ± 26	100.5 ± 0.55	
YKS-35	0.0699 ± 0.0010	0.587 ± 0.039	454 ± 18	469 ± 25	92.6	0.59	YKS-87	0.1723 ± 0.014	3.83 ± 0.23	473 ± 22	438 ± 24	103.0 ± 0.60	
YKS-36	0.0766 ± 0.0011	0.518 ± 0.012	435.4 ± 6.0	423.6 ± 8.1	102.8	0.59	YKS-88	0.0755 ± 0.0037	0.571 ± 0.034	469 ± 22	459 ± 22	102.3 ± 0.69	
YKS-37	0.1702 ± 0.0024	1.550 ± 0.036	475.7 ± 6.5	476.1 ± 8.9	99.9	0.52	YKS-89	0.0727 ± 0.0036	0.579 ± 0.035	452 ± 22	464 ± 22	97.5 ± 0.74	
YKS-38	0.3378 ± 0.0048	4.86 ± 0.11	1876 ± 23	1795 ± 20	104.5	0.93	YKS-90	0.1815 ± 0.0090	1.87 ± 0.11	107.5 ± 49	107.2 ± 40	100.3 ± 0.61	
YKS-39	0.0784 ± 0.0011	0.627 ± 0.015	486.8 ± 6.7	494.4 ± 9.2	94.5	0.45	YKS-91	0.0739 ± 0.0032	0.582 ± 0.036	459 ± 19	446 ± 19	98.6 ± 0.70	
YKS-40	0.1002 ± 0.0038	0.868 ± 0.041	615 ± 22	635 ± 22	97.0	0.28	YKS-92	0.0744 ± 0.0032	0.554 ± 0.035	461 ± 19	448 ± 23	103.0 ± 0.60	
YKS-41	0.0929 ± 0.0035	0.778 ± 0.014	475.7 ± 21	573 ± 21	584 ± 21	98.0	1.8	YKS-93	0.0737 ± 0.0032	0.534 ± 0.033	458 ± 19	434 ± 22	105.5 ± 0.91
YKS-42	0.0944 ± 0.0035	0.770 ± 0.036	1013 ± 13	951 ± 14	106.6	0.32	YKS-94	0.0752 ± 0.0032	0.588 ± 0.037	468 ± 19	470 ± 23	99.5 ± 0.46	
YKS-43	0.0780 ± 0.0029	0.602 ± 0.028	484 ± 11	478 ± 18	101.2	0.66	YKS-95	0.1183 ± 0.0051	1.135 ± 0.071	721 ± 29	770 ± 34	93.6 ± 0.35	
YKS-44	0.0758 ± 0.0028	0.568 ± 0.027	471 ± 17	457 ± 17	103.2	0.84	YKS-96	0.0746 ± 0.0032	0.582 ± 0.036	464 ± 19	446 ± 22	104.2 ± 0.63	
YKS-45	0.1792 ± 0.0067	2.025 ± 0.095	1063 ± 37	1124 ± 32	94.6	0.88	YKS-97	0.0766 ± 0.0033	0.607 ± 0.038	476 ± 20	448 ± 24	98.8 ± 0.54	
YKS-46	0.0744 ± 0.0028	0.594 ± 0.028	462 ± 17	473 ± 18	97.7	0.68	YKS-98	0.0757 ± 0.0033	0.560 ± 0.035	471 ± 20	451 ± 23	104.3 ± 0.47	
YKS-47	0.0706 ± 0.0026	0.526 ± 0.025	440 ± 16	429 ± 16	102.4	0.54	YKS-99	0.0702 ± 0.0030	0.527 ± 0.033	438 ± 18	430 ± 22	101.8 ± 0.60	
YKS-48	0.0734 ± 0.0028	0.604 ± 0.028	457 ± 17	479 ± 18	95.2	0.58	YKS-100	0.0719 ± 0.0031	0.589 ± 0.037	470 ± 23	470 ± 19	95.2 ± 0.43	
YKS-49	0.0675 ± 0.0043	0.561 ± 0.044	421 ± 26	452 ± 28	93.1	0.65							
YKS-50	0.241 ± 0.015	3.13 ± 0.24	1390 ± 79	1439 ± 60	96.6	0.61							
YKS-51	0.0778 ± 0.0049	0.596 ± 0.046	483 ± 30	475 ± 29	101.7	0.54							
YKS-52	0.1325 ± 0.0084	1.168 ± 0.091	802 ± 48	786 ± 43	102.1	0.56							

TABLE 1. (Continued)

Grain	$^{206}\text{Pb}/^{238}\text{U}$	$^{207}\text{Pb}/^{235}\text{U}$	$^{208}\text{Pb}/^{238}\text{U}$	$^{207}\text{Pb}/^{235}\text{U}$ age (Ma)	$^{208}\text{Pb}/^{238}\text{U}$ age (Ma)	$^{207}\text{Pb}/^{235}\text{U}$ age (Ma)	$^{206}\text{Pb}/^{238}\text{U}$	Grain	$^{206}\text{Pb}/^{238}\text{U}$	$^{207}\text{Pb}/^{235}\text{U}$ age (Ma)	$^{208}\text{Pb}/^{238}\text{U}$ age (Ma)	% conc Th/U	
Devonian Tobigamori Formation (08429-5; N39°04'02.0", E141°14'37.0")													
TGM-1	0.0700 ± 0.0035	0.564 ± 0.044	436 ± 21	454 ± 29	96.0	0.47	120611-2-11	0.0592 ± 0.0015	0.443 ± 0.017	370.5 ± 9.5	373 ± 15	99.5	0.51
TGM-2	0.0617 ± 0.0031	0.506 ± 0.040	386 ± 19	416 ± 27	92.9	0.34	120611-2-13	0.0595 ± 0.0016	0.453 ± 0.022	373 ± 10	380 ± 19	98.1	0.35
TGM-3	0.1953 ± 0.0097	2.15 ± 0.17	1150 ± 52	1165 ± 55	98.7	0.57	120611-2-14	0.0734 ± 0.0020	0.512 ± 0.025	409 ± 11	420 ± 21	97.4	0.75
TGM-4	0.239 ± 0.012	3.11 ± 0.25	1384 ± 62	1436 ± 61	96.4	0.93	120611-2-15	0.0570 ± 0.0015	0.456 ± 0.023	357.3 ± 9.7	382 ± 19	93.6	0.68
TGM-5	0.1828 ± 0.0091	1.99 ± 0.16	1082 ± 49	1111 ± 53	97.4	0.33	120611-2-16	0.0584 ± 0.0019	3.49 ± 0.15	1482 ± 40	1525 ± 67	97.2	0.93
TGM-6	0.1388 ± 0.0069	1.38 ± 0.11	838 ± 39	882 ± 47	95.0	0.24	120611-2-17	0.2871 ± 0.0026	4.053 ± 0.089	1627 ± 15	1645 ± 36	98.9	0.30
TGM-7	0.0660 ± 0.0033	0.471 ± 0.037	412 ± 20	392 ± 26	105.2	0.53	120611-2-18	0.05741 ± 0.00060	0.423 ± 0.014	359.9 ± 3.8	358 ± 12	100.5	0.69
TGM-8	0.0694 ± 0.0034	0.591 ± 0.047	432 ± 21	471 ± 30	91.7	0.81	120611-2-19	0.05832 ± 0.00052	0.427 ± 0.014	101.3 ± 12	101.3	1.2	
TGM-9	0.247 ± 0.012	3.22 ± 0.25	1425 ± 63	1462 ± 61	97.5	1.8	120611-2-20	0.05613 ± 0.00059	0.415 ± 0.014	352.1 ± 3.7	353 ± 12	99.8	0.56
TGM-10	0.0709 ± 0.0033	0.576 ± 0.031	442 ± 20	462 ± 20	95.7	0.38	120611-2-21	0.06587 ± 0.00065	0.526 ± 0.014	411.2 ± 4.0	429 ± 12	95.8	0.67
TGM-11	0.0697 ± 0.0032	0.490 ± 0.026	434 ± 20	405 ± 18	107.3	0.59	120611-2-22	0.2314 ± 0.0021	2.891 ± 0.064	1342 ± 12	1380 ± 30	97.2	0.53
TGM-12	0.0691 ± 0.0032	0.539 ± 0.029	431 ± 19	438 ± 19	98.4	0.50	120611-2-23	0.4869 ± 0.0045	12.49 ± 0.27	2557 ± 23	2642 ± 58	96.8	0.35
TGM-13	0.0709 ± 0.0033	0.621 ± 0.033	442 ± 20	490 ± 20	90.1	0.74	120611-2-24	0.05644 ± 0.0010	0.430 ± 0.019	353.4 ± 3.9	363 ± 16	97.4	0.65
TGM-14	0.0776 ± 0.0036	0.628 ± 0.034	482 ± 22	495 ± 21	97.4	0.44	120611-2-25	0.0576 ± 0.0011	0.451 ± 0.020	360.8 ± 6.6	378 ± 17	95.5	0.46
TGM-15	0.0673 ± 0.0031	0.493 ± 0.027	420 ± 19	407 ± 18	103.2	0.80	120611-2-26	0.0365 ± 0.0011	0.459 ± 0.024	354.6 ± 6.8	384 ± 20	92.4	0.58
TGM-16	0.0702 ± 0.0033	0.588 ± 0.032	437 ± 20	470 ± 20	93.1	0.56	120611-2-27	0.2465 ± 0.0043	3.08 ± 0.11	1420 ± 25	1428 ± 51	99.5	0.31
TGM-17	0.0647 ± 0.0027	0.523 ± 0.029	404 ± 16	427 ± 19	94.6	0.59	120611-2-28	0.0588 ± 0.0010	0.430 ± 0.019	350.2 ± 6.4	363 ± 16	96.4	0.53
TGM-18	0.0686 ± 0.0028	0.549 ± 0.030	427 ± 17	444 ± 17	96.3	1.0	120611-2-29	0.2434 ± 0.0042	3.20 ± 0.11	1404 ± 24	1456 ± 51	96.5	0.33
TGM-19	0.0932 ± 0.0038	0.693 ± 0.038	575 ± 23	535 ± 23	107.5	2.2	120611-2-30	0.0673 ± 0.0012	0.507 ± 0.019	419.9 ± 7.4	416 ± 16	100.8	0.55
TGM-20	0.481 ± 0.020	11.78 ± 0.65	2534 ± 86	2587 ± 52	97.9	0.69	120611-2-31	0.05884 ± 0.0010	0.439 ± 0.017	366.2 ± 6.4	370 ± 14	99.1	0.61
TGM-21	0.0674 ± 0.0020	0.499 ± 0.025	420 ± 12	411 ± 17	102.3	0.70	120611-2-32	0.05848 ± 0.00064	0.439 ± 0.014	366.4 ± 4.0	370 ± 12	99.1	0.63
TGM-22	0.1068 ± 0.0032	0.935 ± 0.046	654 ± 19	670 ± 24	97.6	0.63	120611-2-33	0.06830 ± 0.00070	0.531 ± 0.025	1439 ± 14	1428 ± 37	99.8	0.76
TGM-23	0.1544 ± 0.0047	1.523 ± 0.076	925 ± 26	940 ± 30	98.5	0.53	120611-2-34	0.05735 ± 0.00066	0.449 ± 0.016	359.5 ± 4.2	376 ± 14	95.5	0.81
TGM-24	0.611 ± 0.018	21.6 ± 1.1	3072 ± 74	3166 ± 48	97.0	0.76	120611-2-35	0.05746 ± 0.00062	0.443 ± 0.014	360.1 ± 3.9	372 ± 12	96.8	0.74
TGM-25	0.0671 ± 0.0020	0.519 ± 0.026	419 ± 12	425 ± 17	98.7	0.55	120611-2-36	0.05820 ± 0.00065	0.437 ± 0.015	364.7 ± 4.1	368 ± 13	99.1	0.70
TGM-26	0.0680 ± 0.0021	0.517 ± 0.026	424 ± 12	423 ± 17	100.2	0.56	120611-2-37	0.3370 ± 0.0034	5.58 ± 0.14	1872 ± 19	1912 ± 48	97.9	0.75
TGM-27	0.0659 ± 0.0020	0.535 ± 0.027	412 ± 12	435 ± 18	94.7	0.65	120611-2-38	0.2497 ± 0.0025	3.127 ± 0.081	1437 ± 14	1439 ± 37	99.8	0.71
TGM-28	0.2021 ± 0.0061	2.09 ± 0.10	1187 ± 33	1144 ± 34	103.7	0.92	120611-2-39	0.1741 ± 0.0017	2.041 ± 0.053	1034 ± 10	1129 ± 29	91.6	0.25
TGM-29	0.0686 ± 0.0021	0.473 ± 0.023	428 ± 13	393 ± 16	108.8	0.78	120611-2-40	0.07107 ± 0.00071	0.574 ± 0.012	442.6 ± 4.4	461 ± 11	96.1	1.0
TGM-30	0.0636 ± 0.0042	0.513 ± 0.045	398 ± 26	420 ± 30	94.6	0.54	120611-2-41	0.05738 ± 0.00072	0.442 ± 0.019	359.7 ± 4.5	372 ± 16	96.7	0.58
TGM-31	0.553 ± 0.037	15.1 ± 1.3	2839 ± 153	2823 ± 84	100.2	0.25	120611-2-42	0.06157 ± 0.00067	0.450 ± 0.014	3370 ± 4.2	377 ± 12	102.2	0.93
TGM-32	0.0700 ± 0.0047	0.517 ± 0.046	436 ± 28	423 ± 31	103.1	0.62	120611-2-43	0.05825 ± 0.00055	0.439 ± 0.009	364.9 ± 3.5	369.6 ± 7.7	98.8	0.35
TGM-33	0.0667 ± 0.0044	0.475 ± 0.042	416 ± 27	394 ± 29	105.5	0.57	120611-2-44	0.06554 ± 0.00070	0.493 ± 0.015	409.3 ± 4.4	407 ± 12	100.5	0.52
TGM-34	0.0695 ± 0.0046	0.541 ± 0.048	433 ± 28	439 ± 31	98.6	0.46	120611-2-45	0.07487 ± 0.00071	0.587 ± 0.012	465.4 ± 4.4	469 ± 10	99.2	0.62
TGM-35	0.1040 ± 0.0069	0.971 ± 0.086	638 ± 41	689 ± 44	92.6	0.23	120611-2-46	0.05818 ± 0.00062	0.441 ± 0.014	364.6 ± 3.9	371 ± 11	98.3	0.95
TGM-36	0.1024 ± 0.00668	0.931 ± 0.082	629 ± 40	668 ± 43	94.1	0.20	120611-2-47	0.05994 ± 0.00020	0.850 ± 0.036	611 ± 13	625 ± 26	97.8	0.77
TGM-37	0.1197 ± 0.013	2.08 ± 0.18	1144 ± 71	1144 ± 61	101.1	0.52	120611-2-48	0.06032 ± 0.00012	0.465 ± 0.020	377.0 ± 7.8	388 ± 17	97.3	0.99
Lower Carboniferous Karaunedate Formation (120611-2-1; N39°0'25.10", E141°15'57.06")													
120611-2-1	0.1826 ± 0.0036	1.961 ± 0.054	1081 ± 21	1102 ± 30	98.1	0.58	120611-2-53	0.0726 ± 0.0014	0.652 ± 0.022	452.0 ± 8.7	510 ± 17	88.7	0.46
120611-2-2	0.0587 ± 0.0012	0.457 ± 0.015	367.8 ± 7.3	382 ± 13	96.3	0.48	120611-2-54	0.0575 ± 0.0011	0.458 ± 0.017	360.1 ± 7.0	383 ± 14	94.1	0.57
120611-2-3	0.0567 ± 0.0011	0.424 ± 0.015	355.7 ± 7.2	359 ± 13	99.1	0.40	120611-2-56	0.0578 ± 0.0013	0.464 ± 0.028	362.1 ± 7.9	387 ± 23	93.6	0.35
120611-2-4	0.2397 ± 0.0035	2.993 ± 0.099	1385 ± 20	1406 ± 46	98.5	0.24	120611-2-57	0.0684 ± 0.0011	0.532 ± 0.016	426.2 ± 6.9	433 ± 13	98.5	0.67
120611-2-5	0.05688 ± 0.00083	0.434 ± 0.015	336.6 ± 5.2	366 ± 13	97.5	0.49	120611-2-58	0.05601 ± 0.00094	0.436 ± 0.017	351.3 ± 5.9	367 ± 14	95.6	0.41
120611-2-6	0.0824 ± 0.0012	0.663 ± 0.022	510.3 ± 7.5	516 ± 18	98.8	0.54	120611-2-59	0.0688 ± 0.0011	0.542 ± 0.017	428.9 ± 7.0	440 ± 14	97.5	0.41
120611-2-7	0.05879 ± 0.00089	0.448 ± 0.017	368.2 ± 5.6	376 ± 15	98.0	0.45	120611-2-60	0.06632 ± 0.00112	0.540 ± 0.029	413.0 ± 7.7	438 ± 23	94.3	0.55
120611-2-8	0.0583 ± 0.0015	0.445 ± 0.017	365.0 ± 9.3	374 ± 15	97.6	0.47	120611-2-61	0.05838 ± 0.00117	0.445 ± 0.018	365 ± 11	373 ± 15	97.7	0.61
120611-2-9	0.0577 ± 0.0015	0.433 ± 0.016	361.7 ± 9.2	365 ± 13	99.1	0.59	120611-2-62	0.0597 ± 0.00118	0.444 ± 0.016	374 ± 11	373 ± 13	100.2	1.2
120611-2-10	0.0578 ± 0.0015	0.431 ± 0.017	362.2 ± 9.3	364 ± 14	99.5	0.63	120611-2-63	0.0584 ± 0.00118	0.584 ± 0.024	366 ± 11	467 ± 19	78.4	0.64

TABLE I. (Continued)

	Grain	$^{206}\text{Pb}/^{238}\text{U}$	$^{207}\text{Pb}/^{235}\text{U}$	$^{208}\text{Pb}/^{238}\text{U}$	age (Ma)	% conc Th/U	Grain	$^{206}\text{Pb}/^{238}\text{U}$	$^{207}\text{Pb}/^{235}\text{U}$	age (Ma)	% conc Th/U	
Lower Permian Nishikori Formation (120611-8; N38°41'14.17", E141°17'24.39")												
120611-8-1	0.0438 ± 0.0017	0.362 ± 0.045	276 ± 11	374 ± 39	88.2	0.35	120611-8-54	0.448 ± 0.0015	0.341 ± 0.046	282 ± 10	298 ± 40	94.8 ± 0.50
120611-8-2	0.0489 ± 0.0030	0.384 ± 0.093	308 ± 19	330 ± 80	92.0	0.35	120611-8-56	0.490 ± 0.0017	0.307 ± 0.048	291 ± 11	272 ± 43	107.1 ± 0.76
120611-8-3	0.0427 ± 0.0026	0.360 ± 0.083	270 ± 16	312 ± 72	86.4	0.36	120611-8-57	0.480 ± 0.0020	0.274 ± 0.054	272 ± 12	246 ± 48	110.6 ± 0.62
120611-8-4	0.0468 ± 0.0016	0.326 ± 0.031	295 ± 10	287 ± 27	102.8	1.2	120611-8-58	0.463 ± 0.0015	0.362 ± 0.057	271 ± 11	314 ± 50	86.2 ± 0.55
120611-8-5	0.0440 ± 0.0025	0.286 ± 0.069	278 ± 16	255 ± 62	108.9	0.57	120611-8-59	0.445 ± 0.0010	0.317 ± 0.033	270.1 ± 7.7	279 ± 29	96.6 ± 0.51
120611-8-6	0.0455 ± 0.0025	0.307 ± 0.069	287 ± 16	272 ± 61	105.4	0.45	120611-8-60	0.444 ± 0.0012	0.313 ± 0.035	280.0 ± 7.8	276 ± 31	101.4 ± 0.58
120611-8-7	0.0478 ± 0.0028	0.345 ± 0.083	301 ± 18	301 ± 72	100.1	0.51	120611-8-61	0.463 ± 0.0014	0.246 ± 0.085	266 ± 18	223 ± 77	119.1 ± 0.37
120611-8-8	0.0449 ± 0.0017	0.330 ± 0.040	283 ± 11	290 ± 35	97.8	0.49	120611-8-62	0.463 ± 0.0019	0.280 ± 0.043	273.4 ± 9.4	250 ± 38	109.2 ± 0.59
120611-8-9	0.0446 ± 0.0026	0.308 ± 0.072	282 ± 17	273 ± 64	103.3	0.56	120611-8-63	0.452 ± 0.0020	0.348 ± 0.048	292 ± 10	303 ± 42	96.1 ± 0.51
120611-8-10	0.0460 ± 0.0019	0.277 ± 0.030	290 ± 12	248 ± 27	116.7	0.77	120611-8-64	0.445 ± 0.0015	0.329 ± 0.025	280.5 ± 6.2	289 ± 22	97.1 ± 0.91
120611-8-11	0.0481 ± 0.0025	0.337 ± 0.062	303 ± 16	295 ± 54	102.6	0.49	120611-8-65	0.449 ± 0.0020	0.307 ± 0.039	263.0 ± 8.4	272 ± 34	96.8 ± 0.54
120611-8-12	0.0436 ± 0.0023	0.328 ± 0.058	275 ± 14	288 ± 51	95.5	0.31	120611-8-66	0.433 ± 0.0017	0.346 ± 0.041	284.8 ± 8.7	302 ± 35	94.4 ± 0.46
120611-8-13	0.0439 ± 0.0023	0.377 ± 0.063	277 ± 14	325 ± 54	85.2	0.38	120611-8-67	0.442 ± 0.0019	0.295 ± 0.058	266 ± 12	262 ± 52	101.6 ± 0.35
120611-8-14	0.0450 ± 0.0022	0.326 ± 0.054	284 ± 14	287 ± 47	98.9	0.34	120611-8-68	0.463 ± 0.0023	0.349 ± 0.049	272 ± 14	347 ± 69	78.4 ± 0.46
120611-8-15	0.0434 ± 0.0018	0.299 ± 0.035	274 ± 12	264 ± 31	103.6	0.61	120611-8-69	0.420 ± 0.0014	0.380 ± 0.044	285 ± 10	285 ± 46	98.7 ± 0.34
120611-8-16	0.0436 ± 0.0027	0.281 ± 0.084	275 ± 17	252 ± 75	109.4	0.52	120611-8-70	0.478 ± 0.0019	0.341 ± 0.039	296 ± 13	308 ± 46	99.1 ± 0.43
120611-8-17	0.0443 ± 0.0019	0.269 ± 0.053	279 ± 12	242 ± 44	115.2	0.76	120611-8-71	0.448 ± 0.0017	0.354 ± 0.062	277 ± 10	292 ± 43	94.7 ± 0.46
120611-8-18	0.0434 ± 0.0017	0.318 ± 0.051	274 ± 11	281 ± 45	97.6	0.54	120611-8-72	0.475 ± 0.0019	0.317 ± 0.058	268 ± 11	313 ± 37	98.5 ± 0.75
120611-8-19	0.0481 ± 0.0027	0.290 ± 0.080	303 ± 17	258 ± 71	117.3	0.35	120611-8-73	0.449 ± 0.0018	0.363 ± 0.059	302 ± 13	315 ± 52	96.1 ± 0.49
120611-8-20	0.0464 ± 0.0017	0.353 ± 0.052	292 ± 11	307 ± 41	95.1	0.48	120611-8-74	0.445 ± 0.0022	0.352 ± 0.061	290 ± 13	306 ± 53	94.7 ± 0.36
120611-8-21	0.0420 ± 0.0017	0.325 ± 0.054	265 ± 11	285 ± 48	93.0	0.35	120611-8-75	0.454 ± 0.0020	0.348 ± 0.055	308 ± 13	296 ± 48	104.1 ± 0.68
120611-8-22	0.0421 ± 0.0017	0.287 ± 0.049	266 ± 10	256 ± 44	103.6	0.39	120611-8-76	0.475 ± 0.0019	0.337 ± 0.051	309 ± 13	309 ± 54	91.7 ± 0.51
120611-8-23	0.0426 ± 0.0024	0.296 ± 0.076	269 ± 15	263 ± 68	102.2	0.67	120611-8-77	0.450 ± 0.0025	0.354 ± 0.055	291.7 ± 9.4	280 ± 31	104.2 ± 0.51
120611-8-24	0.0439 ± 0.0013	0.309 ± 0.041	276.9 ± 8.4	273 ± 36	101.4	0.45	120611-8-62	0.463 ± 0.0020	0.377 ± 0.061	292 ± 12	325 ± 53	89.9 ± 0.42
120611-8-25	0.0437 ± 0.0018	0.232 ± 0.052	276 ± 11	212 ± 47	130.2	0.64	120611-8-63	0.452 ± 0.0016	0.380 ± 0.044	325 ± 10	327 ± 37	87.2 ± 0.57
120611-8-26	0.0473 ± 0.0015	0.330 ± 0.048	298 ± 10	290 ± 42	102.9	0.48	120611-8-64	0.463 ± 0.0024	0.344 ± 0.055	282.8 ± 9.2	298 ± 34	89.7 ± 0.49
120611-8-27	0.0438 ± 0.0014	0.337 ± 0.047	276.1 ± 8.9	295 ± 41	93.5	0.43	120611-8-65	0.433 ± 0.0015	0.317 ± 0.055	273 ± 10	308 ± 44	88.8 ± 0.57
120611-8-28	0.0438 ± 0.0018	0.290 ± 0.056	276 ± 11	259 ± 50	106.8	0.48	120611-8-66	0.433 ± 0.0016	0.343 ± 0.052	299 ± 12	295 ± 46	101.3 ± 0.45
120611-8-29	0.0465 ± 0.0017	0.348 ± 0.057	293 ± 11	303 ± 50	96.6	0.38	120611-1-1	0.3919 ± 0.00056	0.286 ± 0.013	289 ± 14	299 ± 64	96.4 ± 0.44
120611-8-30	0.0466 ± 0.0018	0.325 ± 0.056	293 ± 11	285 ± 50	102.8	0.42	120611-1-2	0.0724 ± 0.0018	0.327 ± 0.051	283 ± 12	287 ± 44	98.5 ± 0.43
120611-8-31	0.0433 ± 0.0013	0.327 ± 0.042	273.2 ± 8.3	287 ± 37	95.1	0.59	120611-1-3	0.06872 ± 0.00094	0.389 ± 0.073	281 ± 14	334 ± 62	84.2 ± 0.64
120611-8-32	0.0494 ± 0.0020	0.362 ± 0.062	311 ± 13	314 ± 54	99.2	0.35	101001-1-4	0.1293 ± 0.0018	1.200 ± 0.041	784 ± 11	801 ± 27	98.0 ± 1.0
120611-8-33	0.0438 ± 0.0018	0.332 ± 0.054	276 ± 11	291 ± 48	95.0	0.67	101001-1-5	0.03767 ± 0.00052	0.284 ± 0.011	238.4 ± 3.3	253.9 ± 9.8	93.9 ± 1.1
120611-8-34	0.0436 ± 0.0019	0.332 ± 0.062	275 ± 12	291 ± 54	94.4	0.64	101001-1-6	0.03949 ± 0.00051	0.2896 ± 0.0070	249.7 ± 3.2	258.2 ± 6.3	96.7 ± 0.37

Upper Permian Toyoma Formation (101001-1; N38°48'02.3", E141°33'04.0")

TABLE 1. (Continued)

Grain	$^{206}\text{Pb}/^{238}\text{U}$	$^{207}\text{Pb}/^{235}\text{U}$	$^{208}\text{Pb}/^{238}\text{U}$	$^{207}\text{Pb}/^{235}\text{U}$ age (Ma)	$^{208}\text{Pb}/^{238}\text{U}$ age (Ma)	$^{206}\text{Pb}/^{238}\text{U}$	$^{207}\text{Pb}/^{235}\text{U}$	$^{208}\text{Pb}/^{235}\text{U}$ age (Ma)	Grain	$^{206}\text{Pb}/^{238}\text{U}$	$^{207}\text{Pb}/^{235}\text{U}$	$^{208}\text{Pb}/^{235}\text{U}$ age (Ma)	% conc Th/U	
101001-1-7	0.1263 ± 0.0016	1.152 ± 0.019	766.9 ± 9.6	778 ± 1.3	98.5 ± 0.56	101001-1-61	0.0422 ± 0.0012	0.318 ± 0.030	266.3 ± 7.4	280 ± 26	95.0	0.82		
101001-1-8	0.1551 ± 0.0038	1.522 ± 0.044	929 ± 23	939 ± 2.7	98.9 ± 0.34	101001-1-62	0.0538 ± 0.0015	0.403 ± 0.035	337.9 ± 9.1	344 ± 30	98.3	0.46		
101001-1-9	0.0413 ± 0.0011	0.302 ± 0.021	260.9 ± 6.8	268 ± 1.8	97.4 ± 0.68	101001-1-63	0.0838 ± 0.0018	0.672 ± 0.028	519 ± 11	522 ± 22	99.4	0.35		
101001-1-10	0.0394 ± 0.0010	0.286 ± 0.012	249.0 ± 6.2	255 ± 1.1	97.5 ± 0.43	101001-1-64	0.0545 ± 0.0012	0.359 ± 0.029	286.0 ± 7.5	312 ± 25	91.7	0.83		
101001-1-11	0.0403 ± 0.0009	0.329 ± 0.025	254.8 ± 6.8	289 ± 2.2	88.2 ± 0.41	101001-1-65	0.3520 ± 0.0074	5.53 ± 0.048	1944 ± 41	1905 ± 66	102.0	0.25		
101001-1-12	0.0419 ± 0.0011	0.347 ± 0.021	264.8 ± 6.9	303 ± 1.8	87.4 ± 0.89	101001-1-66	0.0477 ± 0.0012	0.354 ± 0.024	300.7 ± 7.3	308 ± 21	97.6	1.0		
101001-1-13	0.04046 ± 0.00056	0.289 ± 0.011	255.7 ± 3.5	257.9 ± 9.4	99.2 ± 0.68	101001-1-67	0.0421 ± 0.0015	0.342 ± 0.028	265.9 ± 9.4	298 ± 25	89.1	0.99		
101001-1-14	0.03938 ± 0.00052	0.3127 ± 0.0081	249.0 ± 3.3	276.3 ± 7.2	90.1 ± 1.8	101001-1-68	0.0502 ± 0.0017	0.353 ± 0.028	316 ± 11	307 ± 25	102.8	0.44		
101001-1-15	0.05875 ± 0.00091	0.430 ± 0.027	368.0 ± 5.7	363 ± 2.3	101.4 ± 0.69	101001-1-69	0.0393 ± 0.0013	0.313 ± 0.019	248.3 ± 8.7	277 ± 17	89.8	0.55		
101001-1-16	0.03914 ± 0.00054	0.287 ± 0.011	247.5 ± 3.4	256.3 ± 9.7	96.6 ± 0.57	101001-1-70	0.0418 ± 0.0014	0.300 ± 0.018	263.8 ± 8.6	266 ± 16	99.2	0.56		
101001-1-17	0.03862 ± 0.00052	0.2802 ± 0.0094	244.3 ± 3.3	250.8 ± 8.4	97.4 ± 0.38									
101001-1-18	0.04039 ± 0.00054	0.281 ± 0.010	247.6 ± 3.4	251.8 ± 9.1	98.3 ± 0.37									
101001-1-19	0.03916 ± 0.00054	0.280 ± 0.011	244.1 ± 3.4	251 ± 10	97.2 ± 1.1									
101001-1-20	0.03859 ± 0.00054	0.2802 ± 0.0094	244.3 ± 3.3	255.3 ± 3.7	256 ± 13	99.7 ± 0.77								
101001-1-21	0.04098 ± 0.00085	0.297 ± 0.013	253.3 ± 5.4	264 ± 12	95.9 ± 0.47									
101001-1-22	0.03832 ± 0.00081	0.314 ± 0.012	242.4 ± 5.1	277 ± 11	87.4 ± 1.0	120612-3-1	0.0439 ± 0.0021	0.302 ± 0.035	277 ± 13	268 ± 31	103.4	0.49		
101001-1-23	0.0454 ± 0.0010	0.343 ± 0.015	286.1 ± 6.1	300 ± 13	95.5 ± 0.48	120612-3-2	0.0418 ± 0.0024	0.307 ± 0.058	264 ± 15	272 ± 51	96.9	0.62		
101001-1-24	0.03936 ± 0.00085	0.287 ± 0.015	248.0 ± 5.4	257 ± 13	90.5 ± 0.58	120612-3-3	0.0455 ± 0.0021	0.343 ± 0.034	287 ± 14	295.8 ± 30	95.8	0.63		
101001-1-25	0.0822 ± 0.0019	0.613 ± 0.033	509 ± 12	485 ± 26	105.0 ± 0.24	120612-3-4	0.0430 ± 0.0020	0.294 ± 0.026	271 ± 12	262 ± 23	103.5	0.67		
101001-1-26	0.0830 ± 0.0019	0.649 ± 0.028	514 ± 12	508 ± 22	101.2 ± 0.47	120612-3-5	0.0453 ± 0.0020	0.324 ± 0.025	286 ± 13	285 ± 22	100.2	0.81		
101001-1-27	0.0409 ± 0.0011	0.315 ± 0.022	258.3 ± 6.6	278 ± 20	93.0 ± 0.77	120612-3-6	0.0425 ± 0.0021	0.254 ± 0.031	268 ± 13	230 ± 28	116.5	0.49		
101001-1-28	0.0415 ± 0.0010	0.311 ± 0.018	262.1 ± 6.3	275 ± 16	95.3 ± 0.47	120612-3-7	0.0412 ± 0.0020	0.302 ± 0.036	260 ± 13	268 ± 32	97.1	0.50		
101001-1-29	0.0405 ± 0.0013	0.275 ± 0.033	259.9 ± 8.2	247 ± 29	103.6 ± 0.41	120612-3-8	0.0441 ± 0.0020	0.312 ± 0.025	278 ± 13	276 ± 22	100.8	0.70		
101001-1-30	0.0475 ± 0.0014	0.334 ± 0.035	298.9 ± 9.0	292 ± 30	102.2 ± 0.46	120612-3-9	0.0429 ± 0.0014	0.315 ± 0.031	270.7 ± 8.8	278 ± 28	97.4	0.51		
101001-1-31	0.0431 ± 0.0011	0.299 ± 0.021	272.3 ± 6.9	266 ± 18	102.5 ± 0.49	120612-3-10	0.0414 ± 0.0014	0.295 ± 0.034	261.3 ± 9.1	262 ± 30	99.7	0.54		
101001-1-32	0.0406 ± 0.0012	0.287 ± 0.025	256.7 ± 7.6	256 ± 22	100.2 ± 0.58	120612-3-11	0.0424 ± 0.0014	0.311 ± 0.032	268.0 ± 8.9	275 ± 28	97.5	0.58		
101001-1-33	0.0403 ± 0.0011	0.297 ± 0.022	254.7 ± 7.2	264 ± 20	96.5 ± 0.72	120612-3-12	0.0443 ± 0.0020	0.320 ± 0.058	273 ± 13	282 ± 51	96.9	0.82		
101001-1-34	0.0417 ± 0.0012	0.293 ± 0.022	263.4 ± 7.4	261 ± 20	100.8 ± 0.53	120612-3-13	0.0424 ± 0.0012	0.294 ± 0.022	267.6 ± 7.8	262 ± 20	102.2	0.66		
101001-1-35	0.0434 ± 0.0021	0.290 ± 0.074	274 ± 13	258 ± 66	105.9 ± 0.74	120612-3-14	0.0454 ± 0.0017	0.311 ± 0.042	286 ± 11	275 ± 37	104.0	0.60		
101001-1-36	0.0422 ± 0.0012	0.308 ± 0.024	266.6 ± 7.6	272 ± 21	97.9 ± 0.45	120612-3-15	0.0461 ± 0.0013	0.355 ± 0.046	291 ± 11	308 ± 40	94.3	0.53		
101001-1-37	0.0435 ± 0.0013	0.310 ± 0.012	256.7 ± 7.6	256 ± 22	100.2 ± 0.58	120612-3-16	0.0424 ± 0.0016	0.273 ± 0.036	279 ± 10	245 ± 33	133.9	0.59		
101001-1-38	0.0496 ± 0.0013	0.408 ± 0.022	254.7 ± 7.2	264 ± 20	96.5 ± 0.72	120612-3-17	0.0443 ± 0.0012	0.310 ± 0.021	279.4 ± 7.4	274 ± 19	101.9	0.62		
101001-1-39	0.1792 ± 0.0018	1.998 ± 0.067	1063 ± 11	1115 ± 37	95.3 ± 0.19	120612-3-18	0.0404 ± 0.0012	0.268 ± 0.026	255.4 ± 7.5	241 ± 23	105.9	0.97		
101001-1-40	0.04388 ± 0.00070	0.315 ± 0.022	276.8 ± 4.4	278 ± 19	99.5 ± 1.0	120612-3-19	0.0433 ± 0.0015	0.286 ± 0.038	273.6 ± 9.3	256 ± 34	107.1	0.79		
101001-1-41	0.04313 ± 0.00064	0.325 ± 0.020	272.2 ± 4.0	286 ± 17	95.2 ± 0.59	120612-3-20	0.0412 ± 0.0013	0.308 ± 0.032	260.2 ± 8.1	273 ± 28	95.4	0.49		
101001-1-42	0.0741 ± 0.0011	0.577 ± 0.037	460.7 ± 7.1	463 ± 29	99.6 ± 0.41	120612-3-21	0.0442 ± 0.0014	0.303 ± 0.033	269.9 ± 8.5	279 ± 30	100.4	0.70		
101001-1-43	0.04192 ± 0.00071	0.289 ± 0.022	264.7 ± 4.5	258 ± 19	102.7 ± 0.38	120612-3-22	0.0472 ± 0.0015	0.355 ± 0.036	297.3 ± 9.2	309 ± 32	96.3	0.55		
101001-1-44	0.04151 ± 0.00060	0.288 ± 0.017	262.2 ± 3.8	257 ± 11	102.1 ± 0.53	120612-3-23	0.0448 ± 0.0016	0.348 ± 0.046	282.5 ± 9.4	303 ± 40	93.2	0.84		
101001-1-45	0.04291 ± 0.00094	0.285 ± 0.029	270.8 ± 5.9	254 ± 26	106.5 ± 0.84	120612-3-24	0.0446 ± 0.0015	0.330 ± 0.031	281.6 ± 9.3	290 ± 27	97.1	0.91		
101001-1-46	0.03984 ± 0.00078	0.315 ± 0.026	251.8 ± 4.9	278 ± 23	90.7 ± 0.55	120612-3-25	0.0469 ± 0.0017	0.357 ± 0.042	295 ± 11	310 ± 36	95.3	0.58		
101001-1-47	0.0433 ± 0.0012	0.343 ± 0.026	273.0 ± 7.5	293 ± 18	92.2 ± 0.48	120612-3-26	0.0428 ± 0.0014	0.303 ± 0.033	269.9 ± 8.5	269 ± 34	106.0	0.88		
101001-1-48	0.0428 ± 0.0011	0.335 ± 0.021	270.2 ± 6.9	293 ± 18	92.2 ± 0.48	120612-3-27	0.0438 ± 0.0016	0.293 ± 0.027	276 ± 10	261 ± 34	105.8	0.71		
101001-1-49	0.0429 ± 0.0013	0.349 ± 0.033	270.6 ± 8.2	304 ± 10	89.1 ± 0.33	120612-3-28	0.0393 ± 0.0013	0.315 ± 0.029	248.2 ± 8.3	278 ± 26	89.3	0.79		
101001-1-50	0.0487 ± 0.0016	0.315 ± 0.040	306 ± 10	278 ± 35	110.3 ± 0.55	120612-3-29	0.0440 ± 0.0014	0.309 ± 0.028	277.4 ± 9.0	273 ± 24	101.4	0.69		
101001-1-51	0.0426 ± 0.0012	0.452 ± 0.034	269.0 ± 7.6	379 ± 28	71.0 ± 0.46	120612-3-30	0.0436 ± 0.0014	0.315 ± 0.028	275.1 ± 8.9	278 ± 24	99.0	1.1		
101001-1-52	0.0392 ± 0.0010	0.281 ± 0.019	247.7 ± 6.4	251 ± 17	98.6 ± 0.46	120612-3-31	0.0448 ± 0.0016	0.286 ± 0.027	270.6 ± 8.9	269 ± 33	105.2	0.69		
101001-1-53	0.03598 ± 0.00078	0.284 ± 0.018	252.1 ± 5.0	254 ± 16	99.3 ± 0.65	120612-3-32	0.0405 ± 0.0013	0.294 ± 0.025	255.7 ± 8.2	262 ± 23	97.7	1.1		
101001-1-54	0.0439 ± 0.0014	0.306 ± 0.041	276.8 ± 8.8	271 ± 36	102.1 ± 0.71	120612-3-33	0.0454 ± 0.0018	0.300 ± 0.033	286 ± 12	267 ± 30	107.4	0.74		
101001-1-55	0.0379 ± 0.0013	0.248 ± 0.036	239.9 ± 8.0	225 ± 33	106.8 ± 0.92	120612-3-34	0.0434 ± 0.0017	0.336 ± 0.033	274 ± 11	294 ± 29	93.1	0.57		
101001-1-56	0.03891 ± 0.00083	0.323 ± 0.023	246.1 ± 5.2	284 ± 20	86.5 ± 0.35	120612-3-35	0.0446 ± 0.0020	0.359 ± 0.043	296 ± 13	312 ± 37	94.9	0.89		
101001-1-57	0.04099 ± 0.00068	0.344 ± 0.015	253.4 ± 4.3	300 ± 13	84.4 ± 0.50	120612-3-36	0.0442 ± 0.0018	0.349 ± 0.038	279 ± 11	304 ± 33	91.8	0.47		
101001-1-58	0.03597 ± 0.00068	0.254 ± 0.015	227.8 ± 4.3	230 ± 14	99.0 ± 0.39	120612-3-37	0.0443 ± 0.0016	0.294 ± 0.026	267 ± 10	262 ± 23	102.2	0.64		
101001-1-59	0.04048 ± 0.0011	0.297 ± 0.027	257.7 ± 7.0	264 ± 24	97.6 ± 0.51</									

TABLE I. (Continued)

Grain	$^{206}\text{Pb}/^{238}\text{U}$	$^{207}\text{Pb}/^{235}\text{U}$	$^{208}\text{Pb}/^{232}\text{U}$	age (Ma)	% conc Th/U	Grain	$^{206}\text{Pb}/^{238}\text{U}$	$^{207}\text{Pb}/^{235}\text{U}$	age (Ma)	% conc Th/U	
120612-3-40	0.0461 ± 0.0019	0.325 ± 0.036	291 ± 12	286 ± 32	101.6 0.54	120612-3-94	0.0439 ± 0.0013	0.312 ± 0.022	276.9 ± 8.0	276 ± 19	100.5 0.74
120612-3-41	0.0438 ± 0.0011	0.307 ± 0.022	276.5 ± 6.9	272 ± 20	101.6 0.55	120612-3-95	0.0421 ± 0.0015	0.334 ± 0.039	266.1 ± 9.6	293 ± 34	91.0 0.57
120612-3-42	0.0442 ± 0.0013	0.333 ± 0.032	278.5 ± 8.0	292 ± 28	95.4 0.65	120612-3-96	0.0447 ± 0.0015	0.285 ± 0.031	281.6 ± 9.4	254 ± 28	110.8 0.51
120612-3-43	0.0393 ± 0.0012	0.298 ± 0.033	248.7 ± 7.7	265 ± 29	93.8 0.51	120612-3-97	0.0450 ± 0.0015	0.315 ± 0.032	283.7 ± 9.3	278 ± 28	102.0 0.48
120612-3-44	0.0458 ± 0.0015	0.342 ± 0.043	288.5 ± 9.7	299 ± 38	96.6 0.60	120612-3-98	0.0419 ± 0.0015	0.312 ± 0.037	264.7 ± 9.5	276 ± 33	95.9 0.48
120612-3-45	0.0440 ± 0.0012	0.335 ± 0.030	277.3 ± 7.7	294 ± 27	94.4 0.53	120612-3-99	0.0462 ± 0.0015	0.339 ± 0.031	290.9 ± 9.2	297 ± 27	98.1 0.64
120612-3-46	0.0426 ± 0.0013	0.335 ± 0.035	269.1 ± 8.2	293 ± 31	91.8 0.76	120612-3-100	0.0441 ± 0.0015	0.335 ± 0.036	278.0 ± 9.5	294 ± 32	94.7 0.55
120612-3-47	0.0458 ± 0.0016	0.337 ± 0.045	289 ± 10	295 ± 40	97.9 0.58	120612-3-101	0.0464 ± 0.0018	0.339 ± 0.039	292 ± 11	296 ± 34	98.7 0.66
120612-3-48	0.0426 ± 0.0017	0.339 ± 0.025	269 ± 11	327 ± 47	82.4 0.43	120612-3-102	0.0422 ± 0.0015	0.396 ± 0.033	266.3 ± 9.3	339 ± 28	78.6 0.85
120612-3-49	0.0408 ± 0.0012	0.288 ± 0.031	257.9 ± 7.8	257 ± 28	100.4 0.54	120612-3-103	0.0423 ± 0.0016	0.274 ± 0.031	267.0 ± 9.8	246 ± 28	108.6 0.52
120612-3-50	0.0414 ± 0.0012	0.312 ± 0.036	261.5 ± 7.6	276 ± 32	94.8 0.63	120612-3-104	0.0416 ± 0.0014	0.369 ± 0.031	262.6 ± 9.7	319 ± 26	82.4 0.64
120612-3-51	0.03931 ± 0.00090	0.295 ± 0.024	248.6 ± 5.7	263 ± 22	94.7 0.75	120612-3-105	0.0444 ± 0.0016	0.334 ± 0.039	280 ± 11	293 ± 34	95.8 0.55
120612-3-52	0.03951 ± 0.00089	0.267 ± 0.022	249.8 ± 5.6	241 ± 20	103.8 0.79	120612-3-106	0.0456 ± 0.0016	0.366 ± 0.034	287 ± 10	317 ± 29	90.7 0.64
120612-3-53	0.0422 ± 0.0011	0.272 ± 0.030	266.6 ± 7.1	244 ± 27	109.3 0.64	120612-3-107	0.0440 ± 0.0016	0.426 ± 0.039	278 ± 10	360 ± 33	77.0 1.1
120612-3-54	0.0457 ± 0.0017	0.396 ± 0.058	288 ± 11	339 ± 50	85.0 0.54	120612-3-108	0.0428 ± 0.0012	0.304 ± 0.023	270.3 ± 7.4	269 ± 21	100.4 0.91
120612-3-55	0.0431 ± 0.0011	0.292 ± 0.029	271.7 ± 6.8	260 ± 26	104.4 0.57	120612-3-109	0.0437 ± 0.0015	0.368 ± 0.042	287.8 ± 9.7	318 ± 36	90.4 0.53
120612-3-56	0.04204 ± 0.00090	0.300 ± 0.022	265.4 ± 5.7	266 ± 20	99.6 0.73	120612-3-110	0.0493 ± 0.0015	0.386 ± 0.047	310 ± 11	332 ± 41	93.5 0.56
120612-3-57	0.0446 ± 0.0015	0.328 ± 0.047	281.5 ± 9.6	288 ± 41	97.7 0.54	120612-3-111	0.0458 ± 0.0013	0.307 ± 0.028	288.5 ± 8.3	322 ± 24	106.2 0.42
120612-3-58	0.0435 ± 0.0015	0.263 ± 0.043	274.6 ± 9.6	237 ± 39	115.7 0.68	120612-3-112	0.0419 ± 0.0014	0.279 ± 0.034	264.7 ± 8.9	250 ± 31	106.0 0.67
120612-3-59	0.0440 ± 0.0018	0.359 ± 0.032	278 ± 11	311 ± 28	89.2 0.72	120612-3-113	0.0463 ± 0.0012	0.316 ± 0.023	291.9 ± 7.8	279 ± 20	104.8 0.72
120612-3-60	0.0406 ± 0.0021	0.290 ± 0.052	256 ± 13	258 ± 46	99.3 0.62	120612-3-114	0.0503 ± 0.0016	0.460 ± 0.045	316 ± 10	384 ± 38	82.3 0.74
120612-3-61	0.0467 ± 0.0020	0.372 ± 0.041	294 ± 13	321 ± 36	91.6 0.69	120612-3-115	0.0443 ± 0.0013	0.333 ± 0.029	279.7 ± 8.1	292 ± 25	95.9 0.71
120612-3-62	0.0421 ± 0.0018	0.418 ± 0.044	266 ± 12	355 ± 37	75.0 0.85	120612-3-116	0.0394 ± 0.0010	0.277 ± 0.028	248.9 ± 6.3	249 ± 25	100.1 0.66
120612-3-63	0.0418 ± 0.0018	0.311 ± 0.031	264 ± 11	275 ± 28	96.1 0.58	120612-3-117	0.0419 ± 0.0010	0.322 ± 0.029	263.4 ± 6.4	284 ± 26	92.9 0.91
120612-3-64	0.0430 ± 0.0018	0.318 ± 0.032	272 ± 11	281 ± 28	96.8 0.97	120612-3-118	0.04212 ± 0.00090	0.300 ± 0.024	265.9 ± 5.7	266 ± 21	99.9 0.64
120612-3-65	0.0431 ± 0.0018	0.298 ± 0.029	272 ± 11	265 ± 26	102.6 0.71	120612-3-119	0.0434 ± 0.0011	0.294 ± 0.030	273.7 ± 6.9	262 ± 27	104.6 0.75
120612-3-66	0.0422 ± 0.0027	0.304 ± 0.078	266 ± 17	269 ± 47	98.9 0.54	120612-3-120	0.04286 ± 0.00092	0.285 ± 0.023	270.5 ± 5.8	254 ± 21	106.3 0.56
120612-3-67	0.0410 ± 0.0014	0.307 ± 0.028	259.0 ± 8.7	272 ± 26	95.3 0.63	120612-3-121	0.0428 ± 0.0013	0.339 ± 0.028	270.4 ± 8.2	296 ± 36	91.2 0.59
120612-3-68	0.0413 ± 0.0014	0.333 ± 0.032	260.6 ± 9.0	292 ± 28	89.3 0.78	120612-3-122	0.0417 ± 0.0010	0.283 ± 0.027	255.1 ± 6.2	253 ± 24	100.8 0.62
120612-3-69	0.0449 ± 0.0014	0.327 ± 0.023	283.0 ± 8.8	287 ± 20	98.6 0.67	120612-3-123	0.0401 ± 0.0010	0.276 ± 0.028	253.7 ± 6.4	248 ± 25	102.4 0.61
120612-3-70	0.0409 ± 0.0015	0.276 ± 0.034	258.2 ± 9.6	247 ± 30	104.5 0.91	120612-3-124	0.04014 ± 0.0014	0.279 ± 0.020	253.7 ± 5.1	250 ± 18	101.6 0.59
120612-3-71	0.0416 ± 0.0015	0.319 ± 0.033	262.9 ± 17	269 ± 47	98.9 0.51	120612-3-125	0.0499 ± 0.0017	0.382 ± 0.033	314 ± 11	329 ± 45	95.4 0.46
120612-3-72	0.0415 ± 0.0015	0.325 ± 0.035	261.9 ± 9.4	286 ± 30	91.6 0.80	120612-3-126	0.0421 ± 0.0010	0.318 ± 0.026	265.8 ± 6.4	280 ± 23	94.9 0.61
120612-3-73	0.0434 ± 0.0016	0.298 ± 0.033	274.1 ± 9.8	265 ± 29	103.6 0.77	120612-3-127	0.0416 ± 0.0010	0.310 ± 0.024	262.8 ± 6.0	274 ± 21	95.8 0.78
120612-3-74	0.0435 ± 0.0015	0.294 ± 0.032	274.4 ± 9.7	261 ± 29	105.0 0.52	120612-3-128	0.0412 ± 0.0011	0.336 ± 0.031	260.5 ± 6.8	294 ± 27	88.5 0.49
120612-3-75	0.0419 ± 0.0017	0.288 ± 0.049	264 ± 11	257 ± 44	102.8 0.66	120612-3-129	0.0412 ± 0.0015	0.314 ± 0.047	260.4 ± 9.5	278 ± 41	93.8 0.81
120612-3-76	0.0453 ± 0.0019	0.368 ± 0.059	286 ± 12	318 ± 51	89.8 0.64	120612-3-130	0.0454 ± 0.0011	0.318 ± 0.026	286.5 ± 6.8	281 ± 23	102.1 0.61
120612-3-77	0.0445 ± 0.0012	0.330 ± 0.027	280.8 ± 7.9	290 ± 24	96.8 0.83	120612-3-131	0.0467 ± 0.0011	0.301 ± 0.025	294.5 ± 6.9	267 ± 23	110.3 0.67
120612-3-78	0.0438 ± 0.0012	0.317 ± 0.024	276.6 ± 7.5	280 ± 22	98.9 1.0	120612-3-132	0.0444 ± 0.0018	0.332 ± 0.058	280 ± 12	291 ± 51	96.2 0.46
120612-3-79	0.0427 ± 0.0012	0.307 ± 0.025	269.7 ± 7.5	272 ± 22	99.3 0.53						
120612-3-80	0.0429 ± 0.0012	0.302 ± 0.025	270.6 ± 7.5	268 ± 22	101.0 0.69						
120612-3-81	0.0429 ± 0.0012	0.336 ± 0.029	271.0 ± 7.8	294 ± 26	92.2 0.57						
120612-3-82	0.0479 ± 0.0016	0.305 ± 0.040	302 ± 10	271 ± 35	111.4 0.82						
120612-3-83	0.0414 ± 0.0011	0.278 ± 0.020	261.5 ± 6.9	249 ± 18	105.1 0.45						
120612-3-84	0.0448 ± 0.0013	0.300 ± 0.027	282.3 ± 8.2	268 ± 26	92.8 0.74						
120612-3-85	0.0420 ± 0.0011	0.341 ± 0.030	276.1 ± 7.0	265.1 ± 20	99.1 0.50						
120612-3-86	0.0418 ± 0.0012	0.295 ± 0.026	259.2 ± 7.5	262 ± 23	98.8 0.66						
120612-3-87	0.0459 ± 0.0015	0.323 ± 0.036	289.0 ± 9.3	284 ± 32	101.7 0.59						
120612-3-88	0.0444 ± 0.0013	0.300 ± 0.027	282.3 ± 8.2	268 ± 24	105.9 0.59						
120612-3-89	0.0420 ± 0.0011	0.301 ± 0.020	265.1 ± 7.0	268 ± 18	99.1 0.50						
120612-3-90	0.0419 ± 0.0011	0.281 ± 0.018	264.6 ± 7.1	251 ± 16	105.3 0.78						
120612-3-91	0.0428 ± 0.0013	0.277 ± 0.027	270.1 ± 8.3	248 ± 24	108.8 0.58						
120612-3-92	0.0408 ± 0.0012	0.298 ± 0.023	257.8 ± 7.6	264 ± 20	97.5 0.85						
120612-3-93	0.0422 ± 0.0013	0.313 ± 0.024	266.7 ± 8.0	276 ± 21	96.5 0.67						

TABLE I. (Continued)

Grain	$^{206}\text{Pb}/^{238}\text{U}$	$^{207}\text{Pb}/^{235}\text{U}$	$^{208}\text{Pb}/^{238}\text{U}$	$^{207}\text{Pb}/^{235}\text{U}$ age (Ma)	$^{208}\text{Pb}/^{238}\text{U}$ age (Ma)	$^{207}\text{Pb}/^{238}\text{U}$ age (Ma)	$^{206}\text{Pb}/^{238}\text{U}$	Grain	$^{206}\text{Pb}/^{238}\text{U}$	$^{207}\text{Pb}/^{235}\text{U}$	$^{208}\text{Pb}/^{238}\text{U}$	% conc Th/U
Lower Triassic Fukkoshi Formation (120613-2; N38°45'28.5", E141°31'39.19")												
120613-2-1	0.0420 ± 0.0011	0.311 ± 0.022	265.0 ± 6.6	275 ± 20	96.3	0.3	120613-2-55	0.0415 ± 0.0013	0.298 ± 0.0018	276 ± 11	265 ± 48	104.3 0.71
120613-2-2	0.0418 ± 0.0011	0.283 ± 0.021	264.1 ± 6.7	253 ± 19	104.4	0.67	120613-2-56	0.0437 ± 0.0011	0.283 ± 0.035	262.4 ± 8.1	253 ± 31	103.6 0.84
120613-2-3	0.0410 ± 0.0011	0.288 ± 0.023	258.8 ± 6.7	257 ± 21	100.6	0.49	120613-2-57	0.0453 ± 0.0014	0.294 ± 0.037	276.0 ± 6.9	282 ± 34	98.0 0.63
120613-2-4	0.0418 ± 0.0012	0.285 ± 0.028	263.8 ± 7.5	255 ± 25	103.5	0.60	120613-2-58	0.0467 ± 0.0014	0.322 ± 0.039	294.4 ± 9.0	283 ± 35	109.0 0.41
120613-2-5	0.0412 ± 0.0016	0.271 ± 0.044	260 ± 10	243 ± 40	106.9	0.71	120613-2-59	0.0452 ± 0.0013	0.285 ± 0.031	284.8 ± 7.9	255 ± 28	111.7 0.56
120613-2-6	0.0434 ± 0.0014	0.290 ± 0.036	273.9 ± 9.0	259 ± 32	105.9	0.72	120613-2-60	0.0425 ± 0.0011	0.314 ± 0.029	268.5 ± 7.1	277 ± 26	96.8 0.56
120613-2-7	0.0408 ± 0.0014	0.293 ± 0.035	257.7 ± 8.7	261 ± 31	98.7	0.53	120613-2-61	0.0453 ± 0.0012	0.334 ± 0.033	285.9 ± 7.9	292 ± 29	97.8 0.54
120613-2-8	0.0450 ± 0.0013	0.307 ± 0.029	283.6 ± 8.2	272 ± 25	104.3	0.58	120613-2-62	0.0416 ± 0.0014	0.308 ± 0.032	262.8 ± 9.0	273 ± 28	96.3 0.50
120613-2-9	0.0449 ± 0.0013	0.316 ± 0.031	283.0 ± 8.2	279 ± 28	101.6	0.58	120613-2-63	0.0441 ± 0.0015	0.306 ± 0.034	278.4 ± 9.6	271 ± 30	102.7 0.79
120613-2-10	0.0414 ± 0.0011	0.318 ± 0.025	261.3 ± 6.7	280 ± 22	93.3	0.76	120613-2-64	0.0439 ± 0.0014	0.303 ± 0.027	277.0 ± 8.8	268 ± 24	103.2 0.66
120613-2-11	0.0433 ± 0.0013	0.316 ± 0.035	273.0 ± 8.5	279 ± 31	97.9	0.48	120613-2-65	0.0516 ± 0.0019	0.359 ± 0.045	324 ± 12	312 ± 39	104.0 0.62
120613-2-12	0.0422 ± 0.0019	0.329 ± 0.059	266 ± 12	289 ± 52	92.1	0.67	120613-2-66	0.0454 ± 0.0019	0.341 ± 0.053	286 ± 12	298 ± 47	96.1 0.72
120613-2-13	0.0405 ± 0.0014	0.312 ± 0.042	255.9 ± 9.1	276 ± 37	92.7	0.86	120613-2-67	0.0455 ± 0.0020	0.278 ± 0.050	287 ± 13	249 ± 45	115.2 0.53
120613-2-14	0.0397 ± 0.0012	0.310 ± 0.033	251.1 ± 7.9	270 ± 30	92.9	0.63	120613-2-68	0.0434 ± 0.0017	0.305 ± 0.042	274 ± 11	270 ± 37	101.4 0.46
120613-2-15	0.0410 ± 0.0011	0.314 ± 0.029	259.3 ± 7.2	278 ± 26	93.4	0.52	120613-2-69	0.0421 ± 0.0020	0.404 ± 0.068	266 ± 13	344 ± 58	77.3 0.54
120613-2-16	0.0418 ± 0.0011	0.296 ± 0.023	264.0 ± 6.6	263 ± 20	100.4	0.66	120613-2-70	0.0430 ± 0.0013	0.300 ± 0.024	271.7 ± 8.3	267 ± 21	101.9 0.62
120613-2-17	0.0463 ± 0.0015	0.321 ± 0.037	291.9 ± 9.2	282 ± 33	103.3	0.37	120613-2-71	0.0426 ± 0.0012	0.295 ± 0.029	269.1 ± 7.3	263 ± 26	102.4 0.51
120613-2-18	0.0396 ± 0.0013	0.285 ± 0.033	250.4 ± 9.0	255 ± 30	98.3	0.64	120613-2-72	0.0404 ± 0.0014	0.294 ± 0.039	255.3 ± 8.7	262 ± 35	97.5 0.52
120613-2-19	0.0424 ± 0.0017	0.309 ± 0.049	268 ± 11	273 ± 43	98.0	0.53	120613-2-73	0.0422 ± 0.0016	0.263 ± 0.044	266 ± 11	270 ± 37	112.4 0.73
120613-2-20	0.0434 ± 0.0012	0.319 ± 0.028	273.8 ± 7.4	281 ± 25	97.5	0.80	120613-2-74	0.0414 ± 0.0011	0.286 ± 0.027	261.6 ± 6.9	255 ± 24	102.4 0.60
120613-2-21	0.0478 ± 0.0022	0.355 ± 0.066	301 ± 14	309 ± 57	97.5	0.43	120613-2-75	0.0482 ± 0.0017	0.417 ± 0.056	303 ± 11	354 ± 48	85.8 0.43
120613-2-22	0.0472 ± 0.0019	0.332 ± 0.055	297 ± 12	291 ± 48	102.3	0.39	120613-2-76	0.0391 ± 0.0010	0.255 ± 0.022	247.1 ± 6.1	231 ± 19	107.0 0.87
120613-2-23	0.0436 ± 0.0026	0.336 ± 0.051	275 ± 17	294 ± 44	93.4	0.44	120613-2-77	0.0458 ± 0.0012	0.336 ± 0.038	288.6 ± 7.8	311 ± 29	92.6 0.52
120613-2-24	0.0456 ± 0.0030	0.325 ± 0.064	288 ± 19	286 ± 56	100.7	0.51	120613-2-78	0.0426 ± 0.0013	0.357 ± 0.039	269.0 ± 8.2	310 ± 34	86.9 0.50
120613-2-25	0.0430 ± 0.0025	0.290 ± 0.039	271 ± 16	259 ± 35	105.0	0.57	120613-2-79	0.0452 ± 0.0023	0.297 ± 0.065	285 ± 14	264 ± 58	107.9 0.56
120613-2-26	0.0409 ± 0.0023	0.307 ± 0.038	259 ± 15	257 ± 33	100.6	0.52	120613-2-80	0.0430 ± 0.0015	0.306 ± 0.037	271.2 ± 9.4	271 ± 33	100.0 0.61
120613-2-27	0.0422 ± 0.0025	0.280 ± 0.039	267 ± 15	251 ± 35	106.2	0.55	120613-2-81	0.0427 ± 0.0014	0.318 ± 0.037	269.3 ± 9.1	281 ± 32	96.0 0.63
120613-2-28	0.0427 ± 0.0024	0.292 ± 0.030	270 ± 15	260 ± 27	103.8	0.42	120613-2-82	0.0424 ± 0.0014	0.336 ± 0.038	267.8 ± 7.8	294 ± 33	91.1 0.82
120613-2-29	0.0413 ± 0.0023	0.307 ± 0.037	261 ± 15	272 ± 33	96.0	0.57	120613-2-83	0.0404 ± 0.0014	0.331 ± 0.039	255.3 ± 9.0	290 ± 34	88.7 0.54
120613-2-30	0.0434 ± 0.0022	0.307 ± 0.039	271 ± 16	259 ± 35	105.0	0.57	120613-2-84	0.0410 ± 0.0017	0.269 ± 0.046	285 ± 14	242 ± 41	107.0 0.72
120613-2-31	0.0462 ± 0.0028	0.308 ± 0.037	259 ± 15	257 ± 33	100.6	0.52	120613-2-85	0.0442 ± 0.0014	0.380 ± 0.035	278.6 ± 8.6	327 ± 30	85.2 0.70
120613-2-32	0.0437 ± 0.0018	0.301 ± 0.033	276 ± 11	267 ± 30	103.3	0.72	120613-2-86	0.0416 ± 0.0018	0.245 ± 0.044	263 ± 11	223 ± 40	118.0 0.77
120613-2-33	0.0421 ± 0.0018	0.292 ± 0.039	266 ± 11	260 ± 27	102.0	0.55	120613-2-87	0.0440 ± 0.0018	0.351 ± 0.039	277 ± 11	305 ± 34	90.9 0.66
120613-2-34	0.0421 ± 0.0020	0.769 ± 0.69	266 ± 13	579 ± 69	45.9	0.69	120613-2-88	0.0449 ± 0.0029	0.297 ± 0.082	283 ± 19	264 ± 73	107.0 0.44
120613-2-35	0.0415 ± 0.0017	0.273 ± 0.030	274 ± 14	272 ± 50	100.8	0.48	120613-2-89	0.0410 ± 0.0017	0.351 ± 0.039	258 ± 11	305 ± 34	84.6 0.33
120613-2-36	0.0414 ± 0.0018	0.271 ± 0.038	291 ± 18	273 ± 73	107.5	0.41	120613-2-90	0.0433 ± 0.0023	0.310 ± 0.057	267 ± 14	267 ± 50	97.2 0.34
120613-2-37	0.0413 ± 0.0018	0.322 ± 0.054	261 ± 13	284 ± 48	92.0	0.49	120613-2-91	0.0437 ± 0.0018	0.289 ± 0.036	240 ± 10	258 ± 32	93.1 0.58
120613-2-38	0.0413 ± 0.0013	0.321 ± 0.033	261.1 ± 8.2	283 ± 29	92.3	0.55	120613-2-92	0.0415 ± 0.0018	0.303 ± 0.040	262 ± 11	269 ± 36	97.5 0.55
120613-2-39	0.0460 ± 0.0014	0.290 ± 0.029	290.1 ± 8.6	259 ± 26	112.2	0.40	120613-2-93	0.0420 ± 0.0017	0.304 ± 0.032	265 ± 11	269 ± 28	98.6 0.53
120613-2-40	0.0436 ± 0.0019	0.299 ± 0.053	262 ± 10	245 ± 27	107.1	0.70	120613-2-94	0.0445 ± 0.0016	0.308 ± 0.039	286 ± 10	273 ± 34	104.7 0.51
120613-2-41	0.0398 ± 0.0106	0.312 ± 0.048	252 ± 11	243 ± 34	107.5	0.50	120613-2-95	0.0470 ± 0.0021	0.297 ± 0.056	267 ± 14	249 ± 26	100.0 0.77
120613-2-42	0.0389 ± 0.0011	0.285 ± 0.024	246.2 ± 7.0	255 ± 22	96.6	0.66	120613-2-96	0.0435 ± 0.0018	0.317 ± 0.057	270 ± 11	279 ± 50	96.8 0.55
120613-2-43	0.0415 ± 0.0017	0.289 ± 0.030	262 ± 11	258 ± 27	101.5	0.68	120613-2-97	0.0437 ± 0.0017	0.317 ± 0.053	276 ± 11	280 ± 47	98.6 0.65
120613-2-44	0.0440 ± 0.0015	0.350 ± 0.041	277.5 ± 9.4	305 ± 35	91.0	0.57	120613-2-98	0.0435 ± 0.0016	0.332 ± 0.043	274 ± 10	291 ± 38	94.3 0.57
120613-2-45	0.0427 ± 0.0018	0.314 ± 0.034	269 ± 12	265 ± 12	97.3	0.69	120613-2-99	0.0447 ± 0.0015	0.491 ± 0.053	261.3 ± 9.5	246 ± 44	64.4 0.58
120613-2-46	0.0445 ± 0.0018	0.308 ± 0.030	281 ± 12	272 ± 26	103.1	0.55	120613-2-100	0.0394 ± 0.0013	0.278 ± 0.029	248.9 ± 8.2	249 ± 26	100.0 0.77
120613-2-47	0.0440 ± 0.0022	0.545 ± 0.064	277 ± 13	442 ± 52	62.8	0.51	120613-2-101	0.0429 ± 0.0017	0.317 ± 0.057	270 ± 11	279 ± 50	96.8 0.55
120613-2-48	0.0415 ± 0.0017	0.289 ± 0.030	262 ± 11	258 ± 27	101.5	0.68	120613-2-102	0.0437 ± 0.0017	0.317 ± 0.053	276 ± 11	280 ± 47	87.7 0.49
120613-2-49	0.0397 ± 0.0018	0.289 ± 0.034	251 ± 11	258 ± 31	97.4	0.57	120613-2-103	0.0422 ± 0.0010	0.276 ± 0.038	248 ± 34	248 ± 34	107.6 0.66
120613-2-50	0.0445 ± 0.0021	0.318 ± 0.035	305 ± 13	280 ± 31	109.0	0.67	120613-2-104	0.0415 ± 0.0015	0.281 ± 0.054	262 ± 11	252 ± 48	104.2 0.33
120613-2-51	0.0425 ± 0.0019	0.319 ± 0.038	268 ± 12	281 ± 34	95.6	0.69	120613-2-105	0.0454 ± 0.0013	0.330 ± 0.038	286.2 ± 8.0	289 ± 33	98.9 0.72
120613-2-52	0.0430 ± 0.0022	0.318 ± 0.053	271 ± 14	281 ± 47	96.7	0.50	120613-2-106	0.0389 ± 0.0013	0.306 ± 0.043	245.8 ± 8.3	271 ± 38	90.7 0.50
120613-2-53	0.0403 ± 0.0022	0.255 ± 0.033	230 ± 14	230 ± 48	110.6	0.57	120613-2-107	0.0401 ± 0.0010	0.290 ± 0.030	253.4 ± 6.5	258 ± 27	98.1 0.75

TABLE I. (Continued)

Grain	$^{206}\text{Pb}/^{238}\text{U}$	$^{207}\text{Pb}/^{235}\text{U}$	$^{208}\text{Pb}/^{238}\text{U}$	$^{207}\text{Pb}/^{235}\text{U}$ age (Ma)	$^{208}\text{Pb}/^{238}\text{U}$ age (Ma)	Grain	$^{206}\text{Pb}/^{238}\text{U}$	$^{207}\text{Pb}/^{235}\text{U}$	$^{208}\text{Pb}/^{238}\text{U}$	$^{207}\text{Pb}/^{235}\text{U}$ age (Ma)	$^{208}\text{Pb}/^{238}\text{U}$ age (Ma)	% conc Th/U	
Middle Triassic Isatomae Formation (130612-7-7; N38°42'48.27", E141°31'25.91")													
120612-7-1	0.6389 ± 0.0014	0.269 ± 0.037	246.2 ± 9.1	241 ± 33	102.0	0.47	120612-7-55	0.03751 ± 0.00084	0.341 ± 0.048	274 ± 11	298 ± 42	91.9	0.81
120612-7-2	0.0381 ± 0.0010	0.301 ± 0.018	251.2 ± 6.4	267 ± 16	102.0	0.86	120612-7-56	0.03792 ± 0.00084	0.274 ± 0.018	237.4 ± 5.3	246 ± 17	96.5	0.68
120612-7-3	0.0405 ± 0.0012	0.279 ± 0.026	256.1 ± 7.8	250 ± 24	102.5	0.52	120612-7-57	0.04353 ± 0.0012	0.335 ± 0.034	274.4 ± 7.7	256 ± 17	93.6	0.78
120612-7-4	0.0402 ± 0.0015	0.376 ± 0.043	253.8 ± 9.2	324 ± 37	78.3	0.57	120612-7-58	0.03917 ± 0.0013	0.331 ± 0.039	247.3 ± 8.0	290 ± 34	85.2	0.53
120612-7-5	0.0403 ± 0.0012	0.288 ± 0.025	254.9 ± 7.6	257 ± 22	99.3	0.68	120612-7-59	0.03632 ± 0.00081	0.285 ± 0.018	230.0 ± 5.1	255 ± 16	90.3	0.68
120612-7-6	0.03852 ± 0.00080	0.268 ± 0.022	243.6 ± 5.0	241 ± 20	100.9	0.57	120612-7-60	0.0380 ± 0.0010	0.291 ± 0.028	240.7 ± 6.6	259 ± 25	92.8	0.53
120612-7-7	0.0408 ± 0.0011	0.329 ± 0.034	257.5 ± 6.7	288 ± 30	89.3	0.51	120612-7-61	0.0413 ± 0.0012	0.294 ± 0.034	261.6 ± 7.9	261 ± 30	99.7	0.49
120612-7-8	0.03987 ± 0.00092	0.313 ± 0.028	252.0 ± 5.8	276 ± 25	91.2	0.54	120612-7-62	0.0414 ± 0.0010	0.320 ± 0.030	261.8 ± 6.3	282 ± 27	92.9	0.63
120612-7-9	0.0398 ± 0.0011	0.308 ± 0.036	251.3 ± 7.1	272 ± 32	92.3	0.70	120612-7-63	0.04054 ± 0.00089	0.306 ± 0.026	256.2 ± 5.6	271 ± 23	94.5	0.56
120612-7-10	0.03830 ± 0.00081	0.289 ± 0.024	242.3 ± 5.1	258 ± 21	93.9	0.37	120612-7-64	0.03933 ± 0.00085	0.280 ± 0.024	248.7 ± 5.4	251 ± 22	99.2	0.46
120612-7-11	0.0404 ± 0.0010	0.306 ± 0.032	255.2 ± 6.6	271 ± 29	94.0	0.52	120612-7-65	0.0411 ± 0.0010	0.334 ± 0.030	263.6 ± 6.1	292 ± 26	90.2	0.48
120612-7-12	0.04242 ± 0.00091	0.306 ± 0.026	267.8 ± 6.7	271 ± 23	98.8	0.41	120612-7-66	0.0436 ± 0.0015	0.366 ± 0.051	274.8 ± 9.3	316 ± 44	86.8	0.56
120612-7-13	0.03830 ± 0.00085	0.272 ± 0.025	242.3 ± 5.4	244 ± 22	99.2	0.80	120612-7-67	0.04048 ± 0.00078	0.291 ± 0.021	255.8 ± 4.9	259 ± 19	98.6	0.46
120612-7-14	0.03773 ± 0.00091	0.279 ± 0.022	238.7 ± 5.7	250 ± 20	95.6	0.70	120612-7-68	0.0401 ± 0.0010	0.283 ± 0.031	253.7 ± 6.6	253 ± 28	100.2	0.96
120612-7-15	0.0389 ± 0.0013	0.328 ± 0.041	246.2 ± 8.1	288 ± 36	85.5	0.58	120612-7-69	0.0406 ± 0.0013	0.404 ± 0.051	256.5 ± 8.5	344 ± 44	74.5	0.58
120612-7-16	0.0379 ± 0.0013	0.320 ± 0.042	251.9 ± 8.3	282 ± 37	94.5	0.57	120612-7-70	0.0407 ± 0.0013	0.303 ± 0.028	257.3 ± 8.2	269 ± 25	95.8	0.50
120612-7-17	0.0398 ± 0.0012	0.299 ± 0.034	251.7 ± 7.5	266 ± 30	94.8	0.66	120612-7-71	0.0389 ± 0.0013	0.338 ± 0.032	245.8 ± 8.7	296 ± 28	83.1	0.54
120612-7-18	0.0389 ± 0.0011	0.306 ± 0.030	245.8 ± 6.8	271 ± 27	90.8	0.55	120612-7-72	0.03732 ± 0.0011	0.268 ± 0.020	235.2 ± 6.9	241 ± 18	97.7	0.69
120612-7-19	0.0442 ± 0.0012	0.321 ± 0.030	278.6 ± 7.3	282 ± 27	98.6	0.72	120612-7-73	0.0420 ± 0.0016	0.382 ± 0.048	265 ± 10	329 ± 41	80.8	0.57
120612-7-20	0.0457 ± 0.0013	0.496 ± 0.046	288.3 ± 8.3	409 ± 38	70.5	0.89	120612-7-74	0.0382 ± 0.0013	0.301 ± 0.030	241.9 ± 8.1	267 ± 27	90.7	0.52
120612-7-21	0.0434 ± 0.0011	0.302 ± 0.026	273.6 ± 6.8	268 ± 23	102.1	0.87	120612-7-75	0.04014 ± 0.00092	0.310 ± 0.020	253.7 ± 7.8	274 ± 44	94.1	0.79
120612-7-22	0.0415 ± 0.0010	0.314 ± 0.019	262.0 ± 6.2	277 ± 17	94.6	0.65	120612-7-76	0.0391 ± 0.0012	0.306 ± 0.023	247.2 ± 7.3	271 ± 20	91.1	1.2
120612-7-23	0.0399 ± 0.0010	0.291 ± 0.021	252.4 ± 6.3	259 ± 19	97.4	0.60	120612-7-77	0.0413 ± 0.0013	0.318 ± 0.030	260.9 ± 8.4	281 ± 26	93.0	0.59
120612-7-24	0.0462 ± 0.0011	0.350 ± 0.024	291.4 ± 7.2	305 ± 21	95.7	0.60	120612-7-78	0.03735 ± 0.00089	0.271 ± 0.020	236.4 ± 5.6	243 ± 18	97.2	0.67
120612-7-25	0.0395 ± 0.0010	0.287 ± 0.024	249.7 ± 6.6	256 ± 21	97.4	0.38	120612-7-79	0.0396 ± 0.0011	0.315 ± 0.033	250.3 ± 7.3	278 ± 29	90.0	0.56
120612-7-26	0.0398 ± 0.0010	0.292 ± 0.022	251.6 ± 6.4	260 ± 21	96.7	0.42	120612-7-80	0.04014 ± 0.00092	0.304 ± 0.020	253.7 ± 5.8	269 ± 18	94.2	0.53
120612-7-27	0.0395 ± 0.0010	0.311 ± 0.019	250.0 ± 6.1	275 ± 18	91.0	0.54	120612-7-81	0.03895 ± 0.00085	0.277 ± 0.017	246.3 ± 5.4	248 ± 15	99.2	0.75
120612-7-28	0.0418 ± 0.0010	0.303 ± 0.021	264.1 ± 6.4	269 ± 18	98.2	0.45	120612-7-82	0.04045 ± 0.0013	0.287 ± 0.038	256.1 ± 8.4	256 ± 34	100.0	0.51
120612-7-29	0.0410 ± 0.0014	0.368 ± 0.046	258.9 ± 9.1	318 ± 40	81.3	0.43	120612-7-83	0.03935 ± 0.00010	0.282 ± 0.023	249.7 ± 6.1	252 ± 20	99.0	1.0
120612-7-30	0.0417 ± 0.0011	0.387 ± 0.031	263.4 ± 7.1	332 ± 26	79.3	0.62	120612-7-84	0.03944 ± 0.0011	0.269 ± 0.024	242.9 ± 6.2	242 ± 22	100.3	0.46
120612-7-31	0.0382 ± 0.0011	0.290 ± 0.029	241.9 ± 7.1	258 ± 26	93.6	0.59	120612-7-85	0.04244 ± 0.0015	0.396 ± 0.054	267.5 ± 9.7	339 ± 46	78.9	0.51
120612-7-32	0.0389 ± 0.0011	0.341 ± 0.032	246.0 ± 7.2	298 ± 28	82.7	0.52	120612-7-86	0.0424 ± 0.0012	0.290 ± 0.033	267.6 ± 7.9	259 ± 29	103.4	0.75
120612-7-33	0.0398 ± 0.0011	0.263 ± 0.025	251.3 ± 7.1	237 ± 23	105.9	0.47							
120612-7-34	0.0401 ± 0.0011	0.289 ± 0.026	253.7 ± 6.9	258 ± 23	98.5	0.76							
120612-7-35	0.03370 ± 0.0010	0.300 ± 0.027	234.3 ± 6.5	267 ± 24	87.9	0.59							
120612-7-36	0.0441 ± 0.0014	0.341 ± 0.040	278.0 ± 9.0	298 ± 35	93.3	0.47							
120612-7-37	0.0417 ± 0.0010	0.310 ± 0.019	263.3 ± 6.2	274 ± 17	96.0	0.65							
120612-7-38	0.0424 ± 0.0015	0.508 ± 0.058	267.7 ± 9.6	417 ± 47	64.2	0.46	120612-8-1	0.04249 ± 0.0013	0.321 ± 0.030	270.6 ± 7.9	282 ± 26	95.9	1.1
120612-7-39	0.0417 ± 0.0010	0.306 ± 0.022	263.2 ± 6.6	271 ± 19	92.4	0.39	120612-8-2	0.04281 ± 0.0018	0.287 ± 0.052	266 ± 12	256 ± 46	103.6	0.62
120612-7-40	0.0382 ± 0.0014	0.293 ± 0.037	241.9 ± 8.7	261 ± 33	92.6	0.65	120612-8-3	0.04642 ± 0.0021	0.410 ± 0.071	291 ± 13	349 ± 60	83.5	0.46
120612-7-41	0.0409 ± 0.0011	0.312 ± 0.019	258.2 ± 6.9	276 ± 17	93.6	0.70	120612-8-4	0.03977 ± 0.0011	0.301 ± 0.025	251.3 ± 7.0	267 ± 22	94.0	0.67
120612-7-42	0.0382 ± 0.0016	0.326 ± 0.048	241.9 ± 9.9	286 ± 42	84.5	0.78	120612-8-5	0.04337 ± 0.0014	0.307 ± 0.033	275.5 ± 8.6	272 ± 29	101.2	0.55
120612-7-43	0.0418 ± 0.0015	0.325 ± 0.040	264.1 ± 9.5	286 ± 35	92.4	0.75	120612-8-6	0.04042 ± 0.0013	0.320 ± 0.038	267.7 ± 8.1	282 ± 34	95.0	0.51
120612-7-44	0.0403 ± 0.0015	0.272 ± 0.037	254.8 ± 9.3	244 ± 33	104.3	0.56	120612-8-7	0.0454 ± 0.0018	0.286 ± 0.051	286 ± 11	256 ± 46	112.0	0.67
120612-7-45	0.0394 ± 0.0010	0.287 ± 0.016	248.8 ± 6.5	256 ± 15	97.3	1.0	120612-8-8	0.04222 ± 0.0011	0.282 ± 0.029	266.4 ± 7.0	252 ± 26	105.6	0.49
120612-7-46	0.0405 ± 0.0013	0.298 ± 0.030	255.6 ± 8.1	265 ± 26	96.6	0.50	120612-8-9	0.0345 ± 0.0014	0.224 ± 0.040	218.9 ± 8.8	205 ± 37	106.5	1.3
120612-7-47	0.0389 ± 0.0011	0.285 ± 0.023	246.3 ± 7.1	255 ± 20	96.6	0.60	120612-8-10	0.0334 ± 0.0016	0.262 ± 0.053	212 ± 10	237 ± 47	89.5	1.1
120612-7-48	0.0384 ± 0.0010	0.293 ± 0.019	243.0 ± 6.6	261 ± 17	93.2	0.62	120612-8-11	0.0424 ± 0.0013	0.320 ± 0.038	267.7 ± 8.1	282 ± 34	95.0	0.51
120612-7-49	0.0402 ± 0.0013	0.349 ± 0.030	254.7 ± 8.3	304 ± 26	83.6	0.52	120612-8-12	0.0454 ± 0.0018	0.286 ± 0.051	286 ± 11	256 ± 46	112.0	0.67
120612-7-50	0.0387 ± 0.0012	0.293 ± 0.023	244.5 ± 7.6	261 ± 21	93.8	0.49	120612-8-13	0.04221 ± 0.0010	0.287 ± 0.025	265.8 ± 6.2	256 ± 22	103.7	0.55
120612-7-51	0.0401 ± 0.0016	0.303 ± 0.040	253.3 ± 9.8	268 ± 36	94.4	0.90	120612-8-14	0.0418 ± 0.0015	0.268 ± 0.041	264.2 ± 9.3	241 ± 37	109.6	0.62
120612-7-52	0.0406 ± 0.0015	0.317 ± 0.037	256.8 ± 9.4	279 ± 33	92.0	0.49	120612-8-15	0.0352 ± 0.0020	0.341 ± 0.076	223 ± 13	298 ± 66	74.8	0.70
120612-7-53	0.0476 ± 0.0016	0.353 ± 0.036	300 ± 10	307 ± 31	97.5	0.95	120612-8-16	0.04053 ± 0.00090	0.302 ± 0.023	256.1 ± 5.7	268 ± 21	95.6	0.52

TABLE 1. (Continued)

Grain	$^{206}\text{Pb}/^{238}\text{U}$	$^{207}\text{Pb}/^{235}\text{U}$	$^{208}\text{Pb}/^{238}\text{U}$	$^{207}\text{Pb}/^{235}\text{U}$ age (Ma)	$^{208}\text{Pb}/^{238}\text{U}$ age (Ma)	$^{206}\text{Pb}/^{238}\text{U}$	Grain	$^{206}\text{Pb}/^{238}\text{U}$	$^{207}\text{Pb}/^{235}\text{U}$ age (Ma)	$^{208}\text{Pb}/^{238}\text{U}$ age (Ma)	% conc Th/U		
120612-8-17	0.0417 ± 0.0019	0.275 ± 0.053	263 ± 12	247 ± 48	106.6	0.61	120612-8-71	0.03224 ± 0.00076	204.6 ± 4.8	199 ± 19	102.6	0.40	
120612-8-18	0.0451 ± 0.0019	0.305 ± 0.052	284 ± 12	270 ± 46	105.3	0.55	120612-8-72	0.03939 ± 0.00017	0.674 ± 0.074	248 ± 11	523 ± 57	47.5	0.39
120612-8-19	0.0380 ± 0.0017	0.666 ± 0.082	241 ± 11	518 ± 64	46.5	0.94	120612-8-73	0.0439 ± 0.0017	0.343 ± 0.040	277 ± 11	299 ± 35	92.6	0.60
120612-8-20	0.0441 ± 0.0018	0.341 ± 0.053	278 ± 11	298 ± 46	93.5	0.58	120612-8-74	0.0392 ± 0.0015	0.294 ± 0.031	247.6 ± 9.3	261 ± 27	94.7	0.48
120612-8-21	0.0412 ± 0.0016	0.319 ± 0.044	260 ± 10	281 ± 39	95.5	0.72	120612-8-75	0.0386 ± 0.0016	0.286 ± 0.037	244.4 ± 9.9	256 ± 33	95.7	0.57
120612-8-22	0.0352 ± 0.0018	0.526 ± 0.084	223 ± 11	429 ± 69	51.9	0.48	120612-8-76	0.0347 ± 0.0017	0.281 ± 0.051	220 ± 11	251 ± 46	87.6	0.66
120612-8-23	0.0421 ± 0.0015	0.315 ± 0.039	266.0 ± 9.4	278 ± 34	95.5	0.95	120612-8-77	0.0405 ± 0.0016	0.275 ± 0.037	256 ± 10	247 ± 33	103.7	0.57
120612-8-24	0.0413 ± 0.0016	0.298 ± 0.041	261.0 ± 9.8	265 ± 37	98.7	0.63	120612-8-78	0.0399 ± 0.0014	0.292 ± 0.027	252.3 ± 9.0	260 ± 24	97.1	0.69
120612-8-25	0.0452 ± 0.0018	0.407 ± 0.058	285 ± 11	347 ± 49	82.2	0.63	120612-8-79	0.0424 ± 0.0019	0.280 ± 0.046	268 ± 12	251 ± 41	106.9	0.69
120612-8-26	0.0384 ± 0.0030	0.337 ± 0.052	243 ± 19	295 ± 54	82.3	0.54	120612-8-80	0.0398 ± 0.0015	0.290 ± 0.033	251.4 ± 9.6	258 ± 29	97.3	0.47
120612-8-27	0.0408 ± 0.0030	0.315 ± 0.031	258 ± 19	278 ± 28	92.8	0.52	120612-8-81	0.0404 ± 0.0015	0.282 ± 0.030	255.0 ± 9.2	252 ± 27	101.3	0.56
120612-8-28	0.0332 ± 0.0030	0.307 ± 0.078	211 ± 19	272 ± 69	77.4	0.89	120612-8-82	0.0420 ± 0.0015	0.288 ± 0.028	265.3 ± 9.2	257 ± 25	103.1	0.93
120612-8-29	0.0344 ± 0.0028	0.250 ± 0.050	218 ± 18	227 ± 45	96.2	0.40	120612-8-83	0.0415 ± 0.0017	0.286 ± 0.040	262 ± 11	255 ± 36	102.8	0.54
120612-8-30	0.0431 ± 0.0031	0.475 ± 0.048	272 ± 20	395 ± 40	68.9	0.52	120612-8-84	0.0420 ± 0.0019	0.250 ± 0.070	214 ± 14	226 ± 64	94.6	0.76
120612-8-31	0.0400 ± 0.0031	0.306 ± 0.051	253 ± 20	271 ± 45	93.4	0.65	120612-8-85	0.0404 ± 0.0016	0.263 ± 0.036	255 ± 10	237 ± 33	107.4	0.53
120612-8-32	0.0435 ± 0.0034	0.276 ± 0.047	275 ± 21	247 ± 42	111.0	0.52	120612-8-86	0.0418 ± 0.0020	0.278 ± 0.050	264 ± 12	249 ± 45	105.8	0.54
120612-8-33	0.0424 ± 0.0034	0.284 ± 0.059	267 ± 22	254 ± 52	105.2	0.55	120612-8-87	0.0422 ± 0.0016	0.311 ± 0.037	266 ± 10	275 ± 33	96.7	0.57
120612-8-34	0.0421 ± 0.0016	0.420 ± 0.057	266 ± 10	356 ± 49	74.6	0.62	120612-8-88	0.0408 ± 0.0014	0.310 ± 0.029	257.9 ± 9.1	274 ± 25	94.1	0.65
120612-8-35	0.0422 ± 0.0017	0.285 ± 0.048	266 ± 11	255 ± 43	104.6	0.60	120612-8-89	0.0372 ± 0.0024	0.201 ± 0.062	236 ± 7	186 ± 57	126.6	0.93
120612-8-36	0.0412 ± 0.0012	0.305 ± 0.032	260.0 ± 7.7	270 ± 28	96.2	0.78	120612-8-90	0.0428 ± 0.0012	0.329 ± 0.035	270.1 ± 7.7	289 ± 31	93.6	0.50
120612-8-37	0.0411 ± 0.0013	0.292 ± 0.035	260.0 ± 8.3	260 ± 32	99.9	0.54	120612-8-91	0.03890 ± 0.00086	0.314 ± 0.023	246.0 ± 5.5	278 ± 20	88.6	0.58
120612-8-38	0.0433 ± 0.0017	0.323 ± 0.051	273 ± 11	284 ± 45	96.3	0.82	120612-8-92	0.0432 ± 0.0017	0.293 ± 0.051	273 ± 11	261 ± 45	104.6	0.47
120612-8-39	0.0435 ± 0.0016	0.340 ± 0.048	274 ± 10	297 ± 42	92.3	0.70	120612-8-93	0.0428 ± 0.0011	0.330 ± 0.030	288.6 ± 7.2	289 ± 27	99.7	0.54
120612-8-40	0.0406 ± 0.0012	0.300 ± 0.032	256.4 ± 7.6	266 ± 28	96.3	0.67	120612-8-94	0.0422 ± 0.0015	0.387 ± 0.051	266.7 ± 9.5	332 ± 44	80.3	0.47
120612-8-41	0.0346 ± 0.0020	0.310 ± 0.079	220 ± 13	274 ± 70	80.7	0.80	120612-8-95	0.04216 ± 0.00094	0.298 ± 0.023	266.2 ± 5.9	265 ± 20	100.4	0.52
120612-8-42	0.0349 ± 0.0016	0.250 ± 0.050	220.9 ± 9.9	227 ± 45	97.4	0.94	120612-8-96	0.0428 ± 0.0017	0.338 ± 0.051	270 ± 11	295 ± 45	91.4	0.49
120612-8-43	0.0443 ± 0.0011	0.302 ± 0.022	279.6 ± 6.7	268 ± 20	104.4	0.53	120612-8-97	0.0425 ± 0.0015	0.304 ± 0.039	268.2 ± 9.5	269 ± 35	99.6	0.87
120612-8-44	0.0361 ± 0.0017	0.302 ± 0.058	229 ± 11	268 ± 31	85.3	1.2	120612-8-98	0.0424 ± 0.0014	0.296 ± 0.034	267.4 ± 8.8	263 ± 30	101.7	0.48
120612-8-45	0.0442 ± 0.0016	0.292 ± 0.046	279 ± 10	260 ± 41	107.1	0.73	120612-8-99	0.0346 ± 0.0022	0.270 ± 0.073	219 ± 14	242 ± 66	90.6	0.81
120612-8-46	0.0356 ± 0.0018	0.314 ± 0.064	226 ± 11	277 ± 56	81.5	0.64	120612-8-100	0.03599 ± 0.00112	0.273 ± 0.028	252.4 ± 7.8	245 ± 25	102.9	0.42
120612-8-47	0.0424 ± 0.0018	0.306 ± 0.033	268 ± 11	271 ± 29	98.7	0.76	120612-8-101	0.03552 ± 0.0010	0.241 ± 0.022	222.8 ± 6.5	219 ± 20	101.6	0.55
120612-8-48	0.0411 ± 0.0016	0.289 ± 0.023	260 ± 10	258 ± 21	100.6	0.48	120612-8-102	0.0346 ± 0.0017	0.236 ± 0.051	219 ± 11	215 ± 47	101.9	1.1
120612-8-49	0.0411 ± 0.0018	0.294 ± 0.035	259 ± 11	262 ± 31	99.1	0.45	120612-8-103	0.0411 ± 0.0015	0.354 ± 0.045	259.5 ± 9.5	308 ± 39	84.2	0.57
120612-8-50	0.0436 ± 0.0022	0.332 ± 0.056	275 ± 14	291 ± 49	94.5	0.73	120612-8-104	0.04225 ± 0.00017	0.380 ± 0.055	268 ± 11	327 ± 48	82.0	0.57
120612-8-51	0.0363 ± 0.0025	0.337 ± 0.086	230 ± 16	295 ± 75	78.0	1.0	120612-8-105	0.04040 ± 0.0012	0.301 ± 0.033	252.5 ± 7.5	267 ± 30	94.5	0.76
120612-8-52	0.0368 ± 0.0015	0.273 ± 0.028	233.2 ± 9.6	245 ± 25	95.1	0.70	120612-8-106	0.0398 ± 0.0010	0.273 ± 0.023	251.5 ± 6.2	245 ± 21	102.5	0.54
120612-8-53	0.0429 ± 0.0020	0.292 ± 0.043	271 ± 13	260 ± 39	104.0	0.70	120612-8-107	0.03241 ± 0.0021	0.300 ± 0.039	219 ± 13	266 ± 70	76.4	0.77
120612-8-54	0.0432 ± 0.0019	0.281 ± 0.036	272 ± 12	251 ± 32	108.4	0.54	120612-8-108	0.04049 ± 0.0013	0.262 ± 0.033	258.3 ± 8.0	236 ± 30	109.4	0.57
120612-8-55	0.0420 ± 0.0016	0.294 ± 0.023	265 ± 10	262 ± 20	101.3	0.72	120612-8-109	0.0419 ± 0.0013	0.282 ± 0.036	264.6 ± 8.3	252 ± 32	104.8	0.61
120612-8-56	0.0439 ± 0.0018	0.334 ± 0.050	277 ± 11	293 ± 44	94.7	0.47	120612-8-110	0.03330 ± 0.0019	0.223 ± 0.062	209 ± 12	204 ± 57	102.5	0.80
120612-8-57	0.0428 ± 0.0016	0.317 ± 0.041	270 ± 10	280 ± 36	96.6	0.56	120612-8-111	0.03317 ± 0.0018	0.266 ± 0.064	270 ± 12	240 ± 58	87.6	0.65
120612-8-58	0.0447 ± 0.0019	0.285 ± 0.047	282 ± 12	254 ± 42	110.9	0.60	120612-8-112	0.03231 ± 0.0018	0.223 ± 0.049	195.1 ± 9.6	204 ± 45	95.6	1.1
120612-8-59	0.0423 ± 0.0014	0.322 ± 0.032	266.8 ± 8.8	283 ± 28	94.1	0.61	120612-8-113	0.0376 ± 0.0014	0.279 ± 0.042	237.7 ± 8.8	250 ± 38	95.3	0.49
120612-8-60	0.0424 ± 0.0016	0.345 ± 0.042	267.7 ± 9.9	301 ± 37	88.9	0.40	120612-8-114	0.04042 ± 0.0015	0.293 ± 0.033	254.1 ± 9.4	261 ± 30	97.5	0.51
120612-8-61	0.0412 ± 0.0014	0.300 ± 0.034	260.2 ± 9.1	266 ± 30	97.7	0.58	120612-8-115	0.0418 ± 0.0018	0.319 ± 0.048	264 ± 11	281 ± 43	93.9	0.57
120612-8-62	0.0355 ± 0.0020	0.239 ± 0.057	225 ± 12	218 ± 52	103.2	0.86	120612-8-116	0.0426 ± 0.0018	0.321 ± 0.045	283 ± 40	95.2 ± 40	95.2	0.48
120612-8-63	0.0413 ± 0.0014	0.305 ± 0.034	260.7 ± 9.1	271 ± 30	96.4	0.56	120612-8-117	0.0409 ± 0.0018	0.290 ± 0.047	258 ± 11	259 ± 42	99.9	0.50
120612-8-64	0.0396 ± 0.0013	0.271 ± 0.028	250.5 ± 8.3	243 ± 25	103.0	0.48	120612-8-118	0.0365 ± 0.0024	0.235 ± 0.071	231 ± 15	215 ± 64	107.8	0.77
120612-8-65	0.0350 ± 0.0018	0.301 ± 0.064	222 ± 11	267 ± 57	83.0	0.95	120612-8-119	0.0372 ± 0.0023	0.304 ± 0.075	236 ± 15	270 ± 66	87.4	0.88
120612-8-66	0.0329 ± 0.0015	0.239 ± 0.050	208.7 ± 9.7	217 ± 45	96.0	0.91	120612-8-120	0.0427 ± 0.0015	0.301 ± 0.033	269.6 ± 9.7	267 ± 29	100.9	0.46
120612-8-67	0.0397 ± 0.0013	0.311 ± 0.042	270 ± 10	254 ± 37	91.1	0.54	120612-8-121	0.0415 ± 0.0018	0.299 ± 0.046	262 ± 11	265 ± 41	98.7	0.70
120612-8-68	0.0332 ± 0.0022	0.277 ± 0.079	210 ± 14	248 ± 71	84.7	0.75							
120612-8-69	0.0359 ± 0.0016	0.248 ± 0.051	227 ± 10	225 ± 46	101.1	0.72							
120612-8-70	0.04244 ± 0.00084	0.312 ± 0.022	267.9 ± 5.3	276 ± 19	97.2	0.76							

TABLE I. (Continued)

	Grain	$^{206}\text{Pb}/^{238}\text{U}$	$^{207}\text{Pb}/^{235}\text{U}$	$^{208}\text{Pb}/^{238}\text{U}$	$^{207}\text{Pb}/^{235}\text{U}$ age (Ma)	$^{206}\text{Pb}/^{238}\text{U}$ age (Ma)	$^{207}\text{Pb}/^{235}\text{U}$ age (Ma)	Grain	$^{206}\text{Pb}/^{238}\text{U}$	$^{207}\text{Pb}/^{235}\text{U}$	$^{208}\text{Pb}/^{238}\text{U}$	$^{207}\text{Pb}/^{235}\text{U}$ age (Ma)	$^{206}\text{Pb}/^{238}\text{U}$ age (Ma)	% conc Th/U		
Lower-Middle Jurassic Nirano-hama Formation (101001-2-2; N38°41'35.3", E141°30'05.0")																
101001-2-1	0.03754 ± 0.00064	0.2634 ± 0.0080	237.6 ± 4.0	237.4 ± 7.2	100.1	0.76	101001-2-55	0.04095 ± 0.00086	0.298 ± 0.013	258.4 ± 5.4	265 ± 11	97.5	0.74			
101001-2-2	0.03902 ± 0.00066	0.2717 ± 0.0073	246.8 ± 4.2	249.4 ± 7.1	98.9	0.74	101001-2-56	0.04023 ± 0.00086	0.306 ± 0.012	258.7 ± 5.3	271 ± 10	95.6	0.73			
101001-2-3	0.03839 ± 0.00064	0.2717 ± 0.0073	242.9 ± 4.1	244.1 ± 6.5	99.5	0.55	101001-2-57	0.0434 ± 0.0011	0.291 ± 0.014	254.2 ± 5.4	260 ± 12	97.9	0.62			
101001-2-4	0.04036 ± 0.00071	0.2933 ± 0.0111	255.0 ± 4.5	261 ± 10	97.9	0.70	101001-2-58	0.0401 ± 0.0011	0.467 ± 0.028	274.1 ± 7.8	389 ± 23	70.4	0.56			
101001-2-5	0.03908 ± 0.00066	0.2782 ± 0.0083	247.1 ± 4.2	249.3 ± 7.4	99.1	0.68	101001-2-59	0.0395 ± 0.0010	0.313 ± 0.015	253.4 ± 6.8	277 ± 14	91.6	0.89			
101001-2-6	0.04058 ± 0.00068	0.2928 ± 0.0077	256.4 ± 4.3	260.8 ± 6.8	98.3	0.79	101001-2-60	0.04040 ± 0.0011	0.286 ± 0.012	249.6 ± 6.6	255 ± 11	97.9	0.26			
101001-2-7	0.04170 ± 0.00070	0.3025 ± 0.0077	263.4 ± 4.4	268.3 ± 6.8	98.2	0.75	101001-2-61	0.0408 ± 0.0011	0.294 ± 0.013	258.0 ± 6.8	261 ± 11	98.7	0.72			
101001-2-8	0.04070 ± 0.00071	0.2933 ± 0.010	257.1 ± 4.5	260.9 ± 8.8	98.6	0.56	101001-2-62	0.0406 ± 0.0011	0.285 ± 0.012	256.6 ± 6.8	254 ± 11	101.0	0.56			
101001-2-9	0.04092 ± 0.00078	0.2755 ± 0.016	258.5 ± 4.9	247 ± 14	104.7	0.69	101001-2-63	0.0413 ± 0.0011	0.300 ± 0.015	260.7 ± 7.0	266 ± 13	97.9	0.95			
101001-2-10	0.0446 ± 0.0011	0.3233 ± 0.0111	281.4 ± 6.8	284.3 ± 9.8	99.0	0.46	101001-2-64	0.0426 ± 0.0012	0.328 ± 0.018	269.2 ± 7.4	288 ± 16	93.3	0.91			
101001-2-11	0.0431 ± 0.0010	0.3052 ± 0.0094	272.6 ± 6.5	270.4 ± 8.3	100.7	0.59	101001-2-65	0.0419 ± 0.0011	0.316 ± 0.015	264.3 ± 7.1	278 ± 13	94.9	0.78			
101001-2-12	0.0440 ± 0.0010	0.3030 ± 0.0084	277.6 ± 6.5	266.5 ± 7.4	104.2	0.83	101001-2-66	0.0391 ± 0.0013	0.292 ± 0.012	252.3 ± 7.9	260 ± 11	97.1	0.65			
101001-2-13	0.0437 ± 0.0010	0.3236 ± 0.010	275.5 ± 6.5	286.7 ± 8.7	96.1	0.77	101001-2-67	0.0433 ± 0.0014	0.325 ± 0.015	273.2 ± 8.6	286 ± 13	95.6	0.96			
101001-2-14	0.06355 ± 0.0015	0.489 ± 0.019	396.6 ± 9.7	404 ± 16	98.2	0.65	101001-2-68	0.0416 ± 0.0013	0.312 ± 0.014	262.9 ± 8.3	275 ± 12	95.4	0.85			
101001-2-15	0.04065 ± 0.00096	0.2948 ± 0.0089	256.9 ± 6.1	262.3 ± 8.0	97.9	0.64	101001-2-69	0.0411 ± 0.0013	0.296 ± 0.019	259.8 ± 8.4	264 ± 17	98.6	0.42			
101001-2-16	0.03985 ± 0.00096	0.276 ± 0.010	251.9 ± 6.1	247.5 ± 9.0	101.8	0.93	101001-2-70	0.0425 ± 0.0013	0.369 ± 0.016	268.6 ± 8.5	319 ± 14	84.3	1.1			
101001-2-17	0.0421 ± 0.0011	0.308 ± 0.016	266.1 ± 6.8	272 ± 14	97.7	0.78	101001-2-71	0.0402 ± 0.0013	0.288 ± 0.012	254.3 ± 8.0	257 ± 11	99.0	0.69			
101001-2-18	0.04046 ± 0.00046	0.2815 ± 0.0083	255.7 ± 2.9	251.9 ± 7.5	101.5	0.59	101001-2-72	0.0427 ± 0.0013	0.319 ± 0.013	269.8 ± 8.5	281 ± 11	96.0	0.75			
101001-2-19	0.04153 ± 0.00044	0.3077 ± 0.0064	262.3 ± 2.8	272.4 ± 5.7	96.3	1.2										
101001-2-20	0.0428 ± 0.0014	0.3722 ± 0.017	270.0 ± 8.8	321 ± 15	84.7	0.88										
101001-2-21	0.0412 ± 0.0013	0.2828 ± 0.013	260.1 ± 8.5	253 ± 12	102.8	0.55										
101001-2-22	0.0434 ± 0.0014	0.3111 ± 0.013	274.2 ± 8.8	275 ± 12	99.8	0.52										
101001-2-23	0.0411 ± 0.0013	0.3036 ± 0.016	259.7 ± 8.5	271 ± 14	95.7	0.78										
101001-2-24	0.0410 ± 0.0013	0.3112 ± 0.015	258.8 ± 8.4	276 ± 13	93.9	1.2	120612-4-1	0.0431 ± 0.0019	0.292 ± 0.045	272 ± 12	237 ± 40	104.4	0.41			
101001-2-25	0.0424 ± 0.0014	0.318 ± 0.014	267.5 ± 8.6	280 ± 12	95.4	1.3	120612-4-2	0.0414 ± 0.0019	0.263 ± 0.045	262 ± 12	237 ± 40	101.3	0.70			
101001-2-26	0.0418 ± 0.0014	0.2922 ± 0.013	263.8 ± 8.5	260 ± 12	101.4	0.52	120612-4-3	0.0416 ± 0.0024	0.388 ± 0.080	262 ± 15	333 ± 69	78.9	0.39			
101001-2-27	0.0414 ± 0.0013	0.2977 ± 0.010	261.3 ± 8.4	264.0 ± 9.3	99.0	0.85	120612-4-4	0.0415 ± 0.0016	0.291 ± 0.033	262 ± 10	260 ± 30	101.0	0.49			
101001-2-28	0.0432 ± 0.0013	0.308 ± 0.014	272.3 ± 8.4	273 ± 12	99.9	0.59	120612-4-5	0.0324 ± 0.0012	0.241 ± 0.021	205.4 ± 7.5	219 ± 19	93.8	0.43			
101001-2-29	0.0427 ± 0.0013	0.3038 ± 0.015	269.3 ± 8.4	273 ± 13	98.8	0.60	120612-4-6	0.0290 ± 0.0010	0.194 ± 0.017	184.4 ± 6.7	180 ± 16	102.4	0.57			
101001-2-30	0.0416 ± 0.0012	0.3141 ± 0.016	262.7 ± 7.8	277 ± 14	94.8	0.58	120612-4-7	0.0285 ± 0.0011	0.205 ± 0.019	178.8 ± 6.7	189 ± 18	94.4	0.54			
101001-2-31	0.0404 ± 0.0012	0.2877 ± 0.013	255.1 ± 7.5	256 ± 12	99.6	0.42	120612-4-8	0.0399 ± 0.0014	0.288 ± 0.022	252.2 ± 9.0	257 ± 20	98.1	0.37			
101001-2-32	0.0392 ± 0.0012	0.3011 ± 0.020	247.8 ± 7.6	267 ± 18	92.7	0.58	120612-4-9	0.0429 ± 0.0015	0.337 ± 0.047	270.7 ± 9.2	295 ± 41	91.8	0.45			
101001-2-33	0.0406 ± 0.0012	0.2944 ± 0.011	256.6 ± 7.6	262 ± 10	97.9	0.59	120612-4-10	0.03124 ± 0.00072	0.212 ± 0.019	198.3 ± 4.6	195 ± 17	101.6	0.40			
101001-2-34	0.0405 ± 0.0012	0.2899 ± 0.012	255.7 ± 7.6	257 ± 11	99.3	0.76	120612-4-11	0.04485 ± 0.00089	0.289 ± 0.020	282.8 ± 5.6	260 ± 18	108.7	0.99			
101001-2-35	0.0401 ± 0.0012	0.2755 ± 0.016	253.3 ± 7.8	247 ± 14	102.6	0.98	120612-4-12	0.0463 ± 0.0017	0.323 ± 0.052	292 ± 11	284 ± 46	102.9	0.46			
101001-2-36	0.0415 ± 0.0012	0.3044 ± 0.012	262.2 ± 7.8	270 ± 11	97.2	0.58	120612-4-13	0.0438 ± 0.0011	0.344 ± 0.030	276.2 ± 6.7	300 ± 27	92.0	0.57			
101001-2-37	0.0416 ± 0.0012	0.2929 ± 0.011	262.7 ± 7.8	260.0 ± 9.9	101.0	0.67	120612-4-14	0.03099 ± 0.00069	0.212 ± 0.018	191.1 ± 4.4	195 ± 17	97.8	0.78			
101001-2-38	0.0413 ± 0.0013	0.2877 ± 0.016	260.7 ± 8.0	256 ± 14	101.9	0.96	120612-4-15	0.04465 ± 0.00087	0.327 ± 0.022	281.6 ± 5.5	287 ± 19	98.2	0.50			
101001-2-39	0.0418 ± 0.0012	0.3036 ± 0.015	258.1 ± 7.8	263.9 ± 12	95.2	1.1	120612-4-16	0.0475 ± 0.0018	0.289 ± 0.033	279 ± 12	258 ± 47	116.1	0.48			
101001-2-40	0.0404 ± 0.0012	0.2909 ± 0.012	263.5 ± 7.4	275 ± 11	95.9	0.63	120612-4-17	0.03416 ± 0.00083	0.211 ± 0.021	216.5 ± 5.2	195 ± 19	111.2	0.34			
101001-2-41	0.0411 ± 0.0012	0.3039 ± 0.012	255.3 ± 7.8	259.8 ± 7.7	274 ± 11	94.9	1.1	120612-4-18	0.0399 ± 0.0012	0.277 ± 0.023	252.3 ± 7.8	248 ± 20	101.7	0.23		
101001-2-42	0.0408 ± 0.0012	0.3448 ± 0.022	257.6 ± 7.7	303 ± 19	85.0	0.47	120612-4-19	0.0422 ± 0.0019	0.283 ± 0.052	266 ± 12	253 ± 46	105.3	0.62			
101001-2-43	0.0408 ± 0.0012	0.3117 ± 0.017	257.9 ± 7.5	280 ± 15	92.3	0.98	120612-4-20	0.04040 ± 0.0012	0.292 ± 0.022	252.6 ± 7.7	260 ± 20	97.1	0.49			
101001-2-44	0.0418 ± 0.0012	0.3036 ± 0.014	254.9 ± 7.5	267 ± 12	98.9	0.92	120612-4-21	0.0439 ± 0.0015	0.305 ± 0.034	276.8 ± 9.6	270 ± 30	102.5	0.36			
101001-2-45	0.0417 ± 0.0012	0.3111 ± 0.012	263.5 ± 7.4	275 ± 11	97.7	0.59	120612-4-22	0.0449 ± 0.0018	0.348 ± 0.048	283 ± 11	303 ± 41	93.3	0.50			
101001-2-46	0.0436 ± 0.0012	0.3133 ± 0.015	275.3 ± 7.9	276 ± 13	99.7	0.58	120612-4-23	0.0372 ± 0.0014	0.355 ± 0.042	235.3 ± 8.9	308 ± 36	76.4	0.71			
101001-2-47	0.0417 ± 0.0012	0.3100 ± 0.012	263.4 ± 7.4	274 ± 11	96.2	1.0	120612-4-24	0.0303 ± 0.0011	0.227 ± 0.025	192.4 ± 6.7	208 ± 22	92.6	0.64			
101001-2-48	0.0409 ± 0.0011	0.3000 ± 0.011	254.8 ± 7.3	267 ± 10	97.0	0.78	120612-4-25	0.022 ± 0.016	0.292 ± 0.016	207.3 ± 6.2	204 ± 15	101.8	0.49			
101001-2-49	0.04034 ± 0.00085	0.2939 ± 0.012	254.9 ± 7.5	262 ± 11	97.4	1.1	120612-4-26	0.0453 ± 0.0016	0.336 ± 0.040	286 ± 10	294 ± 35	97.2	0.49			
101001-2-50	0.04159 ± 0.00087	0.3033 ± 0.012	262.7 ± 5.5	269 ± 11	97.7	0.43	120612-4-27	0.0448 ± 0.0019	0.377 ± 0.063	282 ± 12	325 ± 54	87.0	0.45</td			

TABLE 1. (Continued)

Grain	$^{206}\text{Pb}/^{238}\text{U}$	$^{207}\text{Pb}/^{235}\text{U}$	$^{208}\text{Pb}/^{238}\text{U}$	$^{207}\text{Pb}/^{235}\text{U}$ age (Ma)	$^{208}\text{Pb}/^{238}\text{U}$ age (Ma)	$^{207}\text{Pb}/^{238}\text{U}$ age (Ma)	Grain	$^{206}\text{Pb}/^{238}\text{U}$	$^{207}\text{Pb}/^{235}\text{U}$	$^{208}\text{Pb}/^{238}\text{U}$	$^{207}\text{Pb}/^{235}\text{U}$ age (Ma)	$^{208}\text{Pb}/^{238}\text{U}$ age (Ma)	$^{207}\text{Pb}/^{235}\text{U}$ age (Ma)	% conc Th/U	% conc U	% conc Th/U	% conc U		
Upper Jurassic Sodenohama Formation (101001-3; N38°40'22.9", E141°28'05.3")																			
120612-4-31	0.0458 ± 0.0019	0.321 ± 0.056	288 ± 12	283 ± 49	102.0	0.56	120612-4-85	0.0394 ± 0.0014	0.304 ± 0.044	249.2	± 8.8	270	± 39	92.3	0.57				
120612-4-32	0.0363 ± 0.0011	0.271 ± 0.026	229.9 ± 6.9	243 ± 23	94.4	0.96													
120612-4-33	0.0407 ± 0.0015	0.350 ± 0.047	257.0 ± 9.7	304 ± 41	84.4	0.36													
120612-4-34	0.0462 ± 0.0021	0.343 ± 0.047	291 ± 13	300 ± 41	97.1	0.35													
120612-4-35	0.2281 ± 0.0085	0.339 ± 0.22	1324 ± 50	1503 ± 97	88.1	0.21													
120612-4-36	0.0286 ± 0.0011	0.194 ± 0.016	181.7 ± 7.0	180 ± 15	100.9	0.23													
120612-4-37	0.0472 ± 0.0029	0.321 ± 0.082	297 ± 18	283 ± 7.3	105.1	0.52	101001-3-1	0.04386 ± 0.00058	0.2973 ± 0.0078	276.7	± 3.7	264.3	± 6.9	104.7	0.45				
120612-4-38	0.0380 ± 0.0016	0.246 ± 0.028	240 ± 10	223 ± 26	107.8	0.49	101001-3-2	0.02836 ± 0.00040	0.2194 ± 0.0086	180.3	± 2.6	201.4	± 7.9	89.5	0.38				
120612-4-39	0.0423 ± 0.0019	0.293 ± 0.039	267 ± 12	261 ± 35	102.1	0.50	101001-3-3	0.03574 ± 0.00038	0.2372 ± 0.0071	226.4	± 3.1	216.1	± 6.5	104.8	1.3				
120612-4-40	0.0274 ± 0.0012	0.187 ± 0.026	174.3 ± 7.8	174 ± 59	101001-3-4	0.02792 ± 0.00038	0.2125 ± 0.0061	177.5	± 2.4	195.6	± 5.6	90.7	0.31						
120612-4-41	0.3361 ± 0.0131	5.12 ± 0.37	186.8 ± 73	1839 ± 134	101.6	0.68	101001-3-5	0.02669 ± 0.00037	0.1961 ± 0.0064	169.8	± 2.3	181.8	± 6.0	93.4	0.56				
120612-4-42	0.0468 ± 0.0024	0.341 ± 0.070	295 ± 15	298 ± 61	98.9	0.49	101001-3-6	0.02960 ± 0.00042	0.1812 ± 0.0073	188.1	± 2.6	169.1	± 6.8	111.2	0.38				
120612-4-43	0.3302 ± 0.0090	5.31 ± 0.22	1839 ± 50	1871 ± 77	98.3	0.40	101001-3-7	0.03464 ± 0.00048	0.2317 ± 0.0082	219.5	± 3.0	211.6	± 7.5	103.7	0.82				
120612-4-44	0.0623 ± 0.0022	0.585 ± 0.059	390 ± 14	467 ± 47	83.4	0.46	101001-3-8	0.03002 ± 0.00042	0.2131 ± 0.0063	190.7	± 2.6	196.2	± 5.8	97.0	0.70				
120612-4-45	0.0287 ± 0.0012	0.198 ± 0.031	182.4 ± 7.7	183 ± 29	99.6	0.53	101001-3-9	0.03362 ± 0.00047	0.2497 ± 0.0082	213.2	± 3.0	226.4	± 7.5	94.2	0.74				
120612-4-46	0.0492 ± 0.0018	0.324 ± 0.041	309 ± 11	285 ± 36	108.5	0.55	101001-3-10	0.02836 ± 0.00051	0.1901 ± 0.0060	180.2	± 3.2	176.7	± 5.6	102.0	0.35				
120612-4-47	0.0402 ± 0.0017	0.369 ± 0.050	254 ± 10	319 ± 43	79.6	0.64	101001-3-11	0.02616 ± 0.00047	0.1804 ± 0.0052	166.5	± 3.0	168.4	± 4.9	98.9	0.42				
120612-4-48	0.0447 ± 0.0013	0.290 ± 0.032	281.9 ± 8.2	259 ± 28	108.9	0.23	101001-3-12	0.02821 ± 0.00051	0.1923 ± 0.0051	179.4	± 3.7	178.6	± 4.7	100.5	0.53				
120612-4-49	0.0426 ± 0.0013	0.335 ± 0.038	268.8 ± 8.4	293 ± 33	91.7	0.46	101001-3-13	0.02659 ± 0.00048	0.1852 ± 0.0064	169.2	± 3.1	172.5	± 5.9	98.1	1.5				
120612-4-50	0.02855 ± 0.00085	0.199 ± 0.022	181.5 ± 5.4	184 ± 20	98.6	0.51	101001-3-14	0.02980 ± 0.00053	0.1988 ± 0.0065	184.8	± 3.3	184.1	± 6.1	100.4	0.44				
120612-4-51	0.0451 ± 0.0019	0.299 ± 0.055	284 ± 12	266 ± 49	107.0	0.43	101001-3-15	0.03146 ± 0.00046	0.2226 ± 0.010	199.7	± 3.7	207.0	± 9.3	96.5	0.99				
120612-4-52	0.0320 ± 0.0010	0.274 ± 0.030	202.8 ± 6.4	246 ± 27	82.4	0.71	101001-3-16	0.0478 ± 0.00026	2.108 ± 0.0045	88.9	± 16	151	± 24	77.2	0.23				
120612-4-53	0.0445 ± 0.0017	0.404 ± 0.056	281 ± 11	345 ± 48	81.4	0.59	101001-3-17	0.03037 ± 0.00058	0.204 ± 0.011	192.9	± 3.7	188	± 10	102.4	0.58				
120612-4-54	0.0461 ± 0.0021	0.296 ± 0.059	290 ± 13	263 ± 52	110.3	0.29	101001-3-18	0.02812 ± 0.0006	1.180 ± 0.026	54.5	± 9.6	79.1	± 18	68.9	0.36				
120612-4-55	0.0454 ± 0.0021	0.347 ± 0.065	286 ± 13	302 ± 56	94.6	0.47	101001-3-19	0.03251 ± 0.00049	0.2221 ± 0.0085	206.2	± 3.1	203.7	± 7.8	101.3	0.39				
120612-4-56	0.0408 ± 0.0017	0.288 ± 0.028	258 ± 11	257 ± 25	100.5	0.85	101001-3-20	0.02815 ± 0.00040	0.2002 ± 0.0059	178.9	± 2.6	185.3	± 5.5	96.6	0.45				
120612-4-57	0.0440 ± 0.0020	0.294 ± 0.037	278 ± 12	262 ± 33	106.1	0.69	101001-3-21	0.03842 ± 0.00053	0.2722 ± 0.0066	243.0	± 3.4	244.4	± 5.9	99.4	0.41				
120612-4-58	0.374 ± 0.014	5.86 ± 0.26	204.6 ± 77	1956 ± 87	104.6	0.10	101001-3-22	0.0738 ± 0.0010	0.590 ± 0.013	45.9	± 6.3	47.1	± 11	97.4	1.1				
120612-4-59	0.0290 ± 0.0013	0.200 ± 0.023	184.4 ± 8.0	185 ± 21	99.5	0.36	101001-3-23	0.02678 ± 0.00038	0.1773 ± 0.0054	170.4	± 2.4	165.7	± 5.1	102.8	0.47				
120612-4-60	0.0355 ± 0.0015	0.297 ± 0.026	224.9 ± 9.3	264 ± 23	85.2	0.49	101001-3-24	0.03536 ± 0.00050	0.2504 ± 0.0072	224.0	± 3.2	226.9	± 6.5	98.7	0.58				
120612-4-61	0.287 ± 0.011	4.75 ± 0.22	1627 ± 62	1777 ± 81	91.6	0.14	101001-3-25	0.03591 ± 0.00050	0.2468 ± 0.0060	227.4	± 3.2	224.0	± 5.4	101.5	0.62				
120612-4-62	0.0265 ± 0.0011	0.167 ± 0.018	168.8 ± 7.2	157 ± 17	107.5	0.43	101001-3-26	0.04063 ± 0.00067	0.2910 ± 0.0090	256.8	± 5.1	259.4	± 8.0	99.0	0.81				
120612-4-63	0.0438 ± 0.0014	0.293 ± 0.038	276.6 ± 9.1	261 ± 34	106.1	0.62	101001-3-27	0.03365 ± 0.00067	0.2385 ± 0.0079	213.4	± 4.2	217.2	± 7.2	98.2	0.84				
120612-4-64	0.3016 ± 0.0062	4.65 ± 0.16	169.9 ± 35	1758 ± 60	96.6	0.40	101001-3-28	0.03049 ± 0.00060	0.2016 ± 0.0061	193.6	± 3.8	186.5	± 5.6	103.8	0.56				
120612-4-65	0.02614 ± 0.00085	0.193 ± 0.024	166.4 ± 5.4	179 ± 22	92.8	0.46	101001-3-29	0.02879 ± 0.00057	0.2050 ± 0.0063	183.0	± 3.6	189.4	± 5.8	96.6	0.76				
120612-4-66	0.02826 ± 0.00089	0.217 ± 0.025	179.6 ± 5.7	201 ± 23	89.6	0.59	101001-3-30	0.03186 ± 0.00061	5.00 ± 0.12	178.3	± 34	181.9	± 43	98.0	0.67				
120612-4-67	0.03333 ± 0.00079	0.223 ± 0.016	211.4 ± 5.0	205 ± 14	103.2	0.45	101001-3-31	0.02630 ± 0.00053	0.1791 ± 0.0065	167.4	± 3.3	167.3	± 6.0	100.1	0.64				
120612-4-68	0.3526 ± 0.0071	5.68 ± 0.18	194.7 ± 39	1928 ± 61	101.0	0.43	101001-3-32	0.02878 ± 0.00056	0.2014 ± 0.0055	182.9	± 3.6	186.3	± 5.1	98.2	0.53				
120612-4-69	0.0290 ± 0.0010	0.190 ± 0.027	184.1 ± 6.5	176 ± 26	104.4	0.49	101001-3-33	0.02685 ± 0.00052	0.1875 ± 0.0051	170.8	± 3.3	174.5	± 4.8	97.9	0.25				
120612-4-70	0.0412 ± 0.0011	0.287 ± 0.028	260.5 ± 7.2	256 ± 25	101.7	0.40	101001-3-34	0.03307 ± 0.00041	5.20 ± 0.12	184.2	± 23	185.2	± 44	99.5	0.18				
120612-4-71	0.3372 ± 0.0066	5.37 ± 0.15	187.3 ± 37	1880 ± 53	99.6	0.18	101001-3-35	0.03415 ± 0.00048	0.2536 ± 0.0098	216.5	± 8.9	229.5	± 8.9	94.3	0.81				
120612-4-72	0.02818 ± 0.00081	0.208 ± 0.022	179.1 ± 5.1	192 ± 20	93.4	0.36	101001-3-36	0.03582 ± 0.00047	0.2511 ± 0.0078	226.9	± 3.0	227.4	± 7.1	99.8	0.60				
120612-4-73	0.02849 ± 0.00077	0.204 ± 0.020	181.1 ± 4.9	189 ± 18	96.0	0.35	101001-3-37	0.03412 ± 0.00052	0.2596 ± 0.0083	260.3	± 3.3	266.1	± 7.3	97.9	1.1				
120612-4-74	0.0423 ± 0.0011	0.282 ± 0.028	267.0 ± 7.1	252 ± 25	106.0	0.63													
120612-4-75	0.0439 ± 0.0029	0.45 ± 0.11	277 ± 18	377 ± 95	73.3	0.44													
120612-4-76	0.0411 ± 0.0011	0.316 ± 0.028	259.8 ± 6.8	278 ± 25	93.3	0.46													
120612-4-77	0.0457 ± 0.0018	0.643 ± 0.077	288 ± 11	504 ± 67	5.72	0.51													
120612-4-78	0.3496 ± 0.0064	5.50 ± 0.16	193.3 ± 35	1901 ± 54	101.7	0.26													

TABLE I. (Continued)

	Grain	$^{206}\text{Pb}/^{238}\text{U}$	$^{207}\text{Pb}/^{235}\text{U}$	$^{208}\text{Pb}/^{238}\text{U}$	age (Ma)	% conc Th/U	Grain	$^{206}\text{Pb}/^{238}\text{U}$	$^{207}\text{Pb}/^{235}\text{U}$	age (Ma)	% conc Th/U	
100416-5-7	0.0343 ± 0.0011	0.236 ± 0.011	217.3 ± 6.9	215 ± 10	101.1	0.32	100416-5-61	0.02784 ± 0.00062	0.1582 ± 0.00064	177.0 ± 3.9	149.1 ± 6.1	118.7 ± 0.38
100416-5-8	0.357 ± 0.011	5.76 ± 0.20	1968 ± 62	1941 ± 66	101.4	0.40						
100416-5-9	0.0379 ± 0.0012	0.264 ± 0.012	239.9 ± 7.7	238 ± 11	100.9	0.43						
100416-5-10	0.0412 ± 0.0011	0.316 ± 0.037	260.0 ± 6.8	279 ± 33	93.3	0.92						
100416-5-11	0.02902 ± 0.00053	0.185 ± 0.010	184.4 ± 3.4	172.4 ± 9.6	107.0	0.92						
100416-5-12	0.1592 ± 0.0025	2.585 ± 0.070	952 ± 15	1296 ± 35	73.5	0.20						
100416-5-13	0.02726 ± 0.00060	0.192 ± 0.017	173.4 ± 3.8	178 ± 16	97.3	0.68	101002-1-1	0.02816 ± 0.00064	0.243 ± 0.010	179.1 ± 4.1	220.8 ± 9.2	81.1 ± 0.44
100416-5-14	0.2856 ± 0.0045	4.51 ± 0.12	1619 ± 25	1733 ± 46	93.4	0.22	101002-1-2	0.02925 ± 0.00065	0.2264 ± 0.0079	184.6 ± 4.1	207.2 ± 7.3	89.1 ± 1.4
100416-5-15	0.02617 ± 0.00045	0.1834 ± 0.0084	166.5 ± 2.9	171.0 ± 7.9	97.4	0.58	101002-1-3	0.02943 ± 0.00064	0.2280 ± 0.0074	185.7 ± 4.1	208.5 ± 6.8	89.1 ± 0.32
100416-5-16	0.3816 ± 0.00062	0.2669 ± 0.0095	241.4 ± 3.9	240.2 ± 8.6	100.5	0.36	101002-1-4	0.02962 ± 0.00065	0.2236 ± 0.0072	188.2 ± 4.1	204.9 ± 6.6	91.8 ± 0.39
100416-5-17	0.02467 ± 0.00042	0.0770 ± 0.0034	157.1 ± 2.7	75.4 ± 3.3	208.5	0.53	101002-1-5	0.03437 ± 0.00076	0.2681 ± 0.0086	217.9 ± 4.8	241.1 ± 7.7	90.4 ± 0.65
100416-5-18	0.04010 ± 0.00065	0.286 ± 0.010	253.5 ± 4.1	255.3 ± 9.0	99.3	0.48	101002-1-6	0.03858 ± 0.00086	0.316 ± 0.010	244.0 ± 5.5	279.1 ± 9.3	87.4 ± 0.55
100416-5-19	0.03458 ± 0.00039	0.2403 ± 0.0073	219.1 ± 2.5	218.6 ± 6.7	100.2	0.67	101002-1-7	0.02985 ± 0.00059	0.269 ± 0.010	189.6 ± 3.7	242.1 ± 9.1	78.3 ± 0.47
100416-5-20	0.3431 ± 0.0037	5.73 ± 0.14	190.1 ± 20	193.5 ± 46	98.2	0.56	101002-1-8	0.03060 ± 0.00058	0.2140 ± 0.0067	194.3 ± 3.7	196.9 ± 6.2	98.7 ± 1.1
100416-5-21	0.03316 ± 0.00039	0.2345 ± 0.0079	210.3 ± 2.5	213.9 ± 7.2	98.3	0.55	101002-1-9	0.03905 ± 0.00075	0.290 ± 0.010	246.9 ± 4.7	258.8 ± 9.1	95.4 ± 0.32
100416-5-22	0.3476 ± 0.0037	5.93 ± 0.14	1923 ± 21	1965 ± 47	97.9	0.94	101002-1-10	0.02907 ± 0.00058	0.2431 ± 0.0099	184.7 ± 3.7	220.9 ± 9.0	83.6 ± 0.36
100416-5-23	0.04023 ± 0.00049	0.286 ± 0.011	254.3 ± 3.1	255.3 ± 9.6	99.5	0.94	101002-1-11	0.03428 ± 0.00065	0.2762 ± 0.0091	216.7 ± 4.1	247.6 ± 8.2	87.5 ± 0.63
100416-5-24	0.03377 ± 0.00041	0.2163 ± 0.0082	214.1 ± 2.6	198.8 ± 7.5	107.7	0.67	101002-1-12	0.03355 ± 0.0011	0.297 ± 0.014	212.4 ± 7.1	264 ± 12	80.4 ± 1.2
100416-5-25	0.3089 ± 0.0033	4.89 ± 0.12	1735 ± 19	1800 ± 44	96.4	0.29	101002-1-13	0.322 ± 0.011	5.05 ± 0.18	1802 ± 60	1828 ± 66	98.6 ± 0.15
100416-5-26	0.02752 ± 0.00031	0.1936 ± 0.0056	175.0 ± 2.0	179.7 ± 5.2	97.4	0.34	101002-1-14	0.02714 ± 0.00091	0.2057 ± 0.0094	172.6 ± 5.8	190.0 ± 8.7	90.9 ± 0.45
100416-5-27	0.03444 ± 0.00066	0.2446 ± 0.0080	218.3 ± 4.2	222.1 ± 7.2	98.3	0.54	101002-1-15	0.0325 ± 0.0011	0.243 ± 0.015	10204 ± 7.1	221 ± 13	93.6 ± 1.4
100416-5-28	0.03461 ± 0.00067	0.2607 ± 0.0088	235.3 ± 3.1	235.3 ± 9.6	92.3	0.56	101002-1-16	0.03295 ± 0.00099	0.207 ± 0.012	184.0 ± 6.3	191 ± 11	96.3 ± 0.62
100416-5-29	0.02902 ± 0.00058	0.1965 ± 0.0086	184.4 ± 3.7	182.2 ± 32	101.2	0.32	101002-1-17	0.03030 ± 0.00077	0.2120 ± 0.0071	192.4 ± 4.9	195.2 ± 6.5	98.6 ± 0.59
100416-5-30	0.02887 ± 0.00057	0.1915 ± 0.0083	183.5 ± 3.7	177.9 ± 7.7	103.1	0.29	101002-1-18	0.02882 ± 0.00075	0.2023 ± 0.0089	183.1 ± 4.8	187.1 ± 8.3	97.9 ± 0.69
100416-5-31	0.03902 ± 0.00074	0.2964 ± 0.0091	246.7 ± 4.7	263.5 ± 8.1	93.6	0.92	101002-1-19	0.03620 ± 0.00092	0.2545 ± 0.0082	229.3 ± 5.8	230.2 ± 7.4	99.6 ± 0.67
100416-5-32	0.02735 ± 0.00054	0.1986 ± 0.0076	174.0 ± 3.4	183.9 ± 7.1	94.6	0.50	101002-1-20	0.02912 ± 0.00076	0.2127 ± 0.0095	185.0 ± 4.8	195.8 ± 8.7	94.5 ± 0.45
100416-5-33	0.4202 ± 0.00081	8.85 ± 0.25	2323 ± 67	97.4 ± 59	101.0	0.21	101002-1-21	0.03279 ± 0.00085	0.233 ± 0.010	208.0 ± 5.4	212.4 ± 9.4	97.9 ± 0.31
100416-5-34	0.02828 ± 0.00055	0.2045 ± 0.0078	179.8 ± 3.5	188.9 ± 7.2	95.2	0.74	101002-1-22	0.03115 ± 0.00080	0.2387 ± 0.0092	197.7 ± 5.1	217.3 ± 8.4	91.0 ± 0.63
100416-5-35	0.03885 ± 0.00074	0.2736 ± 0.0086	245.7 ± 4.7	245.6 ± 7.7	100.1	0.21	101002-1-23	0.0395 ± 0.0010	0.2882 ± 0.0088	249.9 ± 6.3	257.2 ± 7.8	97.2 ± 0.53
100416-5-36	0.02838 ± 0.00085	0.1581 ± 0.0070	180.4 ± 5.4	149.1 ± 6.6	121.0	0.54	101002-1-24	0.2945 ± 0.0075	4.60 ± 0.13	1664 ± 42	174.8 ± 51	95.2 ± 0.43
100416-5-37	0.1043 ± 0.0031	1.422 ± 0.048	63.9 ± 19	89.8 ± 30	71.2	0.15	101002-1-25	0.03018 ± 0.00075	0.2141 ± 0.0086	191.7 ± 4.8	197.0 ± 7.9	97.3 ± 0.49
100416-5-38	0.02727 ± 0.00081	0.1742 ± 0.0068	173.5 ± 5.2	163.0 ± 6.4	106.4	0.26	101002-1-26	0.03279 ± 0.00079	0.2701 ± 0.0096	203.5 ± 5.0	242.7 ± 8.7	83.8 ± 0.49
100416-5-39	0.3195 ± 0.0094	4.96 ± 0.16	1787 ± 53	1813 ± 59	98.6	0.16	101002-1-27	0.02526 ± 0.00062	0.1773 ± 0.0061	159.6 ± 3.9	165.8 ± 5.7	96.3 ± 0.33
100416-5-40	0.02802 ± 0.00085	0.1395 ± 0.0071	178.2 ± 5.4	132.6 ± 6.7	134.3	0.55	101002-1-28	0.03079 ± 0.00077	0.2412 ± 0.0098	195.5 ± 4.9	219.4 ± 8.9	89.1 ± 0.66
100416-5-41	0.3446 ± 0.010	6.15 ± 0.20	1914 ± 56	1997 ± 65	95.9	0.25	101002-1-29	0.02524 ± 0.00062	0.1822 ± 0.0067	160.7 ± 4.0	169.9 ± 6.3	94.6 ± 0.52
100416-5-42	0.0345 ± 0.0010	0.252 ± 0.012	218.8 ± 6.6	228 ± 11	96.0	0.72	101002-1-30	0.02864 ± 0.00070	0.2195 ± 0.0074	182.0 ± 4.5	201.5 ± 6.8	90.3 ± 0.44
100416-5-43	0.02724 ± 0.00081	0.1868 ± 0.0077	173.2 ± 5.2	173.9 ± 7.2	99.6	0.46	101002-1-31	0.03566 ± 0.00095	0.270 ± 0.019	225.9 ± 6.0	243 ± 17	93.1 ± 0.65
100416-5-44	0.02587 ± 0.00077	0.1810 ± 0.0074	164.7 ± 4.9	168.9 ± 6.9	97.5	0.35						
100416-5-45	0.02584 ± 0.00049	0.1829 ± 0.0058	164.4 ± 3.1	170.5 ± 5.4	96.4	0.54						
100416-5-46	0.3065 ± 0.0057	4.89 ± 0.14	1724 ± 32	1800 ± 50	95.8	0.20						
100416-5-47	0.3216 ± 0.0060	5.07 ± 0.14	1798 ± 34	1830 ± 50	98.2	0.43						
100416-5-48	0.3023 ± 0.0056	4.79 ± 0.13	1703 ± 32	1783 ± 50	95.5	0.16						
100416-5-49	0.03476 ± 0.00067	0.2450 ± 0.0088	220.3 ± 4.2	222.5 ± 8.0	99.0	0.59	100416-4-1	0.391 ± 0.020	0.0523 ± 0.0024	328 ± 15	335 ± 18	98.0 ± 0.36
100416-5-50	0.2802 ± 0.0053	4.46 ± 0.13	1592 ± 30	1724 ± 51	92.4	0.53	100416-4-2	0.166 ± 0.012	0.0204 ± 0.0010	130.0 ± 6.2	156 ± 11	83.4 ± 1.6
100416-5-51	0.02767 ± 0.00053	0.1949 ± 0.0071	176.0 ± 3.4	180.8 ± 6.6	97.3	0.29	100416-4-3	5.98 ± 0.30	0.298 ± 0.014	1682 ± 78	197.2 ± 98	85.3 ± 0.56
100416-5-52	0.02859 ± 0.00056	0.1885 ± 0.0075	181.7 ± 3.5	175.3 ± 7.0	103.7	0.33	100416-4-4	0.1725 ± 0.0097	0.02221 ± 0.0010	140.7 ± 6.6	161.6 ± 9.7	87.1 ± 1.0
100416-5-53	0.02623 ± 0.00058	0.1373 ± 0.0058	166.9 ± 3.7	130.6 ± 5.5	127.8	0.56	100416-4-5	3.09 ± 0.15	0.2072 ± 0.0097	121.4 ± 57	143.1 ± 71	84.8 ± 0.24
100416-5-54	0.02680 ± 0.00060	0.1863 ± 0.0075	170.5 ± 3.8	173.5 ± 7.0	98.3	0.39	100416-4-6	0.1665 ± 0.0098	0.0209 ± 0.0010	133.5 ± 6.3	156 ± 9	85.4 ± 1.1
100416-5-55	0.03471 ± 0.00076	0.2438 ± 0.0093	218.9 ± 4.8	221.5 ± 8.5	99.3	0.76	100416-4-7	0.0367 ± 0.0017	0.0204 ± 0.0016	233 ± 11	236 ± 14	98.4 ± 0.92
100416-5-56	0.02942 ± 0.00066	0.2083 ± 0.0053	186.9 ± 4.2	192.1 ± 8.7	97.3	0.37	100416-4-8	0.1733 ± 0.012	0.0206 ± 0.0010	131.2 ± 6.2	162 ± 11	81.1 ± 1.7
100416-5-57	0.3055 ± 0.0065	4.79 ± 0.14	1719 ± 37	1782 ± 53	96.4	0.29	100416-4-9	0.331 ± 0.018	0.0461 ± 0.0020	291 ± 13	290 ± 16	100.1 ± 0.14
100416-5-58	0.03357 ± 0.00077	0.221 ± 0.011	212.8 ± 4.9	203.0 ± 9.7	104.8	0.96	100416-4-10	0.252 ± 0.014	0.0358 ± 0.0016	227 ± 10	228 ± 13	99.4 ± 0.54
100416-5-59	0.3676 ± 0.0079	7.27 ± 0.22	2018 ± 43	245 ± 64	94.1	1.1	100416-4-11	0.457 ± 0.0087	0.0219 ± 0.0010	140 ± 6	138 ± 8	101.0 ± 1.2
100416-5-60	0.03368 ± 0.00073	0.2198 ± 0.0076	213.5 ± 4.6	201.7 ± 7.0	105.9	0.48	100416-4-12	0.1520 ± 0.0090	0.02123 ± 0.00071	135.4 ± 4.5	144 ± 8	94.3 ± 0.9

TABLE 1. (Continued)

Grain	$^{206}\text{Pb}/^{238}\text{U}$	$^{207}\text{Pb}/^{235}\text{U}$	$^{208}\text{Pb}/^{238}\text{U}$	$^{207}\text{Pb}/^{235}\text{U}$ age (Ma)	$^{208}\text{Pb}/^{238}\text{U}$ age (Ma)	Grain	$^{206}\text{Pb}/^{238}\text{U}$	$^{207}\text{Pb}/^{235}\text{U}$	$^{208}\text{Pb}/^{238}\text{U}$ age (Ma)	$^{207}\text{Pb}/^{235}\text{U}$ age (Ma)	% conc Th/U	
<i>100416-4-13</i>	0.1504 ± 0.0094	0.02002 ± 0.00069	127.8 ± 4.4	142.3 ± 8.9	89.8 /	1.1	100416-4-60	0.149 ± 0.011	0.02022 ± 0.00069	129 ± 4	141 ± 10	91.6 / 1.3
<i>100416-4-14</i>	0.3668 ± 0.0119	0.03666 ± 0.0012	232.0 ± 7.6	318 ± 16	72.9 / 0.28	100416-4-61	0.1478 ± 0.0080	0.02076 ± 0.00068	132.4 ± 4.3	140.0 ± 7.6	94.6 / 0.6	
<i>100416-4-15</i>	3.28 ± 0.15	0.2178 ± 0.0070	127.0 ± 41	147.5 ± 68	86.1 / 0.1	100416-4-62	0.156 ± 0.010	0.02079 ± 0.00070	133 ± 4	147 ± 9	89.9 / 0.93	
<i>100416-4-16</i>	0.186 ± 0.0111	0.02655 ± 0.0012	168.8 ± 7.8	174 ± 10	97.3 / 0.35	100416-4-63	0.203 ± 0.012	0.02674 ± 0.00089	170.1 ± 5.7	187 ± 11	90.8 / 0.7	
<i>100416-4-17</i>	0.145 ± 0.0110	0.02111 ± 0.0013	135 ± 6	138 ± 10	98.0 / 0.11	100416-4-64	0.1430 ± 0.0085	0.02014 ± 0.00067	129 ± 4	136 ± 8	94.7 / 1.1	
<i>100416-4-18</i>	0.201 ± 0.0111	0.02922 ± 0.0013	186 ± 9	186 ± 9	99.9 / 0.29	100416-4-65	4.71 ± 0.17	0.2990 ± 0.0087	168.6 ± 49	176.9 ± 62	95.3 / 0.2	
<i>100416-4-19</i>	1.387 ± 0.025	0.10422 ± 0.0013	639 ± 8	883 ± 16	72.3 / 0.24	100416-4-66	3.46 ± 0.12	0.2273 ± 0.0066	132.0 ± 3.8	151.7 ± 5.5	87.0 / 0.27	
<i>100416-4-20</i>	0.2958 ± 0.0035	167.1 ± 20	1765 ± 28	94.6 / 0.16	100416-4-67	2.94 ± 0.10	0.1960 ± 0.0057	115.4 ± 3.3	139.2 ± 49	82.9 / 0.20		
<i>100416-4-21</i>	4.762 ± 0.076	0.2695 ± 0.0032	1538 ± 18	1778 ± 29	86.5 / 0.4	100416-4-68	5.85 ± 0.20	0.2927 ± 0.0085	165.5 ± 48	195.3 ± 68	84.7 / 0.6	
<i>100416-4-22</i>	0.2229 ± 0.0078	0.02857 ± 0.00040	181.6 ± 2.5	204.3 ± 7.0	88.9 / 0.61	100416-4-69	1.815 ± 0.0083	0.02133 ± 0.00063	136.0 ± 4.0	169.4 ± 7.7	89.3 / 1.2	
<i>100416-4-23</i>	0.1739 ± 0.0059	0.02098 ± 0.00029	133.8 ± 1.9	162.8 ± 5.5	82.2 / 0.60	100416-4-70	0.1666 ± 0.0098	0.02108 ± 0.00065	134.5 ± 4.1	156.5 ± 9.2	85.9 / 0.7	
<i>100416-4-24</i>	5.50 ± 0.15	0.3324 ± 0.0058	185.0 ± 32	190.1 ± 51	97.3 / 0.9	100416-4-71	0.1889 ± 0.0080	0.02672 ± 0.00078	170.0 ± 5.0	176 ± 7	96.8 / 0.28	
<i>100416-4-25</i>	0.483 ± 0.013	0.04213 ± 0.00072	266.0 ± 4.6	400 ± 11	66.5 / 0.38	100416-4-72	0.171 ± 0.015	0.02091 ± 0.00068	133 ± 4	161 ± 14	83.0 / 1.2	
<i>100416-4-26</i>	0.282 ± 0.0111	0.0391 ± 0.0010	253 ± 10	253 ± 10	97.9 / 0.12	100416-4-73	0.2065 ± 0.0093	0.02914 ± 0.00068	185.5 ± 4.3	191 ± 9	97.1 / 0.69	
<i>100416-4-27</i>	0.1482 ± 0.0062	0.02134 ± 0.00056	136.1 ± 3.6	140.3 ± 5.9	97.0 / 0.87	100416-4-74	0.2492 ± 0.0099	0.03638 ± 0.00084	230.4 ± 5.3	226 ± 9	102.0 / 0.3	
<i>100416-4-28</i>	0.1909 ± 0.0082	0.02622 ± 0.00069	166.9 ± 4.4	177.4 ± 7.6	94.1 / 0.4	100416-4-75	0.284 ± 0.010	0.03270 ± 0.00075	207.4 ± 4.7	254 ± 9	81.6 / 0.75	
<i>100416-4-29</i>	1.215 ± 0.043	0.0920 ± 0.0024	568 ± 15	807 ± 29	70.3 / 0.40	100416-4-76	0.1594 ± 0.0081	0.01989 ± 0.00048	126.9 ± 3.0	150 ± 8	84.5 / 1.0	
<i>100416-4-30</i>	0.1967 ± 0.0069	0.02159 ± 0.00055	137.7 ± 3.5	182.4 ± 6.4	75.5 / 1.6	100416-4-77	0.1732 ± 0.0083	0.02154 ± 0.00051	137 ± 3	162 ± 8	84.7 / 0.80	
<i>100416-4-31</i>	0.1532 ± 0.0088	0.02033 ± 0.00056	130 ± 4	145 ± 8	89.6 / 2.0	100416-4-78	0.1386 ± 0.0058	0.02064 ± 0.00048	132 ± 3	132 ± 5	99.9 / 0.72	
<i>100416-4-32</i>	0.2705 ± 0.0087	0.0380 ± 0.0010	243.0 ± 6.1	243.0 ± 7.8	99.0 / 0.31	100416-4-79	4.43 ± 0.12	0.2821 ± 0.00063	160.2 ± 3.6	171.9 ± 47	93.2 / 0.28	
<i>100416-4-33</i>	0.376 ± 0.014	0.0498 ± 0.0015	313.1 ± 9.6	324 ± 12	96.5 / 0.28	100416-4-80	0.230 ± 0.011	0.02857 ± 0.00068	181.6 ± 4.3	210 ± 10	86.4 / 0.46	
<i>100416-4-34</i>	1.041 ± 0.038	0.0839 ± 0.0026	519 ± 16	724 ± 27	71.7 / 0.35	100416-4-81	0.1818 ± 0.0065	0.02546 ± 0.00058	162 ± 4	170 ± 6	95.5 / 0.33	
<i>100416-4-35</i>	5.05 ± 0.17	0.3191 ± 0.0098	1785 ± 55	1828 ± 62	97.6 / 0.18	100416-4-82	0.423 ± 0.022	0.0561 ± 0.0027	352 ± 17	358 ± 19	98.4 / 0.39	
<i>100416-4-36</i>	4.94 ± 0.17	0.3153 ± 0.0097	1767 ± 54	1810 ± 62	97.6 / 0.70	100416-4-83	0.142 ± 0.013	0.0197 ± 0.0010	125.9 ± 6.3	135 ± 12	93.4 / 0.84	
<i>100416-4-37</i>	0.294 ± 0.012	0.04049 ± 0.0013	258.5 ± 8.0	262 ± 10	98.6 / 0.4	100416-4-84	0.213 ± 0.011	0.0257 ± 0.0012	163.4 ± 7.7	196 ± 10	83.2 / 0.29	
<i>100416-4-38</i>	0.1479 ± 0.0076	0.02113 ± 0.00067	134.8 ± 4.3	140.1 ± 7.2	96.2 / 1.1	100416-4-85	0.1452 ± 0.0089	0.0211 ± 0.0010	134.6 ± 6.4	137.6 ± 8.4	97.8 / 1.10	
<i>100416-4-39</i>	0.256 ± 0.012	0.0365 ± 0.0011	231.1 ± 7.3	231.1 ± 11	99.9 / 0.4	100416-4-86	0.191 ± 0.010	0.0264 ± 0.0013	168 ± 8	177 ± 9	94.8 / 0.45	
<i>100416-4-40</i>	0.260 ± 0.011	0.0370 ± 0.0012	234.4 ± 7.3	234 ± 10	100.0 / 0.3	100416-4-87	0.144 ± 0.012	0.0214 ± 0.0011	136.3 ± 6.7	136 ± 12	100.0 / 1.2	
<i>100416-4-41</i>	0.389 ± 0.011	0.04383 ± 0.00090	276.5 ± 5.7	333.3 ± 9.8	83.0 / 0.19	100416-4-88	0.148 ± 0.012	0.02028 ± 0.0010	130.0 ± 6.5	140 ± 11	94.8 / 1.0	
<i>100416-4-42</i>	0.2892 ± 0.0085	0.03911 ± 0.00080	247.3 ± 5.1	257.9 ± 7.6	95.9 / 0.1	100416-4-89	0.148 ± 0.011	0.0212 ± 0.0010	135.3 ± 6.6	140 ± 11	96.6 / 0.64	
<i>100416-4-43</i>	0.191 ± 0.010	0.02588 ± 0.00058	164.7 ± 3.7	178 ± 9	92.8 / 1.1	100416-4-90	0.1461 ± 0.0085	0.02102 ± 0.00050	134.1 ± 3.2	138 ± 8	96.9 / 1.28	
<i>100416-4-44</i>	0.1432 ± 0.0061	0.02082 ± 0.00045	132.8 ± 2.8	136 ± 6	97.8 / 0.74	100416-4-91	0.427 ± 0.022	0.0560 ± 0.0013	351 ± 8	361 ± 18	97.4 / 0.40	
<i>100416-4-45</i>	0.3009 ± 0.0090	0.04151 ± 0.00085	262.0 ± 5.4	267 ± 8	98.2 / 1.0	100416-4-92	0.268 ± 0.014	0.03766 ± 0.00088	238 ± 6	241 ± 13	98.8 / 0.19	
<i>100416-4-46</i>	3.94 ± 0.11	0.25844 ± 0.00053	1482 ± 30	1622 ± 44	91.3 / 0.2	100416-4-93	0.159 ± 0.013	0.0219 ± 0.0011	140 ± 7	150 ± 12	93.3 / 0.76	
<i>100416-4-47</i>	7.49 ± 0.20	0.3984 ± 0.0081	2162 ± 44	2171 ± 57	99.6 / 0.67	100416-4-94	0.155 ± 0.012	0.0210 ± 0.0010	134.2 ± 6.5	146 ± 11	91.9 / 1.0	
<i>100416-4-48</i>	0.1483 ± 0.0047	0.02084 ± 0.00043	133.0 ± 2.7	140.4 ± 4.4	94.7 / 0.83	100416-4-95	0.263 ± 0.015	0.0396 ± 0.0019	250 ± 12	237 ± 13	105.7 / 0.3	
<i>100416-4-49</i>	0.252 ± 0.018	0.0359 ± 0.0016	227 ± 10	228 ± 16	99.7 / 0.60	100416-4-96	0.147 ± 0.011	0.0201 ± 0.0010	128.5 ± 6.2	139 ± 11	92.1 / 0.99	
<i>100416-4-50</i>	0.180 ± 0.011	0.0258 ± 0.0011	164.1 ± 7.3	168 ± 10	97.7 / 0.61	100416-4-97	0.290 ± 0.020	0.0403 ± 0.0019	254 ± 12	259 ± 18	98.4 / 0.54	
<i>100416-4-51</i>	0.161 ± 0.012	0.02029 ± 0.00093	129.5 ± 5.9	152 ± 12	85.5 / 0.71	100416-4-98	0.200 ± 0.014	0.0280 ± 0.0011	178.2 ± 6.8	185 ± 13	96.2 / 0.47	
<i>100416-4-52</i>	0.177 ± 0.011	0.02533 ± 0.0011	160.9 ± 7.2	165.4 ± 9.9	97.3 / 2.0	100416-4-99	0.261 ± 0.011	0.0369 ± 0.0014	233.5 ± 8.6	236 ± 10	99.1 / 0.12	
<i>100416-4-53</i>	4.17 ± 0.20	0.2711 ± 0.0119	154.6 ± 68	166.7 ± 80	92.8 / 0.3	100416-4-100	0.1713 ± 0.0079	0.02436 ± 0.00090	155.1 ± 5.7	160.5 ± 7.4	96.7 / 0.6	
<i>100416-4-54</i>	0.1389 ± 0.0096	0.02001 ± 0.0016	127.1 ± 9.1	132.1 ± 9.1	96.7 / 0.80	100416-4-101	0.1359 ± 0.0093	0.02072 ± 0.00078	132.2 ± 5.0	129.4 ± 8.9	102.1 / 1.2	
<i>100416-4-55</i>	0.143 ± 0.011	0.02071 ± 0.00095	132.1 ± 6.0	136 ± 11	97.0 / 0.8	100416-4-102	0.1676 ± 0.0078	0.02041 ± 0.00030	130.2 ± 5.0	157.3 ± 7.4	82.8 / 0.8	
<i>100416-4-56</i>	0.248 ± 0.014	0.0351 ± 0.0016	222.3 ± 9.9	225 ± 13	98.7 / 1.2	100416-4-103	0.158 ± 0.011	0.02095 ± 0.00034	134 ± 2	149 ± 10	89.8 / 1.5	
<i>100416-4-57</i>	0.263 ± 0.011	0.0365 ± 0.0012	231.0 ± 7.4	237 ± 10	97.6 / 0.12	100416-4-104	0.2001 ± 0.0089	0.02787 ± 0.00040	177 ± 3	185 ± 8	95.7 / 0.93	
<i>100416-4-58</i>	0.1504 ± 0.0082	0.02068 ± 0.00068	132 ± 4	142 ± 8	92.8 / 0.72	100416-4-105	0.1551 ± 0.0082	0.02103 ± 0.00031	134.2 ± 2.0	146.4 ± 7.7	91.7 / 0.99	
<i>100416-4-59</i>	3.54 ± 0.13	0.2244 ± 0.0071	1305 ± 55	1336 ± 55	85.0 / 0.4							